Analysis-oriented Model for Partially FRP-and-Steel-Confined Circular RC Columns under Compression

Javad Shayanfar [1], Joaquim A. O. Barros [2] and Mohammadali Rezazadeh [3]

[1] PhD Candidate, ISISE, Department of Civil Engineering, University of Minho, Azurém 4800-058 Guimarães, Portugal, arch3d.ir@gmail.com (corresponding author)

[2] Full Prof., ISISE, IBS, Department of Civil Engineering, University of Minho, Azurém 4800-058 Guimarães, Portugal, barros@civil.uminho.pt

[3] Lecturer, Civil Eng., Department of Mechanical and Construction Engineering, Northumbria University, Newcastle upon Tyne, NE1 8ST, United Kingdom, mohammadali.rezazadeh@northumbria.ac.uk

Abstract

Even though analysis-oriented models exist to simulate the axial and dilation behavior of reinforced concrete (RC) columns strengthened with fiber-reinforced-polymer (FRP) full confinement arrangements, a reliable model developed/calibrated for FRP partially imposed confinements is not yet available, identified as a research gap. Therefore, this paper is dedicated to the development of a new analysis-oriented model generalized for fully and partially confined RC columns under compression. In addition to vertical arching action phenomenon, the influence of the concrete expansion distribution along the column height on confining stress is considered in the establishment of the combined confinement from FRP strips and steel transverse reinforcements. A new unified dilation model is proposed, where the substantial effect of additional axial deformations induced by damage evolution in unwrapped zones is formulated by considering available experimental results. This model is coupled with an axial stress-strain formulation that includes a new failure surface function for simulating the dual confinement-induced enhancements, which are strongly dependent on the confinement stiffness. The developed model considers the influence of partially imposed confinement strategy on the axial and dilation behavior of RC columns, whose validation is demonstrated by simulating several experimental tests. Lastly, a parametric study is performed to evidence the dependence of FRP-steel confinement-induced enhancements on steel hoop and FRP spacing, and on the concrete compressive strength.

Keywords: RC columns; FRP confinement; Steel confinement; Dilation model; Stress-strain model;

1 - Introduction

The confinement of existing circular reinforced concrete (RC) columns with fiber-reinforced-polymer (FRP) composites has been progressively demonstrated as a competitive strengthening technique for increasing the axial load carrying and deformation capacity of these structural elements. Numerous studies have been carried out to investigate the influence of FRP confining system on the axial and dilation behavior of concrete/RC columns, leading to the development of several analysis/design-oriented stress-strain models. Nonetheless, most of these models do not consider the confinement provided by existing steel hoop/spiral reinforcements, neither the mutual interference of this hybrid reinforcement (FRP and hoop/spiral) on the final confinement. Furthermore, in general, they are only applicable to full confinement arrangement and, consequently, their applicability for the case of FRP partially imposed confinement is at least arguable. For a comprehensive investigation, existing studies available in the literature were analyzed and classified into two distinctive categories: i) those of experimental and numerical nature that consider the influence of key parameters on full/partial confinement mechanism/performance; ii) those of analysis-oriented framework that simulate theoretically the axial and dilation behavior of concrete/RC columns with dual FRP-steel confinement.

In the first category, for the case of FRP fully confined circular concrete elements (FC as shown in Fig. 1a), Lin e*t al.* [1] experimentally evidenced that the effectiveness of this confinement system remarkably depends on concrete axial compressive strength and FRP thickness. For the case of FRP partially confined circular concrete elements (PC as shown in Fig. 1a), Wang *et al.* [2] demonstrated the FRP strip spacing (s_f) plays a key role in the establishment of their axial and dilation behavior. Zeng *et al.* [3, 4] experimentally revealed that by increasing s_f, the ratio of concrete lateral expansion at the strip mid-plane and at the mid-height of FRP strips grows remarkably, leading to a non-homogenous distribution of concrete expansion and confining stress along the column height. Wang *et al.* [5] performed an experimental study to evaluate axial and dilation responses of FRP fully confined circular RC column (FR as shown in Fig. 1a). It was demonstrated that the dual confinement mechanism of FRP jacket and steel hoops is able to considerably enhance axial strength and deformability of FR, compared to FC, depending on steel hoop spacing (s_s). Kaeseberg *et al.* [6] experimentally demonstrated the substantial influence of s_s on the confinement-induced enhancements of FR, whose level also depends on the volumetric ratio and yield strength of steel hoops, as also confirmed by [7]. Eid *et al.* [8] experimentally showed that steel spiral reinforcements are more effective than steel hoops for the improvement of the axial and dilation responses of FR, which was also shown by [9]. Based on finite element analysis, Zignago and Barbato [10] evidenced the significant influence of the steel hoop confinement on the peak axial strength of FR, but its contribution has decreased with the increase of the concrete compressive strength and FRP confinement stiffness. Barros and Ferreira [11] investigated the axial and dilation behavior of FRP partially confined circular RC columns (PR as shown in Fig. 1a) with different confinement arrangements. The results indicated that even though the partial confining strategy was not as efficient as full confinement, it could be sufficient to assure high levels of load-carrying capacity and deformability with a good compromise between efficiency and cost-effectiveness. Furthermore, it was demonstrated that the confinement-induced enhancements were more significant in PR columns with closely spaced FRP strips and relatively low concrete compressive strength.

On the other hand, in the second category, several theoretical-based models [12-15] have been proposed to simulate axial and dilation behavior of concrete/RC columns with FRP or dual FRP-steel confinement, It is now well-known that at the same level of confinement pressure (f_l), there is a remarkable difference in the level of enhancements provided by passively- and actively-confinement systems (f_l varies and is constant, respectively, during axial loading). This difference is generally known as *Confinement Path Effect*. In general, to determine the axial stress-strain curve of passively-confined concrete (i.e. FRP confined concrete), an axial stress-strain base model, $f_c = g_1\left(f_{cc}\right)$, is adopted, where g_1 represents the mathematical function of the model for determining a certain value of axial stress (f_c) from a specified value of peak axial strength (f_{cc}) at a given axial strain (ε_c), as demonstrated in Fig. 1b. Subsequently, the confinement path effect is considered by using a failure surface function applicable to passively- confining system, $f_{cc} = g_2\left(f_l\right)$, which determines f_{cc} from the confinement pressure (f_l) at a given ε_c through the g_2 .function. Teng *et al.* [12] proposed an analysis-oriented model applicable to FC in which a new failure surface function was developed/calibrated based on test results of FC rather than actively-confined concrete. Zeng *et al.* [3] generalized Teng *et al.* [12]'s models for the case of PC by adopting the well-known concept of confinement efficiency factor (suggested by Mander *et al.* [13]). It was demonstrated that this approach results in misleading predictions of experimental axial and dilation behavior of PC, particularly for specimens with a relatively large s_f . Shayanfar *et al.* [14] proposed a generalized analysis-oriented model for FC and PC, coupled with the dilation model developed by Shayanfar *et al.* [15]. In this model, a new failure surface function applicable to passively-confined concrete was developed based on a large test database of FC/PC. Furthermore, besides the vertical arching action, the effect of non-uniform distribution of concrete lateral expansion along the column height of PC was considered. For the case of FR, Pellegrino and Modena [16] proposed an axial stress-strain model, where the interaction mechanisms between internal FRP full confinement and steel transverse reinforcements were considered based on experimental observations. Hu and Seracino [17] developed a new confinement model for FR, where the contribution of steel hoops and FRP jackets in the failure surface function is evaluated according to the Mander *et al.* [13] (originally developed for steel-confined RC columns) and Jiang and Teng [18]'s models, respectively. Similarly, Teng *et al.* [19] extended the model of Jiang and Teng [18] for the case of FR by using the ratio between the FRP confinement stiffness and the effective confining stiffness of steel transverse reinforcements for considering the effect of their dual confinement mechanism. Even so, to the best of the authors' knowledge, the development of a robust analysis-oriented model for the case of PR to predict the full range of axial- stress–strain response is still lacking.

The present study aims to introduce a robust confinement model generalized for FRP full and partial confinement arrangements (FR and PR), where the key components of this model are calibrated based on existing experimental results. For the establishment of the FRP-steel equivalent confinement pressures uniformly distributed over the column height, the influence of non-homogenous distribution of concrete lateral expansion on their confining stress is required to be addressed, besides vertical arching action. For quantitatively characterizing this influence, a reduction factor with an analytical framework is suggested where the degree of its dominance in the equivalent confinement pressure is strongly dependent on confinement configuration i.e. steel hoop/spiral and FRP spacing and FRP confinement stiffness, in addition to cross-section geometry. Subsequently, an extended version of the dilation model recommended by Teng *et al.* [19], originally developed for FR, is introduced for the case of PR. In this extended/improved model, new parameters are proposed to reflect the substantial effects of additional axial deformations induced by damage evolution in unwrapped zones, peak Poisson's ratio, and non-homogenous concrete expansion distribution on axial strain-lateral strain relation. This model is, then, coupled with axial stress-strain models for concrete core and cover areas that include a confinement stiffness-based failure surface function calibrated for partially imposed FRP-steel confining systems. Lastly, the reliability of the proposed analysis-oriented model is demonstrated by comparison with existing experimental results and those predicted by Teng *et al.* [19]'s model generalized based on the well-known concept of confinement efficiency factor (suggested by Mander *et al.* [13]).

2 - Characteristics of Unconfined Concrete Columns

To calculate the confinement-induced improvements in terms of axial compressive strength and deformability, the characteristics of unconfined concrete compressive strength (f_{c0}) and its corresponding axial strain (ε_{c0}) are necessary to be determined as basic parameters. The studies (i.e. [20-32]) have evidenced a remarkable size effect, resulted from the energy release of the elastic strain when concrete enters in its softening stage, which is also dependent of the relative stiffness of the specimen versus of the adopted testing equipment. This influences the compressive strength of unconfined concrete specimens, being it dependent on the parameters affecting the axial stiffness of the specimen, namely the specimen's aspect ratio (L/D) and concrete elasticity modulus, E_c. This last parameter reflects the concrete stiffness, which is influenced not only on the quality of the matrix and aggregates, but also on the aggregate-matrix interface zone [24-29]. Sim *et al.* [25] proposed an empirical formulation, calibrated by using results from 1509 test specimens of unconfined concrete, having a better performance in predicting experimental f_{c0} compared to Bazant [27] and Kim and Eo [28]. Accordingly, in this study, the well-calibrated model suggested by Sim *et al.* [25] was adopted to calculate f_{c0} as presented by Eq. (1) (with a slight rearrangement):

$$f_{c0}=\left[0.63+0.9\sqrt{\frac{\left(L/D\right)^{-0.6}}{1+0.017D}}\right]f'_{c0}\simeq 1.063\left(\frac{150}{D}\right)^{0.122}\left(\frac{D}{L}\right)^{0.088}f'_{c0} \tag{1}$$

where f'_{c0} is the compressive strength of the standard cylinder with $D=150$ mm and $L=300$ mm (the reference specimen's dimensions), assumed as a representative. Note that for the case of the representative, $f_{c0}=f'_{c0}$.

On the other hand, studies (i.e. [20-22, 30-32]) demonstrated a strong relation between concrete compressive strength (f_{c0}) and its corresponding axial strain (ε_{c0}), where ε_{c0} increases with f_{c0}. Besides the effect of f_{c0}, Jansen and Shah [20] evidenced that the column aspect ratio (L/D) has a noticeable influence on the ε_{c0}, which was also confirmed by [22]. In the present study, for the estimation of ε_{c0} by considering the size effect, a large database including 604 unconfined concrete specimens was collected as presented briefly in Table 1. According to the compiled database, the best-fit expression obtained from regression analysis, as a function of f_{c0} and column aspect ratio (L/D), is proposed:

$$\varepsilon_{c0}=0.0011\left(\frac{f_{c0}D}{L}\right)^{0.25} \tag{2}$$

whose predictive performance over the corresponding collected experimental data ($\varepsilon_{c0}^{Ana}/\varepsilon_{c0}^{Exp}$) is shown in Fig. 2 for the considered variables: f_{c0}, L/D and D. The obtained statistical indicators presented in Table 2 demonstrate that Eq. (2) is able to predict with acceptable accuracy the experimental counterparts. Furthermore, Table 2 shows that the proposed expression has a better predictive performance than those recommended by Lim and Ozbakkaloglu [31] and Popovics [32].

3 - Simulation Procedure of Axial Response for FR and PR

To establish the axial stress versus axial strain relationship of FR/PR with the combined confinement from steel transverse reinforcements and FRP jacket, the following procedure was adopted:

a) Determination of the equivalent confinement pressure imposed by steel transverse reinforcements ($f_{l,s}$) and FRP jacket ($f_{l,f}$) by considering both the effect of non-homogenous distribution of concrete transverse expansibility over the column height and the vertical arching action phenomenon.

b) Determination of the average axial compressive strain along the column height (ε_c) at a certain level of concrete lateral strain ($\varepsilon_{l,j}$) obtained from a unified dilation model.

c) Determination of the axial stresses carried by concrete core and cover areas (f_c^{Core} and f_c^{Cover} , respectively) at a certain level of ε_c based on the 'Active Confinement Approach'. In this approach, the axial stress-strain relation of passively-confined concrete is derived based on an axial stress-strain base relation model developed for actively-confined concrete, where the differences of passive and active confinement systems are reflected in terms of their confinement-induced improvements.

Since full confinement system is a special case of partial confinement configuration where $s_f = 0$, a unified approach that depends on s_f will be established, in order to dealt with both confinement arrangements with the same formulation. Accordingly, as close s_f is to the null value, as close is the behavior of a column when subjected to a full confinement configuration (FR). Likewise, when the spacing of steel transverse reinforcements is above a certain limit (its contribution would be insignificant in dual confinement mechanism with FRP jacket), the prediction continuity between FR/PR and FC/PC can be achieved. Therefore, through a generalized mathematical framework based on unification approach, an unique formulation was developed to be applied to PC, PR, FC and FR.

4 - Confinement Pressure Generated by FRP and Steel Transverse Reinforcements

This section addresses the determination of the confinement pressure generated by FRP full/partial confinement system and steel transverse reinforcements. Fallahpour *et al.* [33] demonstrated experimentally that there is a non-uniform distribution of concrete lateral strain that generates a non-uniform confining pressure along the column height, which is dependent on the confinement stiffness, as was also confirmed by [34-36]. For FC with high level of FRP confinement stiffness, since strong restrictions are imposed against the concrete expansibility, an almost null gradient of concrete expansion along the column height is expected. However, for lightly-confined concrete, the damage evolution cannot be homogenized, leading to strain localization due to the lack of sufficient confinement stiffness [36]. On the other hand, the non-uniform distribution of concrete lateral expansion for the case of PC is more pronounced than in FC, whose level is significantly dependent on the s_f, as evidenced by Zeng *et al.* [4] and Guo *et al.* [37]. For the case of FC/PC, Shayanfar *et al.* [14] have specified a reduction factor for FRP confining stress aiming to develop an equivalent confining stress acting uniformly over the concrete column height. Accordingly, by assuming that the maximum concrete expansion ($\varepsilon_{l,j}$) occurs at the mid-distance between FRP strips in case of PC (Fig. 3) leading to a confining stress equal to $E_f \varepsilon_{l,j}$ (where E_f is the elasticity modulus of FRP strips), the equivalent confining stress can be expressed as $k_{ff} E_f \varepsilon_{l,j}$, where k_{ff} is the reduction factor specified by Shayanfar *et al.* [14].

Therefore, for the case of PR, considering the effect of vertical arching action between FRP strips, the equivalent FRP confinement pressure ($f_{l,f}$) acting uniformly over the column height can be derived based on lateral force equilibrium as (the meaning of the symbols representing geometric entities are shown in Fig. 1):

$$f_{l,f} = 2k_{v,f} \frac{n_f t_f w_f}{D\left(w_f + s_f\right)} E_f k_{ff}{}^{PR} \varepsilon_{l,j} = 2k_{v,f} k_{ff}{}^{PR} \frac{n_f t_f w_f}{D\left(w_f + s_f\right)} E_f \varepsilon_{l,j} \tag{3}$$

Rearranging Eq. (3) yields:

$$f_{l,f} = k_{v,f} k_{ff}{}^{PR} K_{Lc} \frac{w_f}{w_f + s_f} \varepsilon_{l,j} \tag{4}$$

in which

$$K_{Lc} = 2\frac{n_f t_f E_f}{D} \tag{5}$$

where $k_{v,f}$ is the reduction factor reflecting the effect of vertical arching action between FRP strips; $k_{ff}{}^{PR}$ is the reduction factor reflecting the effect of non-homogenous concrete expansion along the height of PR (the superscript represents the type of confined column that this factor is applicable to). Note that to calculate $f_{l,f}$ by Eq. (4), the reduction factors $k_{ff}{}^{PR}$ and $k_{v,f}$ need to be addressed as input parameters, which will be presented in Section 4.1 and Section 4.2, respectively.

By considering the influences of the concrete expansion distribution and vertical arching action between steel transverse reinforcements, the equivalent confinement pressure ($f_{l,s}$), imposed uniformly on the core of PR can be determined from lateral force equilibrium as (the meaning of the symbols representing geometric entities was shown in Fig. 1):

$$f_{l,s} = 2k_{v,s}k_{ff}{}^{PR}\frac{A_{sth}}{D_c s_s}E_s\varepsilon_{l,j} \qquad \text{for } k_{ff}{}^{PR}\varepsilon_{l,j} < \varepsilon_{yh} \tag{6a}$$

$$f_{l,s} = 2k_{v,s}\frac{A_{sth}}{D_c s_s}f_{yh} \qquad \text{for } k_{ff}{}^{PR}\varepsilon_{l,j} \geq \varepsilon_{yh} \tag{6b}$$

where $k_{v,s}$ is the reduction factor reflecting the effect of vertical arching action between steel transverse reinforcements; D_c is the diameter of the concrete core (Fig. 1); A_{sth} is the cross-sectional area of a steel confining spiral/hoop; s_s is the distance between steel transverse reinforcements; E_s, ε_{yh} and f_{yh} are the elasticity modulus, yield strain and stress of steel transverse reinforcements, respectively. To calculate $f_{l,s}$ by Eq. (6), besides $k_{ff}{}^{PR}$, the reduction factor of $k_{v,s}$ should be determined as an input parameter, which will be presented in Section 4.2. To do not introduce unnecessary complexities in the formulation, the hoop strain of steel confining reinforcement was assumed to be identical to the hoop strain of FRP jacket based on Teng *et al.* [19]'s recommendation.

4.1- Non-homogenous Distribution of Concrete Lateral Expansion

Experimental studies (i.e. Zeng *et al.* [4] and Guo *et al.* [37]) have evidenced that concrete regions between FRP strips (unwrapped zone) in a partially confining system experience a larger dilatancy during axial loading, compared to the wrapped ones as typically illustrated in Fig. 3a. Since the concrete expansion produces FRP confining strain/stress, Shayanfar *et al.* [35] have confirmed that by assuming a homogenous concrete expansibility along the column height in the model ($k_{ff} = 1$, representing the same concrete expansion for the unwrapped and wrapped), the real dilation and axial behavior cannot be correctly predicted, particularly for a partial system with a relatively large s_f.

Shayanfar *et al.* [14] evidenced that $k_{ff}{}^{PR}$ (the ratio of average concrete lateral expansion within the strip zone to the maximum concrete expansion ($\varepsilon_{l,j}$) along the damage zone length (L_d), as illustrated in Fig. 3) is strongly dependent on s_f. For a closely spaced FRP strips, $k_{ff}{}^{PR}$ tends to be similar to $k_{ff}{}^{FR}$, being equal in the case of full confinement ($s_f = 0$). However, for a largely spaced FRP strips ($s_f \geq L_{d0}$, where L_{d0} is the damage zone length of unconfined concrete to be latter determined) with marginal FRP confinement effectiveness, $k_{ff}{}^{PR}$ approaches to $k_\varepsilon{}^{SCR}$ similar to the case of RC columns (SCR: confined only by steel transverse reinforcements). Accordingly, $k_{ff}{}^{PR}$ can be reasonably considered on the interval $\left[k_\varepsilon{}^{SCR}, k_{ff}{}^{FR}\right]$. By assuming $k_{ff}{}^{PR}$ as being linearly dependent of s_f / L_{d0}, it can be expressed as (Fig. 3a):

$$k_{ff}{}^{PR} = k_{ff}{}^{FR} - \left(k_{ff}{}^{FR} - k_\varepsilon{}^{SCR}\right)\frac{s_f}{L_{d0}} \geq k_\varepsilon{}^{SCR} \qquad (7)$$

where L_{d0} can be obtained as suggested by Wu and Wei [38]:

$$0.57 \leq \frac{L_{d0}}{\sqrt{A_g}\psi_f} = 1.71 - 3.53\times10^{-5} A_g \leq 1.36 \qquad (8)$$

$$\psi_f = \frac{6.3}{\sqrt{f_{c0}}} \leq 1 \qquad (9)$$

where A_g is the total area of the section; ψ_f is the calibration factor reflecting the effect of concrete compressive strength in terms of damage zone length of unconfined concrete.

In Eq. (7), k_{ε}^{SCR} is the ratio between the minimum and maximum concrete expansion within L_{d0} in the case of steel-confined RC columns. By decreasing s_s, the concrete lateral expansion tends to be smaller and more-homogenously distributed. Hence, k_{ε}^{SCR} approaches to 1, representing uniform concrete expansion over the column height, for the case with very closely spaced steel transverse reinforcements. However, due to its marginal influence when $s_s \geq L_{d0}$ ([39-42]), k_{ε}^{SCR} can be considered almost 0.08 similar to the case of unconfined concrete, as recommended by Shayanfar *et al.* [15]. Consequently, by assuming k_{ε}^{SCR} on the interval $[0.08,1]$ and a linear relation with s_s/L_{d0}, k_{ε}^{SCR} can be expressed as:

$$k_{\varepsilon}^{SCR} = 1 - 0.92\frac{s_s}{L_{d0}} \geq 0.08 \qquad (10)$$

In Eq. (7), k_{ff}^{FR} is the reduction factor to account for non-uniform confinement along the column height of FR, representing the ratio of average concrete lateral expansion along L_d to the maximum concrete expansion ($\varepsilon_{l,j}$) as illustrated in Fig. 3b. In this figure, I_f^* represents the threshold of FRP-based confinement stiffness above which a uniform distribution for concrete lateral expansion along the column height is assumed. Based on an approximate method with analytical framework, Shayanfar *et al.* [14] proposed a reduction factor (k_{ff}^{FC}) applicable to FC, as a main function of a confinement stiffness index (I_f). In this model, above a certain level of confinement stiffness ($I_f \geq I_f^*$), since strong restrictions are imposed to the concrete deformability, an almost null gradient of concrete expansion along the column height was assumed (representing $k_{ff}^{FC} = 1$), as evidenced experimentally by Wei and Wu [36]. Nonetheless, for lightly-confined concrete ($I_f < I_f^*$), the damage evolution is not uniform ($k_{ff}{}^{FC} < 1$), leading to strain localization due to the lack of sufficient confinement stiffness. In the present study, by extending Shayanfar *et al.* [14]'s model in order to be applicable to the case of FR, $k_{ff}{}^{FR}$ is proposed as (Fig. 3b):

$$k_{ff}{}^{FR} = \frac{1}{3} + \frac{2}{3} k_{\varepsilon}{}^{FR} \tag{11}$$

in which

$$k_{\varepsilon}{}^{FR} = k_{\varepsilon}{}^{SCR} + \left(1 - k_{\varepsilon}{}^{SCR}\right)\left[2\frac{I_f}{I_f^*} - \left(\frac{I_f}{I_f^*}\right)^2\right] \le 1 \qquad \text{for } I_f \le I_f^* \tag{12a}$$

$$k_{\varepsilon}{}^{FR} = 1 \qquad \text{for } I_f \ge I_f^* \tag{12b}$$

with

$$I_f^* = 0.06 + 0.0005 f_{c0} \tag{13}$$

$$I_f = \frac{K_{Lc}\varepsilon_{c0}}{f_{c0}} \tag{14}$$

where I_f is the FRP confinement stiffness index; I_f^* is the threshold above which $k_{ff}{}^{FR} = k_{\varepsilon}{}^{FR} = 1$; $k_{\varepsilon}{}^{FR}$ is the ratio between the minimum and the maximum concrete expansion along L_d in a FR. As a result, by calculating $k_{\varepsilon}{}^{SCR}$, $k_{\varepsilon}{}^{FR}$ and $k_{ff}{}^{FR}$ by Eqs. (10), (12) and (11), respectively, $k_{ff}{}^{PR}$ for the case of partially imposed confinement on RC column can be calculated by Eq. (7). The dominance degree of $k_{ff}{}^{PR}$ in $f_{l,f}$ and $f_{l,s}$ is strongly dependent on steel hoop/spiral and FRP spacing (s_s/L_{d0} and s_f/L_{d0}) and FRP confinement stiffness (I_f). Accordingly, for the case of well-confined RC columns ($I_f \geq I_f^*$) with closely spaced steel hoop/spiral and FRP strips, k_{ff}^{PR} tends to be equal to one, representing a uniform concrete expansion distribution over the column height.

It is noteworthy that for the case of FR/ PR with $s_s \geq L_{d0}$, Eq. (10) provides $k_{\varepsilon}^{SCR} = 0.08$, and the equations for determining k_{ff}^{PR} (Eq. (7)) and k_{ff}^{FR} (Eq. (11)) degenerate on those proposed by Shayanfar *et al.* [14] for FC/PC. It confirms the unified character of the extended model developed for FR/PR with FC/PC.

4.2- Vertical Arching Action

Due to vertical arching action, the concrete regions of a partially confined column can be distinguished in two distinct confined areas: i) effective confinement area, and ii) ineffective confinement area, as illustrated in Fig. 4. In order the entire cross-section area at transverse and longitudinal directions could be considered as a uniformly confined concrete volume, an effective confinement pressure is used by applying a reduction factor, k_v, to the confinement pressure.

Considering the effect of vertical arching action for the case of FRP partial confinement (Fig. 4a), Shayanfar *et al.* [15] proposed a new formulation to calculate $k_{v,f}$ as follows:

$$k_{v,f} = \frac{w_f + s_f\left(1 - \frac{s_f}{D} + 0.43\left(\frac{s_f}{D}\right)^2 - 0.07\left(\frac{s_f}{D}\right)^3\right)}{w_f + s_f} \tag{15}$$

which can be conveniently simplified to:

$$k_{v,f} = \frac{w_f + s_f \exp\left(-0.98 R_f\right)}{w_f + s_f} \leq 1 \tag{16}$$

where

$$R_f = \frac{s_f}{D} \tag{17}$$

For the case of steel-confined concrete (as a partial confinement system), a reduction factor $k_{v,s}$, reflecting the influence of vertical arching action (Fig. 4b), can be determined following the same principles adopted in the development of Eq. (16) resulting

$$k_{v,s} = C_{shc} \exp\left(-0.98R_s\right) \le 1 \tag{18}$$

where

$$R_s = \frac{s_s}{D_c} \tag{19a}$$

$$C_{shc} = \begin{cases} 1 + 0.84R_s & \text{for steel spirals} \\ 1 & \text{for steel hoops} \end{cases} \tag{19b}$$

The equation of C_{shc} parameter was derived based on Mander *et al.* [13] ($k_{v,s} = 1 - R_s/2$ and $k_{v,s} = \left(1 - R_s/2\right)^2$ for spiral and hoop cases, respectively).

As a result, by using $k_{v,f}$, $k_{v,s}$ and k_{ff}^{PR} by Eqs. (16), (18) and (7), the equivalent confinement pressures generated by FRP jacket and steel transverse reinforcements at a given $\varepsilon_{l,j}$ can be calculated by Eqs. (4) and (6), respectively.

5- Dilation Model of FR/PR

The methodology for determining the dilation response of FR and PR during axial compressive loading is addressed in this section. For the case of FC, the initial transversal expansion of the confined concrete is almost the same of unconfined one of same strength class. However, above a certain axial compressive deformation, which depends on the concrete strength class, the micro defects in the concrete microstructure degenerate in meso-defects, and the lateral concrete expansion start increase significantly, which is reflected in the pronounced increase of the Poisson's ratio and a transition zone starts being visible as shown in Fig. 5 (discussed in detail later). The magnitude of concrete expansion rate is dependent on the stiffness of the confinement systems. With the degeneration of meso- into macro-defects, the concrete experiences its maximum expansion rate, which is followed by a descending trend with a lower dilatancy. Further information about the influence of the confinement on dilation behavior of FC under compression can be found in [43-48].

To highlight the influence of steel confining hoops on dilation characteristics of FR, the dilation results obtained from the experimental study conducted by Wang *et al.* [5] for the cases of FR and FC are compared in Fig. 5. For this purpose, the test specimens of C2H0L1 (FC) and C2H1L1 (FR), fully confined by one layer of CFRP jacket, were selected. For C2H1L1, the distance between steel hoops was reported as 120 mm ($R_s = 0.71$). As can be seen in Fig. 5a, beyond the transition zone, at a certain level of axial strain (ε_c), the concrete lateral expansion ($\varepsilon_{l,j}$) of FC was larger than that of FR. Based on the volumetric strain ($\varepsilon_v = \varepsilon_c - 2\varepsilon_{l,j}$) versus ε_c relation presented in Fig. 5b, FC developed a larger volumetric expansion due to the higher increase of concrete lateral expansibility, compared to FR. Fig. 5c presents the relation between the secant Poisson's ratio ($\nu_s = \varepsilon_{l,j} / \varepsilon_c$; positive values are considered for both strain components) and ε_c, which confirms a smaller dilation response of FR with a lower maximum concrete secant Poisson's ratio ($\nu_{s,\max}$) than that of FC.

To predict the lateral strain versus the axial strain of FRP confined concrete, several models have been proposed (i.e. [15, 19, 43-48]). In the present study, the well-calibrated dilation model conducted by Teng *et al.* [19], developed for circular RC columns with full confinement arrangements (FR), having a unified character for FC, will be, hereafter, adapted for being applicable to FRP-based partial confinement arrangements. In this model, the average axial strain along the column height (ε_c) at a certain level of $\varepsilon_{l,j}$ can be obtained from:

$$\varepsilon_c = 0.85\varepsilon_{c0}F_T\left\{\left[1+0.75\left(\frac{\varepsilon_{l,j}}{\varepsilon_{c0}}\right)\right]^{0.7} - \exp\left[-7\left(\frac{\varepsilon_{l,j}}{\varepsilon_{c0}}\right)\right]\right\} \tag{20}$$

in which

$$F_T = 1+8\frac{f_{l,f}}{f_{c0}}+\alpha\frac{f_{l,s}}{f_{c0}} \tag{21}$$

$$\alpha = 1.59+15.1\rho_{FS} \tag{22}$$

$$\rho_{FS} = \frac{K_{Lat}^{FRP}}{K_{Lat}^{Steel}} = \frac{n_f t_f E_f s_s D_c}{k_{v,s}E_s A_{st} D} = \frac{K_{Lc}s_s D_c}{2k_{v,s}E_s A_{st}} \quad \text{for FC/FR} \tag{23a}$$

$$\rho_{FS} = \frac{k_{v,f}K_{Lc}s_s D_c}{2k_{v,s}E_s A_{st}}\left(\frac{w_f}{w_f+s_f}\right) \quad \text{for PC/PR} \tag{23b}$$

where ρ_{FS} is the ratio between the confinement stiffness of the FRP jacket and steel confining systems; F_T is the term reflecting the influence of the combined confinement from FRP jacket and steel transverse reinforcements on concrete dilation behavior. Note that in the present study, Eq. (23b) was derived/extended for the case of partial confinement based on the approach used for Eq. (23a) ($\rho_{FS} = K_{Lat}^{FRP}/K_{Lat}^{Steel}$). It is clear that the maximum secant Poisson's ratio ($\nu_{s,\max} = \left(\varepsilon_{l,j}/\varepsilon_c\right)_{\max}$

) cannot be directly determined from Eq. (20). Since the secant Poisson's ratio (v_s as the ratio of hoop/lateral strain and axial strain) must be lower than $v_{s,\max}$ during axial compressive loading ($v_s \le v_{s,\max}$), the axial strain (ε_c) obtained from Eq. (20) should be consequently higher than $\varepsilon_{l,j}/v_{s,\max}$, as a threshold. On the other hand, for the case of partial confining systems, since the concrete regions between FRP strips of PC/PR (unwrapped zone) are indirectly subjected to a certain confinement pressure, more damage-induced axial deformation would be expected, compared to FC/FR, depending on s_f, as evidenced by [2-4, 49-51]. Accordingly, to simulate the dilation response of PC/PR, the preliminary evaluations using Eq. (20), exclusively developed for FC/FR, revealed that this model would result in misleading predictions. Consequently, based on the aforementioned discussion, in the present study, the dilation model developed by Teng *et al.* [19] was extended to the case of PC/PR as follows:

$$\varepsilon_c = 0.85\varepsilon_{c0}F_T\left\{\left[1+0.75\beta\frac{\varepsilon_{l,j}}{\varepsilon_{c0}}\right]^{0.7} - \exp\left[-7\beta\frac{\varepsilon_{l,j}}{\varepsilon_{c0}}\right]\right\} + \Delta_{\varepsilon c} \ge \frac{\varepsilon_{l,j}}{v_{s,\max}} \tag{24}$$

in which

$$\beta = 1-5\left(1-k_\varepsilon^{PR}\right)\frac{s_f}{L_{d0}} \ge k_\varepsilon^{PR} \tag{25}$$

$$k_\varepsilon^{PR} = k_\varepsilon^{FR} - \left(k_\varepsilon^{FR} - k_\varepsilon^{SCR}\right)\frac{s_f}{L_{d0}} \ge k_\varepsilon^{SCR} \tag{26}$$

$$v_{s,\max} = \frac{0.256}{\left(1+\frac{L_{d0}}{D}\right)\sqrt{\rho_{K,T}}} \tag{27}$$

$$\rho_{K,T} = \left(\frac{f_{l,T}}{f_{c0}}\right)\frac{\varepsilon_{c0}}{\varepsilon_{l,j}} = \left(\frac{f_{l,f}}{f_{c0}} + \frac{D_c f_{l,s}}{D f_{c0}}\right)\frac{\varepsilon_{c0}}{\varepsilon_{l,j}} \tag{28}$$

where β reflects the influence of non-uniform distribution of concrete expansion along the column height, which is equal to 1 for the case of full confinement. k_{ε}^{PR} is the ratio between the minimum and the maximum concrete expansion, which was derived based on the approach adopted for developing k_{ff}^{PR} (Eq. (7) as also shown in Fig. 3a) due to the similarity of concepts. In Eq. (24), $\Delta_{\varepsilon c}$ is the calibration term representing the influence of the additional axial strain for PC/PR, compared to FC/FR; $v_{s,\max}$ defines the maximum secant Poisson's ratio, which was proposed by Shayanfar *et al.* [35] having a unified character for both cases of full and partial FRP arrangements. It is noted that in Eq. (28), total confinement pressure ($f_{l,T}$) acting on the entire cross-section imposed by FRP jacket (on the entire cross-section with D) and steel jacket (on the concrete core with D_c) was derived based on the equilibrium of lateral forces in the entire cross-section with D diameter.

To develop $\Delta_{\varepsilon c}$, by assuming $\varepsilon_{l,i}$ and $\varepsilon_{l,j}$ as the concrete lateral expansion at the strip mid-plane and at mid-height between two consecutive strips, the following expression was empirically suggested as $\Delta_{\varepsilon c} = A_1\left(\varepsilon_{l,j} - \varepsilon_{l,i}\right)^{A_2}$ where A_1 and A_2 are calibration factors. To minimize the complexity of this expression, $\Delta_{\varepsilon c}$ was rearranged by considering $\varepsilon_{l,i}/\varepsilon_{l,j} = 1 - 0.92\, s_f / L_{d,0}$ as recommended by [15], resulting:

$$\Delta_{\varepsilon c} = A_1\left(\varepsilon_{l,j} - \varepsilon_{l,i}\right)^{A_2} = A_1\left(\varepsilon_{l,j} - \left(1 - 0.92\frac{s_f}{L_{d,0}}\right)\varepsilon_{l,j}\right)^{A_2} = A_1\left(0.92\frac{s_f \varepsilon_{l,j}}{L_{d,0}}\right)^{A_2} \tag{29}$$

A regression analysis was performed to achieve the best-fit values for A_1 and A_2 based on 92 test specimens of PC and PR conducted by Barros and Ferreira [11], Zeng *et al.* [3, 4, 51] and Guo *et al.* [37]. It is noteworthy that the experimental values of A_1 and A_2 were derived by trial-and-error procedure in such a way that full range lateral strain versus axial strain curves predicted by the developed dilation model could virtually coincide with those of the experimental relations. Based on a preliminary regression analysis, A_1 and A_2 were determined equal to 0.085 and 0.65, respectively. It was, however, verified that considering the influence of FRP confinement stiffness and $R_f = s_f / D$ on the evaluation of A_1, a better prediction of $\Delta_{\varepsilon c}$ was obtained, therefore the following equation was determined:

$$A_1 = \frac{0.0048}{\exp\left(1.75 R_f\right)} \left(\frac{K_{Lc}}{f_{c0}} \right)^{0.9} \tag{30}$$

Hence, $\Delta_{\varepsilon c}$ was proposed as

$$\Delta_{\varepsilon c} = A_1 \left(\varepsilon_{l,j} - \varepsilon_{l,i} \right)^{A_2} \simeq 0.0045 e^{-1.75 R_f} \left(\frac{K_{Lc}}{f_{c0}} \right)^{0.9} \left(\frac{s_f \varepsilon_{l,j}}{L_{d,0}} \right)^{0.65} \tag{31}$$

where $\Delta_{\varepsilon c} = 0$ for the cases of FC and FR. Fig. 6 demonstrates the predictive performance of Eq. (31). It can be seen that the calibration factor of A_1 has a good agreement with experimental counterparts.

Fig. 7 compares the existing approach and that proposed in the present study in the establishment of dilation response of PC based on experimental tests conducted by Zeng *et al.* [3]. For this purpose, the model proposed by Teng *et al.* [19] (developed exclusively for the case of full confinement) was selected as the representative of existing approaches, where the original concept of confinement efficiency factor ($k_{v,f} = \left[1 - s_f / 2D\right]^2$, suggested by Mander *et al.* [13]) was adopted to generalize this model for the case of partial confinement (presented in Appendix A). It is noteworthy that the hoop strain in FRP strip in Teng *et al.* [19]'s model is equal to $\varepsilon_{l,j}$ representing the assumption of uniform distribution of concrete expansion along the column height ($k_\varepsilon{}^{PC} = 1$). However, in the present study, FRP hoop strain is considered $k_\varepsilon{}^{PC}\varepsilon_{l,j}$ (or $k_\varepsilon{}^{PR}\varepsilon_{l,j}$ in the case of PR). As can be seen in Fig. 7, the initial dilation responses obtained from the developed model and the generalized Teng *et al.* [19]'s model were almost identical. However, as shown in Fig. 7a, beyond the transition zone, at a certain level of ε_c, the generalized Teng *et al.* [19]'s model resulted in significant overestimates in the prediction of the corresponding FRP hoop strain, compared to the experimental records, which were captured correctly by the developed dilation model. Fig. 7b shows that the generalized Teng *et al.* [19]'s model overestimates $v_{s,\max}$ and is not able to accurately simulate v_s versus ε_c, while a suitable agreement is observed between the responses registered experimentally and obtained with the developed dilation model. Furthermore, the ε_c versus ε_v relations presented in Fig. 7c demonstrate that the developed dilation model is capable of simulating more closely the ε_c-ε_v response registered experimentally than the generalized Teng *et al.* [19]'s model.

For further evaluation of the developed dilation model, Fig. 8 and Fig. 9 compare experimental lateral strain versus axial strain curves of PC and PR with different confinement arrangements reported by Barros and Ferreira [11], Zeng *et al.* [3, 51], Guo *et al.* [37] with those obtained from the proposed model and the generalized Teng *et al.* [19]'s model. It can be seen, the generalized Teng *et al.* [19]'s model predicts non-conservatively the experimental dilation responses of PC and PR, which consequently overestimates the confinement pressure generated by FRP strips. The suitable predictive performance of the developed dilation model validates its reliability to simulate experimental lateral strain versus axial strain curves, working for both PC and PR.

6- Axial Stress-strain Model of FR/PR

This section establishes the axial stress (f_c) versus axial strain (ε_c) relationship for FR/PR. Under axial loading, the compressive load carried by the entire cross-section of FR/PR can be comprised of three distinct parts: i) the load carried by concrete cover area subjected to only FRP confinement, ii) the load carried by concrete core area under the combined confinement from steel transverse reinforcements and FRP jacket, and iii) the load carried by steel longitudinal bars. Accordingly, at a given axial strain (ε_c), the corresponding average axial load (N) can be expressed as:

$$N = f_c^{Core} A_c + f_c^{Cover}\left(A_g - A_c\right) + f_{sl} A_{slb} \tag{32}$$

in which

$$f_{sl} = E_{sl}\varepsilon_c \le f_{yl} \tag{33}$$

where f_c^{Core} and f_c^{Cover} are the axial stress acting on the concrete core and cover areas, respectively; A_g is the total area of the concrete section; A_c is the total area of the concrete core; A_{slb} is the total cross-section area of steel longitudinal bars; f_{sl} is the axial stress of steel longitudinal bars corresponding to ε_c; E_{sl} and f_{yl} are the elasticity modulus and yield stress of steel longitudinal bars, respectively. Accordingly, by calculating f_c^{Core} and f_c^{Cover} for a range of ε_c, not only can the axial stress-strain relations of the concrete core and cover areas be found, but also the axial load (N) versus axial strain relation of FR/PR can be calculated using Eq. (32).

421 In this study, the well- known concept of '*Active Confinement Approach*' was adopted to determine the axial responses of f_c^{Core} and f_c^{Cover} of FR/PR subjected to different confinement pressures. The axial response of FRP confined concrete (passive confinement) is derived based on an axial stress-strain base relation model originally developed for actively-confined concrete, by modifying its failure surface function to make it applicable to passively-confined ones [14, 19, 35, 53-56]. By following the axial stress-strain base relation model suggested by Popovics [32], at a given ε_c, f_c^{Core} carried by concrete core area under $f_{l,f}$ and $f_{l,s}$ can be obtained as

$$f_c^{Core} = f_{cc}^{Core} \frac{\left(\varepsilon_c / \varepsilon_{cc}^{Core}\right) n_1}{n_1 - 1 + \left(\varepsilon_c / \varepsilon_{cc}^{Core}\right)^{n_1}} \tag{34}$$

in which

$$\frac{\varepsilon_{cc}^{Core}}{\varepsilon_{c0}} = 1 + 5\left[\frac{f_{cc}^{Core}}{f_{c0}} - 1\right] \tag{35}$$

$$n_1 = \frac{E_c}{E_c - f_{cc}^{Core} / \varepsilon_{cc}^{Core}} \simeq \frac{1}{1 - 0.27 f_{c0}^{0.25}\left(1 - \alpha_1\right)} \tag{36}$$

$$\alpha_1 = 1.15 f_{c0}^{-0.1}\left(\frac{f_{l,f} + f_{l,s}}{f_{c0}}\right)^{0.4} \leq 0.85 \tag{37}$$

where f_{cc}^{Core} is the failure surface function as the peak axial stress of the axial stress-strain base relation of the confined (by steel transverse reinforcement and FRP) concrete core; ε_{cc}^{Core} is the axial strain corresponding to f_{cc}^{Core} to be determined using Eq. (35) recommended by Mander *et al.* [13]; n_1 introduces the concrete brittleness term that can be calculated using the recommendation of Carreira and Chu [52] by Eq. (36) (with a slight rearrangement); E_c defines the elasticity modulus of concrete.

Similarly, for the case of the concrete cover, the axial stress-strain base relation model can be expressed by

$$f_c^{Cover} = f_{cc}^{Cover} \frac{\left(\varepsilon_c / \varepsilon_{cc}^{Cover}\right) n_2}{n_2 - 1 + \left(\varepsilon_c / \varepsilon_{cc}^{Cover}\right)^{n_2}} \tag{38}$$

in which

$$\frac{\varepsilon_{cc}^{Cover}}{\varepsilon_{c0}} = 1 + 5\left[\frac{f_{cc}^{Cover}}{f_{c0}} - 1\right] \tag{39}$$

$$n_2 = \frac{1}{1 - 0.27 f_{c0}^{0.25}\left(1 - \alpha_2\right)} \tag{40}$$

$$\alpha_2 = 1.15 f_{c0}^{-0.1}\left(\frac{f_{l,f}}{f_{c0}}\right)^{0.4} \leq 0.85 \tag{41}$$

where f_{cc}^{Cover} is the failure surface function as the peak axial stress of the axial stress-strain base relation of the confined (by FRP) concrete cover; ε_{cc}^{Cover} is the axial strain corresponding to f_{cc}^{Cover}; n_2 introduces the brittleness term of the concrete cover. According to Eqs. (34-41), to calculate the axial stress-strain relations of the concrete core and cover areas (f_c^{Core} versus ε_c curve, and f_c^{Cover} versus ε_c curve), f_{cc}^{Core} and f_{cc}^{Cover} as failure surface functions are required to be determined as input parameters.

It is now well-known that at the same level of confinement pressure, there is a remarkable difference in the level of enhancements provided by passively- and actively-confinement systems in which the confinement pressure is varying and constant, respectively, during axial loading. According to the studies conducted by Lai *et al.* [57, 58] and Ho et al. [59], the confinement path effect (Φ) can be computed quantitatively as the difference of the peak strength obtained from the failure surface functions of passively- and actively-confined concrete ($f_{cc}^{Passive}$ and f_{cc}^{Active}, respectively). Hence, Φ can be calculated by $\Phi = f_{cc}^{Passive} - f_{cc}^{Active}$ where $\Phi < 0$ reveals that confinement-induced enhancements in a passively-confined concrete is less than those in an actively-confined concrete system. Studies [14, 35, 56-59] evidenced that by using a failure surface function (f_{cc}^{Active}) derived/calibrated based on actively-confined concrete columns, the enhancements offered by a passive confinement system (as confinement path-dependent) are overestimated, due to the significant difference of their confinement pressure paths ($\Phi < 0$). This phenomenon has been evaluated comprehensively in Lai *et al.* [57, 58], Ho *et al.* [59] and Shayanfar *et al.* [14, 35].

In the present study, the confinement stiffness-based failure surface function recommended by Shayanfar *et al.* [14], calibrated based on a large test database of both FC and PC (passively-confined concrete columns), was adopted. Accordingly, f_{cc}^{Core} and f_{cc}^{Cover} can be calculated as:

$$\frac{f_{cc}^{Core}}{f_{c0}} = 1 + \frac{R_1}{R_2}\left(\frac{f_{l,f} + f_{l,s}}{f_{c0}}\right)^{R_2} \tag{42}$$

$$\frac{f_{cc}^{Cover}}{f_{c0}} = 1 + \frac{R_1}{R_2}\left(\frac{f_{l,f}}{f_{c0}}\right)^{R_2} \tag{43}$$

where R_1 and R_2 are the calibration terms. It should be noted that since the confinement pressure generated by steel transverse reinforcements ($f_{l,s}$) remains constant beyond steel yielding, the application of a failure surface function developed exclusively for passively-confined concrete might lead to underestimation in the calculation of the improvements induced by dual confinement mechanism of steel transverse reinforcements and FRP jacket ([56]). However, in this study, in a slight conservative manner, the effect of steel confinement on the determination of R_1 and R_2 was ignored, which can be considered practically correct for the case of RC columns with largely spaced steel transverse reinforcements due to its negligible effectiveness. Accordingly, by following the Shayanfar *et al.* [14]'recommendations, R_1 and R_2 can be calculated as (with a slight modification):

$$R_1 = \frac{24\rho_{K,f}^{\ 0.67}}{\lambda_{fc}\lambda_{Rf}} \leq 4.25 \qquad (44)$$

$$R_2 = 1.82\rho_{K,f}^{\ 0.26} \geq 0.3 \qquad (45)$$

in which

$$\rho_{K,f} = \frac{f_{l,f}\varepsilon_{c0}}{f_{c0}\varepsilon_{l,j}} = k_{v,f} k_{ff}^{\ PR} \frac{K_{Lc} w_f \varepsilon_{c0}}{\left(w_f + s_f\right) f_{c0}} \qquad (46)$$

$$\lambda_{fc} = 0.75 + 0.008 f_{c0} \qquad (47)$$

$$\lambda_{Rf} = 1 + 0.15 R_f^{\ 0.25} \qquad (48)$$

where $\rho_{K,f}$ represents FRP confinement stiffness that considers the effect of non-homogenous distribution of concrete expansibility through $k_{ff}^{\ PR}$ in addition to vertical arching action ($k_{v,f}$) and FRP volumetric ratio in a partial confinement system (the term of $w_f / \left(w_f + s_f\right)$); λ_{fc} and λ_{Rf} are the partial calibration factors representing the impact of f_{c0} and R_f on R_1, respectively.

It should be noted that a lag between the axial strain development and confining strain/stress generation occurs with the increase of the concrete compressive strength (f_{c0}) due to the decrease of its lateral deformation [57-59]. Consequently, more confinement-induced enhancements would be achieved with the decrease of the concrete compressive strength class, which was reflected in the development of the proposed failure surface function through the consideration of the calibration term of λ_{fc} as a reduction factor for R_1. On the other hand, the dilation model developed in the present study for PR differs from that used by Shayanfar *et al.* [14] applicable to PC. Accordingly, since the dilation model has a significant influence on the confinement pressure and is coupled to the axial stress-strain relation, in this study, λ_{Rf} (Eq. (48)) was recalibrated based on regression analysis performed on the experimental axial stress-strain relations of 109 PC and PR specimens to ensure its reliability. The experimental values of λ_{Rf} were derived by trial-and-error procedure in such a way that full range axial stress-strain curves predicted by the developed analysis-oriented model could virtually coincide with those of the experimental relations. Fig. 10 demonstrates the variation of λ_{Rf}^{Exp} with $R_f = s_f / D$. As can be seen, there is an upward trend of λ_{Rf}^{Exp} by increasing R_f. Furthermore, Eq. (48) has a good agreement with experimental counterparts.

As a result, by calculating R_1 and R_2 by Eqs. (44) and (45), f_{cc}^{Core} and f_{cc}^{Cover} can be determined using Eqs. (42) and (43), respectively. Then, based on Eqs. (34) to (37) and Eqs. (38) to (41), the f_c^{Core} and f_c^{Cover} corresponding to ε_c are obtained, respectively. The incremental calculation process for determining the axial stress-strain response of FR/PR based on the developed analysis-oriented model is the following one:

1) Calculate k_{ff}^{PR} with Eq. (7)

2) Calculate $k_{v,f}$ with Eq. (16)

3) Calculate $k_{v,s}$ with Eq. (18)

4) Assume a value of concrete lateral strain ($\varepsilon_{l,j}$)

5) Calculate FRP confinement pressure ($f_{l,f}$) by Eq. (4)

6) Calculate steel confinement pressure ($f_{l,s}$) by Eq. (6)

7) Calculate axial strain (ε_c) by Eq. (24)

8) Calculate failure surface function of the concrete core (f_{cc}^{Core}) by Eq. (42)

9) Calculate failure surface function of the concrete cover (f_{cc}^{Cover}) by Eq. (43)

10) Calculate axial stress (f_c^{Core}) by Eqs. (34) to (37)

11) Calculate axial stress (f_c^{Cover}) by Eqs. (38) to (41)

12) Calculate the average axial load (N) by Eq. (32)

13) Continue the steps 4-12 up to ultimate axial strain

Accordingly, not only can N versus ε_c relation of FR/PR be found, but also f_c^{Core} versus ε_c and f_c^{Cover} versus ε_c relations of the concrete core and cover areas can be calculated.

It should be noted that a more reliable model could be always conducted by regression analysis through providing a comprehensive dataset having a broader range of the model variables. According to the database used to develop/calibrate Eqs. (42) and (43), concrete strength variable (f_{c0}) varies from 16 to 171 MPa with the mean and CoV values equal to 40 MPa and 0.53, respectively; confinement stiffness of the external jacket ($\rho_{K,f}$) has a range of 0.002 to 0.262 with the mean and CoV values equal to 0.037 and 0.85, respectively; column's diameter to total FRP's thickness ratio ($D/n_f t_f$) varies in the range of 40 to 1796 with mean and CoV values equal to 166 and 0.26, respectively; column aspect ratio (L/D) is in the range of 2 to 5 with mean and CoV values equal to 2.09 and 0.2, respectively. Accordingly, the proposed model is limited to the aforementioned range of the variables covered by the assembled database.

Studies [60-62] evidenced that slenderness effects have a detrimental influence on the load carrying and deformability capacity of FRP confined concrete/RC columns, leading to an underutilization of the FRP confinement potentialities and the necessity of considering the column buckling. However, in the present stage of the research program, the applicability of the developed model was only validated to the aforementioned interval of the relevant variables that govern the response of fully/partially FRP confined concrete/RC columns, and do not cover the cases where buckling is a design concern. Nevertheless, by developing the slenderness limit and its relative reduction factors in terms of load carrying and deformability capacity, the methodology proposed in the present work can be potentially extended to slender FRP confined RC columns, which will be the focus of a future study.

7- Model Validation

This section presents the verification of the proposed model to predict the axial and dilation responses of FR/PR under axial compressive loading. For this purpose, the results obtained from the developed analysis-oriented model were compared with those measured experimentally by [5-8, 11]. Furthermore, for the case of comparative assessment, the well-established model suggested by Teng *et al.* [19], developed exclusively for fully FRP confined circular columns, was selected and generalized for the case of partial confinement strategy based on the concept of confinement efficiency factor (Mander *et al.* 1988 as one of the most-cited approach). The generalized model of Teng *et al.* [19] can be found in Appendix A.

Fig. 11 compares the axial force(N)/stress ($f_c = N/A_g$)/versus axial strain (ε_c) curves of FR and PR obtained from the proposed model with those conducted experimentally by Barros and Ferreira [11], Eid *et al.* [8], and Wang *et al.* [5]. As shown in Fig. 11a, the developed model is able to predict accurately the global axial stress-strain curves of the FR specimens with the different values of R_s. In Fig. 11b-c, the developed model reveals efficient capability in simulating the experimental responses of FR with different values of f_{c0}, and with/without concrete cover, even though the initial axial behavior was underestimated slightly (in Fig. 11c, C2MP2N and C2N1P2N specimens were constructed without concrete cover). The comparisons in Fig. 11d-e demonstrate that the model is able to capture sufficiently the influence of FRP confining system on the axial stress-strain curves of FR and PR, regardless an underestimation associated with FL3S2C32. In Fig. 11f, a suitable performance of the developed model for the case of PR with the different values of R_f can be confirmed.

Fig. 12 and Fig. 13 compare the axial stress/force-strain curves of PR and FR obtained from the proposed model and the generalized Teng *et al.* [19]'s model with those conducted experimentally by Wang *et al.* [5], Kaeseberg *et al.* [6], Chastre and Silva [7], Eid *et al.* [8], and Barros and Ferreira [11]. In general, the developed model is able to predict closely the full range of the experimental counterparts. Furthermore, compared to the generalized Teng *et al.* [19]'s model, the developed model reveals a better predictive performance in terms of axial behavior of PR and FR with different types of confining arrangement.

For the further examination of the developed model in terms of axial and dilation responses, the axial stress versus volumetric strain (ε_v) curves of PC specimens reported by Barros and Ferreira [11] were simulated by the proposed model and the generalized Teng *et al.* [19]'s model, as shown in Fig. 14. Note that ε_v in this figure represents the concrete volumetric strain at the mid-plane of FRP strips during axial compressive loading. As can be seen, the developed model is capable of simulating closely the experimental volumetric variation. It is mainly attributable to the consideration of the effect of non-homogenous distribution of concrete lateral expansion along the height of PR in the developed model. By using Teng *et al.* [19]'s generalized model based on the concept of confinement efficiency factor suggested by Mander *et al.* [13], exclusively devoted to steel-confined RC columns, misleading predictions are obtained in terms of volumetric change evolutions.

The comparative assessment demonstrated in Figs. 11-14 not only evidences the reliability of the proposed analysis-oriented model for the prediction of axial and dilation behavior of FR and PR, but also confirms the validity of the conducted assumptions in the consideration of the effects of dual confinement mechanism of steel transverse reinforcements and FRP full/partial arrangement. Furthermore, the proposed model has a unified character for the case of FRP confined concrete (FC and PC) confirming its wide applicability.

Lastly, using the proposed model analysis on PR, Fig. 15 evaluates the dependence of FRP-steel confinement-induced enhancements on the distance between steel hoops (s_s), the distance between FRP strips (s_f) and the concrete compressive strength (f_{c0}). In this parametric study, an RC column with a diameter and height of 200 and 1000 mm was assumed. The data for the parameters of FRP confinement configuration were $n_f = 5$, $t_f = 0.167$ mm, $E_f = 249$ GPa and $w_f = 50$ mm

, while for the parameters of steel hoops were $d_{sth} = 6$ mm, $f_{yh} = 400$ MPa, $E_s = 200$ GPa. Furthermore, for the case of the parameters of steel longitudinal reinforcements, the data were $d_{sth} = 10$ mm, $f_{yl} = 400$ MPa, $E_{sl} = 200$ GPa. The concrete cover was considered 25 mm. Fig. 15a reveals the effect of s_s on the normalized concrete axial stress (f_c^{ave}/f_{c0}) versus ε_v relation of PR with $R_f = s_f/D = 0.4$ and $f_{c0} = 25$ MPa, where f_c^{ave} represents the area-weighted average axial stress carried by concrete core and cover areas. As can be seen, while s_s decreases from 150 mm to 50 mm, the volumetric change evolution tends to be reversed resulting in a higher axial strength and smaller volumetric expansion. It highlights the influence of steel hoop confinement in limiting the concrete tendency for an abrupt expansion. Similarly, as shown in Fig. 15b, for the case of PR with $s_s = 100$ mm and $f_{c0} = 25$ MPa, by decreasing R_f, the response changes from volumetric expansion to volumetric compaction, indicating a remarkable increase in FRP effectiveness in restraining concrete lateral dilation. In Fig. 15c-d, shows the effects of steel hoop and FRP spacing on f_c^{ave}/f_{c0} versus ε_v relation of PR with a higher concrete compressive strength ($f_{c0} = 50$ MPa). As can be seen, FRP-steel confinement induced enhancements in the case of $f_{c0} = 50$ MPa are not so pronounced compared to those in the case of $f_{c0} = 25$ MPa (Fig. 15c-d), mainly attributable to smaller lateral deformations and a longer lag between the axial strain development and the confining strain/stress generation for higher strength concrete.

8- Summary and conclusions

In the present study, a generalized analysis-oriented model was developed for determining the axial compressive stress-strain relationship for circular cross-section RC columns of fully and partially confined with FRP systems and also including transverse steel reinforcements (FR and

PR, respectively). To derive the equivalent confinement pressures imposed by FRP jacket and steel transverse reinforcements, the effects of non-homogenous concrete transverse expansion along the column height and the vertical arching action were considered. An already existing dilation model was extended to the cases with partially imposed confinement pressure and dual FRP-steel confinement mechanism. With this information, a unified axial stress-strain model was developed for the establishment of the axial stress-strain relations of FR and PR. A comprehensive comparison to axial responses registered experimentally in available literature demonstrated that the proposed analysis-oriented model has a suitable agreement with the experimental counterparts. Based on the work presented in the current study, the conclusions can be drawn as follows:

- In contrast to the original concept of confinement efficiency factor, it is found that the consideration of the effect of non-homogenous concrete transverse expansion along the column height is critical to develop a rational and robust model for PC/PR. This consideration led to a significant enhancement in the model performance to simulate accurately axial and dilation responses of PC/PR concrete columns.
- An extended/improved version of Teng et al. (2015)'s dilation model for PC/PR is proposed, which demonstrated a suitable level of reliability for predicting lateral-to-axial strain relation of PC/PR, through addressing the substantial effects of additional axial deformations induced by damage evolution in unwrapped zones, peak Poisson's ratio, and non-homogenous concrete expansion distribution.
- The axial stress versus axial/lateral/volumetric strain relationship of PC/PR and FC/FR can be predicted accurately through the developed analysis-oriented model, consisting of a new confinement stiffness-based failure surface function that addresses the confinement path effect.

- The investigation undertaken in the current study has demonstrated that $R_f = s_f / D$ is the most influencing parameter on the confinement-induced improvements in PC/PR. By decreasing this parameter, the column response would drive from volumetric expansion to volumetric compaction, dependent on the confinement stiffness.
- The methodology adopted for the model development can be taken to recalibrate the key components of this model, resulting in a more reliable model, when more comprehensive databases are available. Furthermore, this methodology can be extended potentially to develop new confinement models for other concrete-type and confining materials, through the recalibration of the failure surface function of the proposed confinement model and its coupled dilation model.

Acknowledgments

This study is a part of the project ‘‘Sticker –Innovative technique for the structural strengthening based on using CFRP laminates with multifunctional attributes and applied with advanced cement adhesives’’, with the reference POCI-01-0247-FEDER-039755. The firs author also acknowledges the support provided by FCT PhD individual fellowship 2019 with the reference of “SFRH/BD/148002/2019”.

Data Availability Statement

All data, models, and code generated or used during the study appear in the submitted article.

References

[1] Lin, S., Zhao, Y. G., Li, J., & Lu, Z. H. (2021). Confining stress path-based compressive strength model of axially loaded FRP-confined columns. Journal of Composites for Construction, 25(1), 04020077.

[2] Wang, W., Martin, P. R., Sheikh, M. N., & Hadi, M. N. (2018). Eccentrically loaded FRP confined concrete with different wrapping schemes. Journal of Composites for Construction, 22(6), 04018056.

[3] Zeng, J. J., Guo, Y. C., Gao, W. Y., Chen, W. P., & Li, L. J. (2018). Stress-strain behavior of concrete in circular concrete columns partially wrapped with FRP strips. Composite Structures, 200, 810-828.

[4] Zeng, J., Guo, Y., Li, L., & Chen, W. (2018). Behavior and three-dimensional finite element modeling of circular concrete columns partially wrapped with FRP strips. Polymers, 10(3), 253.

[5] Wang, Z., Wang, D., Smith, S. T., & Lu, D. (2012). Experimental testing and analytical modeling of CFRP-confined large circular RC columns subjected to cyclic axial compression. Engineering Structures, 40, 64-74.

[6] Kaeseberg, S., Messerer, D., & Holschemacher, K. (2020). Experimental study on concrete under combined FRP–Steel confinement. Materials, 13(20), 4467.

[7] Chastre, C., & Silva, M. A. (2010). Monotonic axial behavior and modelling of RC circular columns confined with CFRP. Engineering Structures, 32(8), 2268-2277.

[8] Eid, R., Roy, N., & Paultre, P. (2009). Normal-and high-strength concrete circular elements wrapped with FRP composites. Journal of composites for construction, 13(2), 113-124.

[9] Yin, P., Huang, L., Yan, L., & Zhu, D. (2016). Compressive behavior of concrete confined by CFRP and transverse spiral reinforcement. Part A: experimental study. Materials and Structures, 49(3), 1001-1011.

[10] Zignago, D., & Barbato, M. (2021). Effects of Transverse Steel on the Axial-Compression Strength of FRP-Confined Reinforced Concrete Columns Based on a Numerical Parametric Study. Journal of Composites for Construction, 25(4), 04021024.

[11] Barros, J. A., & Ferreira, D. R. (2008). Assessing the efficiency of CFRP discrete confinement systems for concrete cylinders. Journal of composites for construction, 12(2), 134-148.

[12] Teng, J., Huang, Y. L., Lam, L., & Ye, L. P. (2007). Theoretical model for fiber-reinforced polymer-confined concrete. Journal of composites for construction, 11(2), 201-210.

[13] Mander, J. B., Priestley, M. J., & Park, R. (1988). Theoretical stress-strain model for confined concrete. Journal of structural engineering, 114(8), 1804-1826.

[14] Shayanfar, J., Barros, J. A., & Rezazadeh, M. (2021). Generalized Analysis-oriented model of FRP confined concrete circular columns. Composite Structures, 270, 114026.

[15] Shayanfar, J., Rezazadeh, M., & Barros, J. A. (2020). Analytical model to predict dilation behavior of FRP confined circular concrete columns subjected to axial compressive loading. Journal of Composites for Construction, 24(6), 04020071.

[16] Pellegrino, C., & Modena, C. (2010). Analytical model for FRP confinement of concrete columns with and without internal steel reinforcement. Journal of Composites for Construction, 14(6), 693-705.

[17] Hu, H., & Seracino, R. (2014). Analytical model for FRP-and-steel-confined circular concrete columns in compression. Journal of Composites for Construction, 18(3), A4013012.

[18] Jiang, T., & Teng, J. G. (2007). Analysis-oriented stress–strain models for FRP–confined concrete. Engineering Structures, 29(11), 2968-2986.

[19] Teng, J. G., Lin, G., & Yu, T. (2015). Analysis-oriented stress-strain model for concrete under combined FRP-steel confinement. Journal of Composites for Construction, 19(5), 04014084.

[20] Jansen, D. C., & Shah, S. P. (1997). Effect of length on compressive strain softening of concrete. Journal of engineering mechanics, 123(1), 25-35.

[21] Yang, K. H., Lee, Y., & Mun, J. H. (2019). A Stress-Strain Model for Unconfined Concrete in Compression considering the Size Effect. Advances in Materials Science and Engineering, 2019.

[22] Watanabe, K., Niwa, J., Yokota, H., & Iwanami, M. (2004). Experimental study on stress-strain curve of concrete considering localized failure in compression. Journal of Advanced Concrete Technology, 2(3), 395-407.

[23] ACI (American Concrete Institute) (2008). "Building code requirements for structural concrete (ACI 318-08) and commentary." ACI 318–08, Detroit.

[24] Bamforth P, Chisholm D, Gibbs J, Harrison T. Properties of Concrete for use in Eurocode 2. Blackwater, Camberley, Surrey, UK: The Concrete Center; 2008. 59 p.

[25] Sim, J. I., Yang, K. H., Kim, H. Y., & Choi, B. J. (2013). Size and shape effects on compressive strength of lightweight concrete. Construction and Building Materials, 38, 854-864.

[26] Bazant ZP, Planas J. Fracture and size effect in concrete and other quasibrittle materials. New York: CRC Press; 1998.

[27] Bazant ZP. Size effect in blunt fracture: concrete, rock, metal. J Eng Mech ASCE 1984;110(4):518–35.

[28] Kim JK, Eo SH. Size effect in concrete specimens with dissimilar initial cracks. Mag Concr Res 1990;42(153):233–8.

[29] Carpinteri, A., Ferro, G., & Monetto, I. (1999). Scale effects in uniaxially compressed concrete specimens. Magazine of Concrete Research, 51(3), 217-225.

[30] Dahl, K. K. B. (1992). "Uniaxial stress-strain curves for normal and high strength concrete." ABK Rep. No. R282, Dept. of Structural Engineering, Technical Univ. of Denmark, Kongens Lyngby, Denmark.

[31] Lim, J. C., & Ozbakkaloglu, T. (2014). Stress–strain model for normal-and light-weight concretes under uniaxial and triaxial compression. Construction and Building Materials, 71, 492-509.

[32] Popovics, S. (1973). A numerical approach to the complete stress-strain curve of concrete. Cement and concrete research, 3(5), 583-599.

[33] Fallahpour, A., Nguyen, G. D., Vincent, T., & Ozbakkaloglu, T. (2020). Investigation of the compressive behavior and failure modes of unconfined and FRP-confined concrete using digital image correlation. Composite Structures, 252, 112642.

[34] Shayanfar, J., Rezazadeh, M., & Barros, J. A. (2021). Theoretical Prediction of Axial Response of FRP Fully/partially Confined Circular Concrete Under Axial Loading. In International Conference on Fibre-Reinforced Polymer (FRP) Composites in Civil Engineering (pp. 1439-1449). Springer, Cham.

[35] Shayanfar, J., Barros, J. A., & Rezazadeh, M. (2022). Unified model for fully and partially FRP confined circular and square concrete columns subjected to axial compression. Engineering Structures, 251, 113355.

[36] Wei, Y., & Wu, Y. F. (2016). Experimental study of concrete columns with localized failure. Journal of Composites for Construction, 20(5), 04016032.

[37] Guo, Y. C., Gao, W. Y., Zeng, J. J., Duan, Z. J., Ni, X. Y., & Peng, K. D. (2019). Compressive behavior of FRP ring-confined concrete in circular columns: Effects of specimen size and a new design-oriented stress-strain model. Construction and Building Materials, 201, 350-368.

[38] Wu, Y. F., & Wei, Y. (2016). Stress–strain modeling of concrete columns with localized failure: An analytical study. Journal of Composites for Construction, 20(3), 04015071.

[39] Razvi, S., & Saatcioglu, M. (1999). Confinement model for high-strength concrete. Journal of Structural Engineering, 125(3), 281-289.

[40] Assa, B., Nishiyama, M., & Watanabe, F. (2001). New approach for modeling confined concrete. I: Circular columns. Journal of Structural Engineering, 127(7), 743-750.

[41] Shayanfar, J., Omidalizadeh, M., & Nematzadeh, M. (2020). Analysis-oriented model for seismic assessment of RC jacket retrofitted columns. Steel and Composite Structures, An International Journal, 37(3), 371-390.

[42] Shayanfar, J., & Akbarzadeh Bengar, H. (2017). Nonlinear analysis of RC frames considering shear behaviour of members under varying axial load. Bulletin of Earthquake Engineering, 15(5), 2055-2078.

[43] Kwan, A. K. H., Dong, C. X., & Ho, J. C. M. (2015). Axial and lateral stress–strain model for FRP confined concrete. Engineering Structures, 99, 285-295.

[44] Dong, C. X., Kwan, A. K. H., & Ho, J. C. M. (2015). A constitutive model for predicting the lateral strain of confined concrete. Engineering Structures, 91, 155-166.

[45] Lai, M., Hanzic, L., & Ho, J. C. (2019). Fillers to improve passing ability of concrete. Structural Concrete, 20(1), 185-197.

[46] Moran, D. A., & Pantelides, C. P. (2012). Elliptical and circular FRP-confined concrete sections: A Mohr–Coulomb analytical model. International Journal of Solids and Structures, 49(6), 881-898.

[47] Lim, J. C., & Ozbakkaloglu, T. (2015). Lateral strain-to-axial strain relationship of confined concrete. Journal of Structural Engineering, 141(5), 04014141.

[48] Shayanfar, J., Rezazadeh, M., Barros, J.A., Ramezansefat H. (2020). A new dilation model for FRP fully/partially confined concrete column under axial loading. The 3RD RILEM Spring Convention 2020 Ambitioning a Sustainable Future for Built Environment: Comprehensive Strategies for Unprecedented Challenges, Guimarães, Portugal.

[49] Yang, J., Wang, J., & Wang, Z. (2020). Axial compressive behavior of partially CFRP confined seawater sea-sand concrete in circular columns–Part I: Experimental study. Composite Structures, 246, 112373.

[50] Yang, J., Wang, Z., & Wang, J. (2022). Compressive Performance of Partially CFRP-Confined Square Seawater–Sea Sand Concrete Columns with Internal Epoxy-Coated Reinforcement. Journal of Composites for Construction, 26(2), 04021073.

[51] Zeng, J. J., Guo, Y. C., Gao, W. Y., Li, J. Z., & Xie, J. H. (2017). Behavior of partially and fully FRP-confined circularized square columns under axial compression. Construction and Building Materials, 152, 319-332.

[52] Carreira and Chu (1985). Stress-strain relationship for plain concrete in compression. In Journal Proceedings 1985;82(6):797–804.

[53] Shayanfar, J., & Akbarzadeh Bengar, H. (2018). A practical model for simulating nonlinear behaviour of FRP strengthened RC beam-column joints. Steel and Composite Structures, An International Journal, 27(1), 49-74.

[54] Nematzadeh, M., Mousavimehr, M., Shayanfar, J., & Omidalizadeh, M. (2021). Eccentric compressive behavior of steel fiber-reinforced RC columns strengthened with CFRP wraps: Experimental investigation and analytical modeling. Engineering Structures, 226, 111389.

[55] Yang, J. Q., & Feng, P. (2020). Analysis-oriented models for FRP-confined concrete: 3D interpretation and general methodology. Engineering Structures, 216, 110749.

[56] Lim, J. C., & Ozbakkaloglu, T. (2014). Unified stress-strain model for FRP and actively confined normal strength and high-strength concrete. Journal of Composites for Construction, 19(4), 04014072.

[57] Lai, M. H., Liang, Y. W., Wang, Q., Ren, F. M., Chen, M. T., & Ho, J. C. M. (2020). A stress-path dependent stress-strain model for FRP-confined concrete. Engineering Structures, 203, 109824.

[58] Lai, M. H., Song, W., Ou, X. L., Chen, M. T., Wang, Q., & Ho, J. C. M. (2020). A path dependent stress-strain model for concrete-filled-steel-tube column. Engineering Structures, 211, 110312.

[59] Ho, J. C. M., Ou, X. L., Chen, M. T., Wang, Q., & Lai, M. H. (2020). A path dependent constitutive model for CFFT column. Engineering Structures, 210, 110367.

[60] Mirmiran, A., Shahawy, M., & Beitleman, T. (2001). Slenderness limit for hybrid FRP-concrete columns. Journal of composites for construction, 5(1), 26-34.

[61] Fitzwilliam, J., & Bisby, L. A. (2010). Slenderness effects on circular CFRP confined reinforced concrete columns. Journal of Composites for Construction, 14(3), 280-288.

[62] Jiang, T., & Teng, J. G. (2013). Behavior and design of slender FRP-confined circular RC columns. Journal of Composites for Construction, 17(4), 443-453.

Appendix A

To determine axial stress versus axial strain curves of FRP fully confined RC columns (FR), Teng *et al.* [19] proposed an analysis-oriented model based on active confinement approach. In the present study, for the generalization of this model for the case of partial confinement arrangement (PR), the original concept of confinement efficiency factor recommended by Mander *et al.* (1988) was adopted.

Based on Teng *et al.* [19]'s model, at a certain level of concrete transverse expansion ($\varepsilon_{l,j}$) representing FRP hoop strain, the corresponding confinement pressures imposed by FRP strips ($f_{l,f}$) and steel transverse reinforcements ($f_{l,s}$) can be calculated as:

For the case of FRP full/partial arrangement:

$$f_{l,f} = 2k_{v,f}\,\frac{n_f t_f w_f}{b\left(s_f + w_f\right)} E_f \varepsilon_{l,j} \qquad \text{B-1}$$

in which

$$k_{v,f} = \left(1 - \frac{s_f}{2D}\right)^2 \qquad \text{B-2}$$

where $k_{v,f}$ is the reduction factor reflecting the effect of vertical arching action between FRP strips; n_f is the number of FRP layers; t_f is the thickness of a FRP layer; E_f is the FRP modulus of elasticity; w_f is the FRP width; s_f is the distance between FRP strips; D is the diameter of the circular cross-section.

For the case of steel transverse reinforcement:

$$f_{l,s} = 2k_{v,s}\frac{A_{sth}}{D_c s_s}E_s\varepsilon_{l,j} \qquad \text{for } \varepsilon_{l,j} < \varepsilon_{yh} \qquad \text{B-3a}$$

$$f_{l,s} = 2k_{v,s}\frac{A_{sth}}{D_c s_s}f_{yh} \qquad \text{for } \varepsilon_{l,j} \geq \varepsilon_{yh} \qquad \text{B-3b}$$

in which

$$k_{v,s} = \left(1 - \frac{s_s}{2D_c}\right)^2 \qquad \text{for steel hoop reinforcement} \qquad \text{B-4a}$$

$$k_{v,s} = \left(1 - \frac{s_s}{2D_c}\right) \qquad \text{for steel spiral reinforcement} \qquad \text{B-4b}$$

where $k_{v,s}$ is the reduction factor reflecting the effect of vertical arching action between reinforcements; D_c is the diameter of the concrete core; A_{sth} is the cross-sectional area of a steel spiral/hoop; s_s is the distance between reinforcements ; E_s , ε_{yh} and f_{yh} are the elasticity modulus, yield strain and stress of reinforcements, respectively. Subsequently, based on the dilation model, the average axial strain along the column height (ε_c) corresponding to $\varepsilon_{l,j}$ can be calculated as:

$$\varepsilon_c = 0.85\varepsilon_{c0}F_T\left\{\left[1+0.75\left(\frac{\varepsilon_{l,j}}{\varepsilon_{c0}}\right)\right]^{0.7} - \exp\left[-7\left(\frac{\varepsilon_{l,j}}{\varepsilon_{c0}}\right)\right]\right\} \qquad \text{B-5}$$

in which

$$F_T = 1 + 8\frac{f_{l,f}}{f_{c0}} + \alpha\frac{f_{l,s}}{f_{c0}} \qquad \text{B-6}$$

$$\alpha = 1.59 + 15.1\rho_{FS} \quad \text{B-7}$$

$$\rho_{FS} = \frac{K_{Lc} s_s D_c}{2k_{v,s} E_s A_{st}} \quad \text{for FR} \quad \text{B-8}$$

$$\rho_{FS} = \frac{k_{v,f} K_{Lc} s_s D_c}{2k_{v,s} E_s A_{st}} \left(\frac{w_f}{w_f + s_f} \right) \quad \text{for PR} \quad \text{B-9}$$

$$\varepsilon_{c0} = 0.000937 f_{c0}^{\ 0.25} \quad \text{B-10}$$

834 where ρ_{FS} is the ratio between the confinement stiffness of the FRP jacket and steel confining

835 systems; ε_{c0} is the axial strain corresponding to f_{c0}. Based on the active confinement approach,

836 the axial stress carried by concrete core area ($f_c^{\ Core}$) corresponding to ε_c can be calculated as

$$f_c^{\ Core} = f_{cc}^{\ Core} \frac{\left(\varepsilon_c / \varepsilon_{cc}^{\ Core} \right) n_1}{n_1 - 1 + \left(\varepsilon_c / \varepsilon_{cc}^{\ Core} \right)^{n_1}} \quad \text{B-11}$$

837 in which

$$\frac{f_{cc}^{\ Core}}{f_{c0}} = 1 + 3.5 \left(\frac{f_{l,f}}{f_{c0}} \right) + 3.12 \left(\frac{f_{l,s}}{f_{c0} \left[1 + 0.202 \rho_{FS}^{\ 0.145} \right]} \right)^{0.736} \quad \text{B-12}$$

$$\frac{\varepsilon_{cc}^{\ Core}}{\varepsilon_{c0}} = 1 + 3.9 \left[\frac{f_{cc}^{\ Core}}{f_{c0}} - 1 \right]^{1.2} \quad \text{B-13}$$

$$n_1 = \frac{E_c}{E_c - f_{cc}^{\ Core} / \varepsilon_{cc}^{\ Core}} \quad \text{B-14}$$

$$E_c = 4730 \sqrt{f_{c0}} \quad \text{B-15}$$

838 where $f_{cc}^{\ Core}$ is the failure surface function as the peak axial stress of the axial stress-strain base

839 relation of the concrete core; $\varepsilon_{cc}^{\ Core}$ is the axial strain corresponding to $f_{cc}^{\ Core}$; n_1 introduces the

concrete brittleness term; E_c defines the elasticity modulus of concrete. Similarly, the axial stress carried by concrete cover area (f_c^{Cover}) corresponding to ε_c can be calculated as

$$f_c^{Cover} = f_{cc}^{Cover} \frac{\left(\varepsilon_c / \varepsilon_{cc}^{Cover}\right) n_2}{n_2 - 1 + \left(\varepsilon_c / \varepsilon_{cc}^{Cover}\right)^{n_2}} \qquad \text{B-16}$$

in which

$$\frac{f_{cc}^{Cover}}{f_{c0}} = 1 + 3.5\left(\frac{f_{l,f}}{f_{c0}}\right) \qquad \text{B-17}$$

$$\frac{\varepsilon_{cc}^{Cover}}{\varepsilon_{c0}} = 1 + 17.5\left(\frac{f_{l,f}}{f_{c0}}\right)^{1.2} \qquad \text{B-18}$$

$$n_2 = \frac{E_c}{E_c - f_{cc}^{Cover} / \varepsilon_{cc}^{Cover}} \qquad \text{B-19}$$

where f_{cc}^{Cover} is the failure surface function as the peak axial stress of the axial stress-strain base relation of the concrete cover; ε_{cc}^{Cover} is the axial strain corresponding to f_{cc}^{Cover}; n_2 introduces the brittleness term of the concrete cover.

The incremental calculation process of the generalized Teng *et al.* [19]'s model for determining the response of FR/PR in terms of f_c^{Core} versus ε_c and f_c^{Cover} versus ε_c relations of the concrete core and cover areas is as the following one:

1) Calculate $k_{v,s}$ with Eq. (B-4)
2) Calculate $k_{v,f}$ with Eq. (B-2)
3) Assume a value of concrete lateral strain ($\varepsilon_{l,j}$)

4) Calculate FRP confinement pressure ($f_{l,f}$) by Eq. (B-1)

5) Calculate steel confinement pressure ($f_{l,s}$) by Eq. (B-3)

6) Calculate axial strain (ε_c) by Eq. (B-5)

7) Calculate failure surface function of the concrete core (f_{cc}^{Core}) by Eq. (B-12)

8) Calculate failure surface function of the concrete cover (f_{cc}^{Cover}) by Eq. (B-17)

9) Calculate axial stress (f_c^{Core}) by Eqs. (B-11) to (B-15)

10) Calculate axial stress (f_c^{Cover}) by Eqs. (B-16) to (B-19)

11) Continue the steps 3-10 up to ultimate axial strain

By repeating the aforementioned calculation procedure for a range of $\varepsilon_{l,j}$, f_c^{Cover} versus ε_c and f_c^{Core} versus ε_c relations of the concrete core and cover areas can be determined. It is noted that that for large-sized RC specimens, Teng *et al.* [19] considered f_{c0} to be $0.85 f'_{c0}$ based on ACI 318's recommendation [23].

Analysis-oriented Model for Partially FRP-and-Steel-Confined Circular RC Columns under Compression

Javad Shayanfar [1], Joaquim A. O. Barros [2] and Mohammadali Rezazadeh [3]

[1] PhD Candidate, ISISE, Department of Civil Engineering, University of Minho, Azurém 4800-058 Guimarães, Portugal, arch3d.ir@gmail.com (corresponding author)

[2] Full Prof., ISISE, IBS, Department of Civil Engineering, University of Minho, Azurém 4800-058 Guimarães, Portugal, barros@civil.uminho.pt

[3] Lecturer, Civil Eng., Department of Mechanical and Construction Engineering, Northumbria University, Newcastle upon Tyne, NE1 8ST, United Kingdom, mohammadali.rezazadeh@northumbria.ac.uk

Abstract

Even though analysis-oriented models exist to simulate the axial and dilation behavior of reinforced concrete (RC) columns strengthened with fiber-reinforced-polymer (FRP) full confinement arrangements, a reliable model developed/calibrated for FRP partially imposed confinements is not yet available, identified as a research gap. Therefore, this paper is dedicated to the development of a new analysis-oriented model generalized for fully and partially confined RC columns under compression. In addition to vertical arching action phenomenon, the influence of the concrete expansion distribution along the column height on confining stress is considered in the establishment of the combined confinement from FRP strips and steel transverse reinforcements. A new unified dilation model is proposed, where the substantial effect of additional axial deformations induced by damage evolution in unwrapped zones is formulated by considering available experimental results. This model is coupled with an axial stress-strain formulation that includes a new failure surface function for simulating the dual confinement-induced enhancements, which are strongly dependent on the confinement stiffness. The developed model considers the influence of partially imposed confinement strategy on the axial and dilation behavior of RC columns, whose validation is demonstrated by simulating several experimental tests. Lastly, a parametric study is performed to evidence the dependence of FRP-steel confinement-induced enhancements on steel hoop and FRP spacing, and on the concrete compressive strength.

Keywords: RC columns; FRP confinement; Steel confinement; Dilation model; Stress-strain model;

1 - Introduction

The confinement of existing circular reinforced concrete (RC) columns with fiber-reinforced-polymer (FRP) composites has been progressively demonstrated as a competitive strengthening technique for increasing the axial load carrying and deformation capacity of these structural elements. Numerous studies have been carried out to investigate the influence of FRP confining system on the axial and dilation behavior of concrete/RC columns, leading to the development of several analysis/design-oriented stress-strain models. Nonetheless, most of these models do not consider the confinement provided by existing steel hoop/spiral reinforcements, neither the mutual interference of this hybrid reinforcement (FRP and hoop/spiral) on the final confinement. Furthermore, in general, they are only applicable to full confinement arrangement and, consequently, their applicability for the case of FRP partially imposed confinement is at least arguable. For a comprehensive investigation, existing studies available in the literature were analyzed and classified into two distinctive categories: i) those of experimental and numerical nature that consider the influence of key parameters on full/partial confinement mechanism/performance; ii) those of analysis-oriented framework that simulate theoretically the axial and dilation behavior of concrete/RC columns with dual FRP-steel confinement.

In the first category, for the case of FRP fully confined circular concrete elements (FC as shown in Fig. 1a), Lin e*t al.* [1] experimentally evidenced that the effectiveness of this confinement system remarkably depends on concrete axial compressive strength and FRP thickness. For the case of FRP partially confined circular concrete elements (PC as shown in Fig. 1a), Wang *et al.* [2] demonstrated the FRP strip spacing (s_f) plays a key role in the establishment of their axial and dilation behavior. Zeng *et al.* [3, 4] experimentally revealed that by increasing s_f, the ratio of concrete lateral expansion at the strip mid-plane and at the mid-height of FRP strips grows remarkably, leading to a non-homogenous distribution of concrete expansion and confining stress along the column height. Wang *et al.* [5] performed an experimental study to evaluate axial and dilation responses of FRP fully confined circular RC column (FR as shown in Fig. 1a). It was demonstrated that the dual confinement mechanism of FRP jacket and steel hoops is able to considerably enhance axial strength and deformability of FR, compared to FC, depending on steel hoop spacing (s_s). Kaeseberg *et al.* [6] experimentally demonstrated the substantial influence of s_s on the confinement-induced enhancements of FR, whose level also depends on the volumetric ratio and yield strength of steel hoops, as also confirmed by [7]. Eid *et al.* [8] experimentally showed that steel spiral reinforcements are more effective than steel hoops for the improvement of the axial and dilation responses of FR, which was also shown by [9]. Based on finite element analysis, Zignago and Barbato [10] evidenced the significant influence of the steel hoop confinement on the peak axial strength of FR, but its contribution has decreased with the increase of the concrete compressive strength and FRP confinement stiffness. Barros and Ferreira [11] investigated the axial and dilation behavior of FRP partially confined circular RC columns (PR as shown in Fig. 1a) with different confinement arrangements. The results indicated that even though the partial confining strategy was not as efficient as full confinement, it could be sufficient to assure high levels of load-carrying capacity and deformability with a good compromise between efficiency and cost-effectiveness. Furthermore, it was demonstrated that the confinement-induced enhancements were more significant in PR columns with closely spaced FRP strips and relatively low concrete compressive strength.

On the other hand, in the second category, several theoretical-based models [12-15] have been proposed to simulate axial and dilation behavior of concrete/RC columns with FRP or dual FRP-steel confinement. It is now well-known that at the same level of confinement pressure (f_l), there is a remarkable difference in the level of enhancements provided by passively- and actively-confinement systems (f_l varies and is constant, respectively, during axial loading). This difference is generally known as *Confinement Path Effect*. In general, to determine the axial stress-strain curve of passively-confined concrete (i.e. FRP confined concrete), an axial stress-strain base model, $f_c = g_1(f_{cc})$, is adopted, where g_1 represents the mathematical function of the model for determining a certain value of axial stress (f_c) from a specified value of peak axial strength (f_{cc}) at a given axial strain (ε_c), as demonstrated in Fig. 1b. Subsequently, the confinement path effect is considered by using a failure surface function applicable to passively- confining system, $f_{cc} = g_2(f_l)$, which determines f_{cc} from the confinement pressure (f_l) at a given ε_c through the g_2 .function. Teng *et al.* [12] proposed an analysis-oriented model applicable to FC in which a new failure surface function was developed/calibrated based on test results of FC rather than actively-confined concrete. Zeng *et al.* [3] generalized Teng *et al.* [12]'s models for the case of PC by adopting the well-known concept of confinement efficiency factor (suggested by Mander *et al.* [13]). It was demonstrated that this approach results in misleading predictions of experimental axial and dilation behavior of PC, particularly for specimens with a relatively large s_f . Shayanfar *et al.* [14] proposed a generalized analysis-oriented model for FC and PC, coupled with the dilation model developed by Shayanfar *et al.* [15]. In this model, a new failure surface function applicable to passively-confined concrete was developed based on a large test database of FC/PC. Furthermore, besides the vertical arching action, the effect of non-uniform distribution of concrete lateral expansion along the column height of PC was considered. For the case of FR, Pellegrino and Modena [16] proposed an axial stress-strain model, where the interaction mechanisms between internal FRP full confinement and steel transverse reinforcements were considered based on experimental observations. Hu and Seracino [17] developed a new confinement model for FR, where the contribution of steel hoops and FRP jackets in the failure surface function is evaluated according to the Mander *et al.* [13] (originally developed for steel-confined RC columns) and Jiang and Teng [18]'s models, respectively. Similarly, Teng *et al.* [19] extended the model of Jiang and Teng [18] for the case of FR by using the ratio between the FRP confinement stiffness and the effective confining stiffness of steel transverse reinforcements for considering the effect of their dual confinement mechanism. Even so, to the best of the authors' knowledge, the development of a robust analysis-oriented model for the case of PR to predict the full range of axial- stress–strain response is still lacking.

The present study aims to introduce a robust confinement model generalized for FRP full and partial confinement arrangements (FR and PR), where the key components of this model are calibrated based on existing experimental results. For the establishment of the FRP-steel equivalent confinement pressures uniformly distributed over the column height, the influence of non-homogenous distribution of concrete lateral expansion on their confining stress is required to be addressed, besides vertical arching action. For quantitatively characterizing this influence, a reduction factor with an analytical framework is suggested where the degree of its dominance in the equivalent confinement pressure is strongly dependent on confinement configuration i.e. steel hoop/spiral and FRP spacing and FRP confinement stiffness, in addition to cross-section geometry. Subsequently, an extended version of the dilation model recommended by Teng *et al.* [19], originally developed for FR, is introduced for the case of PR. In this extended/improved model, new parameters are proposed to reflect the substantial effects of additional axial deformations induced by damage evolution in unwrapped zones, peak Poisson's ratio, and non-homogenous concrete expansion distribution on axial strain-lateral strain relation. This model is, then, coupled with axial stress-strain models for concrete core and cover areas that include a confinement stiffness-based failure surface function calibrated for partially imposed FRP-steel confining systems. Lastly, the reliability of the proposed analysis-oriented model is demonstrated by comparison with existing experimental results and those predicted by Teng *et al.* [19]'s model generalized based on the well-known concept of confinement efficiency factor (suggested by Mander *et al.* [13]).

2 - Characteristics of Unconfined Concrete Columns

To calculate the confinement-induced improvements in terms of axial compressive strength and deformability, the characteristics of unconfined concrete compressive strength (f_{c0}) and its corresponding axial strain (ε_{c0}) are necessary to be determined as basic parameters. The studies (i.e. [20-32]) have evidenced a remarkable size effect, resulted from the energy release of the elastic strain when concrete enters in its softening stage, which is also dependent of the relative stiffness of the specimen versus of the adopted testing equipment. This influences the compressive strength of unconfined concrete specimens, being it dependent on the parameters affecting the axial stiffness of the specimen, namely the specimen's aspect ratio (L/D) and concrete elasticity modulus, E_c . This last parameter reflects the concrete stiffness, which is influenced not only on the quality of the matrix and aggregates, but also on the aggregate-matrix interface zone [24-29]. Sim *et al.* [25] proposed an empirical formulation, calibrated by using results from 1509 test specimens of unconfined concrete, having a better performance in predicting experimental f_{c0} compared to Bazant [27] and Kim and Eo [28]. Accordingly, in this study, the well-calibrated model suggested by Sim *et al.* [25] was adopted to calculate f_{c0} as presented by Eq. (1) (with a slight rearrangement):

$$f_{c0} = \left[0.63 + 0.9\sqrt{\frac{(L/D)^{-0.6}}{1+0.017D}} \right] f'_{c0} \simeq 1.063 \left(\frac{150}{D} \right)^{0.122} \left(\frac{D}{L} \right)^{0.088} f'_{c0} \qquad (1)$$

where f'_{c0} is the compressive strength of the standard cylinder with $D = 150$ mm and $L = 300$ mm (the reference specimen's dimensions), assumed as a representative. Note that for the case of the representative, $f_{c0} = f'_{c0}$.

On the other hand, studies (i.e. [20-22, 30-32]) demonstrated a strong relation between concrete compressive strength (f_{c0}) and its corresponding axial strain (ε_{c0}), where ε_{c0} increases with f_{c0}. Besides the effect of f_{c0}, Jansen and Shah [20] evidenced that the column aspect ratio (L/D) has a noticeable influence on the ε_{c0}, which was also confirmed by [22]. In the present study, for the estimation of ε_{c0} by considering the size effect, a large database including 604 unconfined concrete specimens was collected as presented briefly in Table 1. According to the compiled database, the best-fit expression obtained from regression analysis, as a function of f_{c0} and column aspect ratio (L/D), is proposed:

$$\varepsilon_{c0} = 0.0011 \left(\frac{f_{c0} D}{L} \right)^{0.25} \qquad (2)$$

whose predictive performance over the corresponding collected experimental data ($\varepsilon_{c0}^{Ana} / \varepsilon_{c0}^{Exp}$) is shown in Fig. 2 for the considered variables: f_{c0}, L/D and D. The obtained statistical indicators presented in Table 2 demonstrate that Eq. (2) is able to predict with acceptable accuracy the experimental counterparts. Furthermore, Table 2 shows that the proposed expression has a better predictive performance than those recommended by Lim and Ozbakkaloglu [31] and Popovics [32].

3 - Simulation Procedure of Axial Response for FR and PR

To establish the axial stress versus axial strain relationship of FR/PR with the combined confinement from steel transverse reinforcements and FRP jacket, the following procedure was adopted:

a) Determination of the equivalent confinement pressure imposed by steel transverse reinforcements ($f_{l,s}$) and FRP jacket ($f_{l,f}$) by considering both the effect of non-homogenous distribution of concrete transverse expansibility over the column height and the vertical arching action phenomenon.

b) Determination of the average axial compressive strain along the column height (ε_c) at a certain level of concrete lateral strain ($\varepsilon_{l,j}$) obtained from a unified dilation model.

c) Determination of the axial stresses carried by concrete core and cover areas (f_c^{Core} and f_c^{Cover}, respectively) at a certain level of ε_c based on the 'Active Confinement Approach'. In this approach, the axial stress-strain relation of passively-confined concrete is derived based on an axial stress-strain base relation model developed for actively-confined concrete, where the differences of passive and active confinement systems are reflected in terms of their confinement-induced improvements.

Since full confinement system is a special case of partial confinement configuration where $s_f = 0$, a unified approach that depends on s_f will be established, in order to dealt with both confinement arrangements with the same formulation. Accordingly, as close s_f is to the null value, as close is the behavior of a column when subjected to a full confinement configuration (FR). Likewise, when the spacing of steel transverse reinforcements is above a certain limit (its contribution would be insignificant in dual confinement mechanism with FRP jacket), the prediction continuity between FR/PR and FC/PC can be achieved. Therefore, through a generalized mathematical framework based on unification approach, an unique formulation was developed to be applied to PC, PR, FC and FR.

4 - Confinement Pressure Generated by FRP and Steel Transverse Reinforcements

This section addresses the determination of the confinement pressure generated by FRP full/partial confinement system and steel transverse reinforcements. Fallahpour *et al.* [33] demonstrated experimentally that there is a non-uniform distribution of concrete lateral strain that generates a non-uniform confining pressure along the column height, which is dependent on the confinement stiffness, as was also confirmed by [34-36]. For FC with high level of FRP confinement stiffness, since strong restrictions are imposed against the concrete expansibility, an almost null gradient of concrete expansion along the column height is expected. However, for lightly-confined concrete, the damage evolution cannot be homogenized, leading to strain localization due to the lack of sufficient confinement stiffness [36]. On the other hand, the non-uniform distribution of concrete lateral expansion for the case of PC is more pronounced than in FC, whose level is significantly dependent on the s_f, as evidenced by Zeng *et al.* [4] and Guo *et al.* [37]. For the case of FC/PC, Shayanfar *et al.* [14] have specified a reduction factor for FRP confining stress aiming to develop an equivalent confining stress acting uniformly over the concrete column height. Accordingly, by assuming that the maximum concrete expansion ($\varepsilon_{l,j}$) occurs at the mid-distance between FRP strips in case of PC (Fig. 3) leading to a confining stress equal to $E_f \varepsilon_{l,j}$ (where E_f is the elasticity modulus of FRP strips), the equivalent confining stress can be expressed as $k_{ff} E_f \varepsilon_{l,j}$, where k_{ff} is the reduction factor specified by Shayanfar *et al.* [14].

Therefore, for the case of PR, considering the effect of vertical arching action between FRP strips, the equivalent FRP confinement pressure ($f_{l,f}$) acting uniformly over the column height can be derived based on lateral force equilibrium as (the meaning of the symbols representing geometric entities are shown in Fig. 1):

$$f_{l,f} = 2k_{v,f} \frac{n_f t_f w_f}{D\left(w_f + s_f\right)} E_f k_{ff}{}^{PR} \varepsilon_{l,j} = 2k_{v,f} k_{ff}{}^{PR} \frac{n_f t_f w_f}{D\left(w_f + s_f\right)} E_f \varepsilon_{l,j} \tag{3}$$

Rearranging Eq. (3) yields:

$$f_{l,f} = k_{v,f} k_{ff}{}^{PR} K_{Lc} \frac{w_f}{w_f + s_f} \varepsilon_{l,j} \tag{4}$$

in which

$$K_{Lc} = 2\frac{n_f t_f E_f}{D} \tag{5}$$

where $k_{v,f}$ is the reduction factor reflecting the effect of vertical arching action between FRP strips; $k_{ff}{}^{PR}$ is the reduction factor reflecting the effect of non-homogenous concrete expansion along the height of PR (the superscript represents the type of confined column that this factor is applicable to). Note that to calculate $f_{l,f}$ by Eq. (4), the reduction factors $k_{ff}{}^{PR}$ and $k_{v,f}$ need to be addressed as input parameters, which will be presented in Section 4.1 and Section 4.2, respectively.

By considering the influences of the concrete expansion distribution and vertical arching action between steel transverse reinforcements, the equivalent confinement pressure ($f_{l,s}$), imposed uniformly on the core of PR can be determined from lateral force equilibrium as (the meaning of the symbols representing geometric entities was shown in Fig. 1):

$$f_{l,s} = 2k_{v,s} k_{ff}{}^{PR} \frac{A_{sth}}{D_c s_s} E_s \varepsilon_{l,j} \qquad \text{for } k_{ff}{}^{PR} \varepsilon_{l,j} < \varepsilon_{yh} \tag{6a}$$

$$f_{l,s} = 2k_{v,s} \frac{A_{sth}}{D_c s_s} f_{yh} \qquad \text{for } k_{ff}{}^{PR} \varepsilon_{l,j} \geq \varepsilon_{yh} \tag{6b}$$

where $k_{v,s}$ is the reduction factor reflecting the effect of vertical arching action between steel transverse reinforcements; D_c is the diameter of the concrete core (Fig. 1); A_{sth} is the cross-sectional area of a steel confining spiral/hoop; s_s is the distance between steel transverse reinforcements; E_s, ε_{yh} and f_{yh} are the elasticity modulus, yield strain and stress of steel transverse reinforcements, respectively. To calculate $f_{l,s}$ by Eq. (6), besides $k_{ff}{}^{PR}$, the reduction factor of $k_{v,s}$ should be determined as an input parameter, which will be presented in Section 4.2. To do not introduce unnecessary complexities in the formulation, the hoop strain of steel confining reinforcement was assumed to be identical to the hoop strain of FRP jacket based on Teng *et al.* [19]'s recommendation.

4.1- Non-homogenous Distribution of Concrete Lateral Expansion

Experimental studies (i.e. Zeng *et al.* [4] and Guo *et al.* [37]) have evidenced that concrete regions between FRP strips (unwrapped zone) in a partially confining system experience a larger dilatancy during axial loading, compared to the wrapped ones as typically illustrated in Fig. 3a. Since the concrete expansion produces FRP confining strain/stress, Shayanfar *et al.* [35] have confirmed that by assuming a homogenous concrete expansibility along the column height in the model ($k_{ff} = 1$, representing the same concrete expansion for the unwrapped and wrapped), the real dilation and axial behavior cannot be correctly predicted, particularly for a partial system with a relatively large s_f.

Shayanfar *et al.* [14] evidenced that k_{ff}^{PR} (the ratio of average concrete lateral expansion within the strip zone to the maximum concrete expansion ($\varepsilon_{l,j}$) along the damage zone length (L_d), as illustrated in Fig. 3) is strongly dependent on s_f. For a closely spaced FRP strips, k_{ff}^{PR} tends to be similar to k_{ff}^{FR}, being equal in the case of full confinement ($s_f = 0$). However, for a largely spaced FRP strips ($s_f \geq L_{d0}$, where L_{d0} is the damage zone length of unconfined concrete to be latter determined) with marginal FRP confinement effectiveness, k_{ff}^{PR} approaches to k_ε^{SCR} similar to the case of RC columns (SCR: confined only by steel transverse reinforcements). Accordingly, k_{ff}^{PR} can be reasonably considered on the interval $\left[k_\varepsilon^{SCR}, k_{ff}^{FR}\right]$. By assuming k_{ff}^{PR} as being linearly dependent of s_f / L_{d0}, it can be expressed as (Fig. 3a):

$$k_{ff}^{PR} = k_{ff}^{FR} - \left(k_{ff}^{FR} - k_\varepsilon^{SCR}\right)\frac{s_f}{L_{d0}} \geq k_\varepsilon^{SCR} \tag{7}$$

where L_{d0} can be obtained as suggested by Wu and Wei [38]:

$$0.57 \leq \frac{L_{d0}}{\sqrt{A_g}\psi_f} = 1.71 - 3.53 \times 10^{-5} A_g \leq 1.36 \tag{8}$$

$$\psi_f = \frac{6.3}{\sqrt{f_{c0}}} \leq 1 \tag{9}$$

where A_g is the total area of the section; ψ_f is the calibration factor reflecting the effect of concrete compressive strength in terms of damage zone length of unconfined concrete.

In Eq. (7), k_{ε}^{SCR} is the ratio between the minimum and maximum concrete expansion within L_{d0} in the case of steel-confined RC columns. By decreasing s_s, the concrete lateral expansion tends to be smaller and more-homogenously distributed. Hence, k_{ε}^{SCR} approaches to 1, representing uniform concrete expansion over the column height, for the case with very closely spaced steel transverse reinforcements. However, due to its marginal influence when $s_s \geq L_{d0}$ ([39-42]), k_{ε}^{SCR} can be considered almost 0.08 similar to the case of unconfined concrete, as recommended by Shayanfar *et al.* [15]. Consequently, by assuming k_{ε}^{SCR} on the interval $[0.08,1]$ and a linear relation with s_s/L_{d0}, k_{ε}^{SCR} can be expressed as:

$$k_{\varepsilon}^{SCR} = 1 - 0.92\frac{s_s}{L_{d0}} \geq 0.08 \tag{10}$$

In Eq. (7), k_{ff}^{FR} is the reduction factor to account for non-uniform confinement along the column height of FR, representing the ratio of average concrete lateral expansion along L_d to the maximum concrete expansion ($\varepsilon_{l,j}$) as illustrated in Fig. 3b. In this figure, I_f^* represents the threshold of FRP-based confinement stiffness above which a uniform distribution for concrete lateral expansion along the column height is assumed. Based on an approximate method with analytical framework, Shayanfar *et al.* [14] proposed a reduction factor (k_{ff}^{FC}) applicable to FC, as a main function of a confinement stiffness index (I_f). In this model, above a certain level of confinement stiffness ($I_f \geq I_f^*$), since strong restrictions are imposed to the concrete deformability, an almost null gradient of concrete expansion along the column height was assumed (representing $k_{ff}^{FC} = 1$), as evidenced experimentally by Wei and Wu [36]. Nonetheless, for lightly-confined concrete ($I_f < I_f^*$), the damage evolution is not uniform ($k_{ff}{}^{FC} < 1$), leading to strain localization due to the lack of sufficient confinement stiffness. In the present study, by extending Shayanfar *et al.* [14]'s model in order to be applicable to the case of FR, $k_{ff}{}^{FR}$ is proposed as (Fig. 3b):

$$k_{ff}{}^{FR} = \frac{1}{3} + \frac{2}{3} k_{\varepsilon}{}^{FR} \tag{11}$$

in which

$$k_{\varepsilon}{}^{FR} = k_{\varepsilon}{}^{SCR} + \left(1 - k_{\varepsilon}{}^{SCR}\right)\left[2\frac{I_f}{I_f^*} - \left(\frac{I_f}{I_f^*}\right)^2\right] \le 1 \qquad \text{for } I_f \le I_f^* \tag{12a}$$

$$k_{\varepsilon}{}^{FR} = 1 \qquad \text{for } I_f \ge I_f^* \tag{12b}$$

with

$$I_f^* = 0.06 + 0.0005 f_{c0} \tag{13}$$

$$I_f = \frac{K_{Lc}\varepsilon_{c0}}{f_{c0}} \tag{14}$$

where I_f is the FRP confinement stiffness index; I_f^* is the threshold above which $k_{ff}{}^{FR} = k_{\varepsilon}{}^{FR} = 1$; $k_{\varepsilon}{}^{FR}$ is the ratio between the minimum and the maximum concrete expansion along L_d in a FR. As a result, by calculating $k_{\varepsilon}{}^{SCR}$, $k_{\varepsilon}{}^{FR}$ and $k_{ff}{}^{FR}$ by Eqs. (10), (12) and (11), respectively, $k_{ff}{}^{PR}$ for the case of partially imposed confinement on RC column can be calculated by Eq. (7). The dominance degree of $k_{ff}{}^{PR}$ in $f_{l,f}$ and $f_{l,s}$ is strongly dependent on steel hoop/spiral and FRP spacing (s_s/L_{d0} and s_f/L_{d0}) and FRP confinement stiffness (I_f). Accordingly, for the case of well-confined RC columns ($I_f \geq I_f^*$) with closely spaced steel hoop/spiral and FRP strips, $k_{ff}{}^{PR}$ tends to be equal to one, representing a uniform concrete expansion distribution over the column height.

It is noteworthy that for the case of FR/ PR with $s_s \geq L_{d0}$, Eq. (10) provides $k_\varepsilon{}^{SCR} = 0.08$, and the equations for determining $k_{ff}{}^{PR}$ (Eq. (7)) and $k_{ff}{}^{FR}$ (Eq. (11)) degenerate on those proposed by Shayanfar *et al.* [14] for FC/PC. It confirms the unified character of the extended model developed for FR/PR with FC/PC.

4.2- Vertical Arching Action

Due to vertical arching action, the concrete regions of a partially confined column can be distinguished in two distinct confined areas: i) effective confinement area, and ii) ineffective confinement area, as illustrated in Fig. 4. In order the entire cross-section area at transverse and longitudinal directions could be considered as a uniformly confined concrete volume, an effective confinement pressure is used by applying a reduction factor, k_v, to the confinement pressure.

Considering the effect of vertical arching action for the case of FRP partial confinement (Fig. 4a), Shayanfar *et al.* [15] proposed a new formulation to calculate $k_{v,f}$ as follows:

$$k_{v,f} = \frac{w_f + s_f\left(1 - \frac{s_f}{D} + 0.43\left(\frac{s_f}{D}\right)^2 - 0.07\left(\frac{s_f}{D}\right)^3\right)}{w_f + s_f} \tag{15}$$

which can be conveniently simplified to:

$$k_{v,f} = \frac{w_f + s_f \exp\left(-0.98 R_f\right)}{w_f + s_f} \leq 1 \tag{16}$$

290 where

$$R_f = \frac{s_f}{D} \quad (17)$$

291 For the case of steel-confined concrete (as a partial confinement system), a reduction factor $k_{v,s}$,
292 reflecting the influence of vertical arching action (Fig. 4b), can be determined following the same
293 principles adopted in the development of Eq. (16) resulting

$$k_{v,s} = C_{shc} \exp\left(-0.98 R_s\right) \le 1 \quad (18)$$

294 where

$$R_s = \frac{s_s}{D_c} \quad (19a)$$

$$C_{shc} = \begin{cases} 1 + 0.84 R_s & \text{for steel spirals} \\ 1 & \text{for steel hoops} \end{cases} \quad (19b)$$

295 The equation of C_{shc} parameter was derived based on Mander *et al.* [13] ($k_{v,s} = 1 - R_s/2$ and
296 $k_{v,s} = \left(1 - R_s/2\right)^2$ for spiral and hoop cases, respectively).

297 As a result, by using $k_{v,f}$, $k_{v,s}$ and $k_{ff}^{\,PR}$ by Eqs. (16), (18) and (7), the equivalent confinement
298 pressures generated by FRP jacket and steel transverse reinforcements at a given $\varepsilon_{l,j}$ can be
299 calculated by Eqs. (4) and (6), respectively.

300 5- Dilation Model of FR/PR

301 The methodology for determining the dilation response of FR and PR during axial compressive
302 loading is addressed in this section. For the case of FC, the initial transversal expansion of the
303 confined concrete is almost the same of unconfined one of same strength class. However, above a

certain axial compressive deformation, which depends on the concrete strength class, the micro defects in the concrete microstructure degenerate in meso-defects, and the lateral concrete expansion start increase significantly, which is reflected in the pronounced increase of the Poisson's ratio and a transition zone starts being visible as shown in Fig. 5 (discussed in detail later). The magnitude of concrete expansion rate is dependent on the stiffness of the confinement systems. With the degeneration of meso- into macro-defects, the concrete experiences its maximum expansion rate, which is followed by a descending trend with a lower dilatancy. Further information about the influence of the confinement on dilation behavior of FC under compression can be found in [43-48].

To highlight the influence of steel confining hoops on dilation characteristics of FR, the dilation results obtained from the experimental study conducted by Wang *et al.* [5] for the cases of FR and FC are compared in Fig. 5. For this purpose, the test specimens of C2H0L1 (FC) and C2H1L1 (FR), fully confined by one layer of CFRP jacket, were selected. For C2H1L1, the distance between steel hoops was reported as 120 mm ($R_s = 0.71$). As can be seen in Fig. 5a, beyond the transition zone, at a certain level of axial strain (ε_c), the concrete lateral expansion ($\varepsilon_{l,j}$) of FC was larger than that of FR. Based on the volumetric strain ($\varepsilon_v = \varepsilon_c - 2\varepsilon_{l,j}$) versus ε_c relation presented in Fig. 5b, FC developed a larger volumetric expansion due to the higher increase of concrete lateral expansibility, compared to FR. Fig. 5c presents the relation between the secant Poisson's ratio ($\nu_s = \varepsilon_{l,j} / \varepsilon_c$; positive values are considered for both strain components) and ε_c, which confirms a smaller dilation response of FR with a lower maximum concrete secant Poisson's ratio ($\nu_{s,\max}$) than that of FC.

To predict the lateral strain versus the axial strain of FRP confined concrete, several models have been proposed (i.e. [15, 19, 43-48]). In the present study, the well-calibrated dilation model conducted by Teng *et al.* [19], developed for circular RC columns with full confinement arrangements (FR), having a unified character for FC, will be, hereafter, adapted for being applicable to FRP-based partial confinement arrangements. In this model, the average axial strain along the column height (ε_c) at a certain level of $\varepsilon_{l,j}$ can be obtained from:

$$\varepsilon_c = 0.85\varepsilon_{c0}F_T\left\{\left[1+0.75\left(\frac{\varepsilon_{l,j}}{\varepsilon_{c0}}\right)\right]^{0.7} - \exp\left[-7\left(\frac{\varepsilon_{l,j}}{\varepsilon_{c0}}\right)\right]\right\} \tag{20}$$

in which

$$F_T = 1+8\frac{f_{l,f}}{f_{c0}}+\alpha\frac{f_{l,s}}{f_{c0}} \tag{21}$$

$$\alpha = 1.59+15.1\rho_{FS} \tag{22}$$

$$\rho_{FS} = \frac{K_{Lat}^{FRP}}{K_{Lat}^{Steel}} = \frac{n_f t_f E_f s_s D_c}{k_{v,s}E_s A_{st} D} = \frac{K_{Lc}s_s D_c}{2k_{v,s}E_s A_{st}} \quad \text{for FC/FR} \tag{23a}$$

$$\rho_{FS} = \frac{k_{v,f}K_{Lc}s_s D_c}{2k_{v,s}E_s A_{st}}\left(\frac{w_f}{w_f+s_f}\right) \quad \text{for PC/PR} \tag{23b}$$

where ρ_{FS} is the ratio between the confinement stiffness of the FRP jacket and steel confining systems; F_T is the term reflecting the influence of the combined confinement from FRP jacket and steel transverse reinforcements on concrete dilation behavior. Note that in the present study, Eq. (23b) was derived/extended for the case of partial confinement based on the approach used for Eq. (23a) ($\rho_{FS} = K_{Lat}^{FRP}/K_{Lat}^{Steel}$). It is clear that the maximum secant Poisson's ratio ($v_{s,\max} = \left(\varepsilon_{l,j}/\varepsilon_c\right)_{\max}$

) cannot be directly determined from Eq. (20). Since the secant Poisson's ratio (v_s as the ratio of hoop/lateral strain and axial strain) must be lower than $v_{s,\max}$ during axial compressive loading ($v_s \le v_{s,\max}$), the axial strain (ε_c) obtained from Eq. (20) should be consequently higher than $\varepsilon_{l,j}/v_{s,\max}$, as a threshold. On the other hand, for the case of partial confining systems, since the concrete regions between FRP strips of PC/PR (unwrapped zone) are indirectly subjected to a certain confinement pressure, more damage-induced axial deformation would be expected, compared to FC/FR, depending on s_f , as evidenced by [2-4, 49-51]. Accordingly, to simulate the dilation response of PC/PR, the preliminary evaluations using Eq. (20), exclusively developed for FC/FR, revealed that this model would result in misleading predictions. Consequently, based on the aforementioned discussion, in the present study, the dilation model developed by Teng *et al.* [19] was extended to the case of PC/PR as follows:

$$\varepsilon_c = 0.85\varepsilon_{c0}F_T\left\{\left[1+0.75\beta\frac{\varepsilon_{l,j}}{\varepsilon_{c0}}\right]^{0.7}-\exp\left[-7\beta\frac{\varepsilon_{l,j}}{\varepsilon_{c0}}\right]\right\}+\Delta_{\varepsilon c}\ge\frac{\varepsilon_{l,j}}{v_{s,\max}} \tag{24}$$

in which

$$\beta = 1-5\left(1-k_\varepsilon^{\ PR}\right)\frac{s_f}{L_{d0}}\ge k_\varepsilon^{\ PR} \tag{25}$$

$$k_\varepsilon^{\ PR} = k_\varepsilon^{\ FR}-\left(k_\varepsilon^{\ FR}-k_\varepsilon^{\ SCR}\right)\frac{s_f}{L_{d0}}\ge k_\varepsilon^{\ SCR} \tag{26}$$

$$v_{s,\max} = \frac{0.256}{\left(1+\dfrac{L_{d0}}{D}\right)\sqrt{\rho_{K,T}}} \tag{27}$$

$$\rho_{K,T} = \left(\frac{f_{l,T}}{f_{c0}}\right)\frac{\varepsilon_{c0}}{\varepsilon_{l,j}} = \left(\frac{f_{l,f}}{f_{c0}} + \frac{D_c f_{l,s}}{D f_{c0}}\right)\frac{\varepsilon_{c0}}{\varepsilon_{l,j}} \quad (28)$$

where β reflects the influence of non-uniform distribution of concrete expansion along the column height, which is equal to 1 for the case of full confinement. k_{ε}^{PR} is the ratio between the minimum and the maximum concrete expansion, which was derived based on the approach adopted for developing k_{ff}^{PR} (Eq. (7) as also shown in Fig. 3a) due to the similarity of concepts. In Eq. (24), $\Delta_{\varepsilon c}$ is the calibration term representing the influence of the additional axial strain for PC/PR, compared to FC/FR; $v_{s,\max}$ defines the maximum secant Poisson's ratio, which was proposed by Shayanfar *et al.* [35] having a unified character for both cases of full and partial FRP arrangements. It is noted that in Eq. (28), total confinement pressure ($f_{l,T}$) acting on the entire cross-section imposed by FRP jacket (on the entire cross-section with D) and steel jacket (on the concrete core with D_c) was derived based on the equilibrium of lateral forces in the entire cross-section with D diameter.

To develop $\Delta_{\varepsilon c}$, by assuming $\varepsilon_{l,i}$ and $\varepsilon_{l,j}$ as the concrete lateral expansion at the strip mid-plane and at mid-height between two consecutive strips, the following expression was empirically suggested as $\Delta_{\varepsilon c} = A_1\left(\varepsilon_{l,j} - \varepsilon_{l,i}\right)^{A_2}$ where A_1 and A_2 are calibration factors. To minimize the complexity of this expression, $\Delta_{\varepsilon c}$ was rearranged by considering $\varepsilon_{l,i}/\varepsilon_{l,j} = 1 - 0.92\, s_f / L_{d,0}$ as recommended by [15], resulting:

$$\Delta_{\varepsilon c} = A_1\left(\varepsilon_{l,j} - \varepsilon_{l,i}\right)^{A_2} = A_1\left(\varepsilon_{l,j} - \left(1 - 0.92\frac{s_f}{L_{d,0}}\right)\varepsilon_{l,j}\right)^{A_2} = A_1\left(0.92\frac{s_f \varepsilon_{l,j}}{L_{d,0}}\right)^{A_2} \quad (29)$$

A regression analysis was performed to achieve the best-fit values for A_1 and A_2 based on 92 test specimens of PC and PR conducted by Barros and Ferreira [11], Zeng *et al.* [3, 4, 51] and Guo *et al.* [37]. It is noteworthy that the experimental values of A_1 and A_2 were derived by trial-and-error procedure in such a way that full range lateral strain versus axial strain curves predicted by the developed dilation model could virtually coincide with those of the experimental relations. Based on a preliminary regression analysis, A_1 and A_2 were determined equal to 0.085 and 0.65, respectively. It was, however, verified that considering the influence of FRP confinement stiffness and $R_f = s_f / D$ on the evaluation of A_1, a better prediction of $\Delta_{\varepsilon c}$ was obtained, therefore the following equation was determined:

$$A_1 = \frac{0.0048}{\exp\left(1.75 R_f\right)} \left(\frac{K_{Lc}}{f_{c0}}\right)^{0.9} \tag{30}$$

Hence, $\Delta_{\varepsilon c}$ was proposed as

$$\Delta_{\varepsilon c} = A_1 \left(\varepsilon_{l,j} - \varepsilon_{l,i}\right)^{A_2} \simeq 0.0045 e^{-1.75 R_f} \left(\frac{K_{Lc}}{f_{c0}}\right)^{0.9} \left(\frac{s_f \varepsilon_{l,j}}{L_{d,0}}\right)^{0.65} \tag{31}$$

where $\Delta_{\varepsilon c} = 0$ for the cases of FC and FR. Fig. 6 demonstrates the predictive performance of Eq. (31). It can be seen that the calibration factor of A_1 has a good agreement with experimental counterparts.

Fig. 7 compares the existing approach and that proposed in the present study in the establishment of dilation response of PC based on experimental tests conducted by Zeng *et al.* [3]. For this purpose, the model proposed by Teng *et al.* [19] (developed exclusively for the case of full confinement) was selected as the representative of existing approaches, where the original concept of confinement efficiency factor ($k_{v,f}=\left[1-s_f/2D\right]^2$, suggested by Mander *et al.* [13]) was adopted to generalize this model for the case of partial confinement (presented in Appendix A). It is noteworthy that the hoop strain in FRP strip in Teng *et al.* [19]'s model is equal to $\varepsilon_{l,j}$ representing the assumption of uniform distribution of concrete expansion along the column height ($k_{\varepsilon}^{PC}=1$). However, in the present study, FRP hoop strain is considered $k_{\varepsilon}^{PC}\varepsilon_{l,j}$ (or $k_{\varepsilon}^{PR}\varepsilon_{l,j}$ in the case of PR). As can be seen in Fig. 7, the initial dilation responses obtained from the developed model and the generalized Teng *et al.* [19]'s model were almost identical. However, as shown in Fig. 7a, beyond the transition zone, at a certain level of ε_c, the generalized Teng *et al.* [19]'s model resulted in significant overestimates in the prediction of the corresponding FRP hoop strain, compared to the experimental records, which were captured correctly by the developed dilation model. Fig. 7b shows that the generalized Teng *et al.* [19]'s model overestimates $v_{s,\max}$ and is not able to accurately simulate v_s versus ε_c, while a suitable agreement is observed between the responses registered experimentally and obtained with the developed dilation model. Furthermore, the ε_c versus ε_v relations presented in Fig. 7c demonstrate that the developed dilation model is capable of simulating more closely the ε_c-ε_v response registered experimentally than the generalized Teng *et al.* [19]'s model.

For further evaluation of the developed dilation model, Fig. 8 and Fig. 9 compare experimental lateral strain versus axial strain curves of PC and PR with different confinement arrangements reported by Barros and Ferreira [11], Zeng *et al.* [3, 51], Guo *et al.* [37] with those obtained from the proposed model and the generalized Teng *et al.* [19]'s model. It can be seen, the generalized Teng *et al.* [19]'s model predicts non-conservatively the experimental dilation responses of PC and PR, which consequently overestimates the confinement pressure generated by FRP strips. The suitable predictive performance of the developed dilation model validates its reliability to simulate experimental lateral strain versus axial strain curves, working for both PC and PR.

6- Axial Stress-strain Model of FR/PR

This section establishes the axial stress (f_c) versus axial strain (ε_c) relationship for FR/PR. Under axial loading, the compressive load carried by the entire cross-section of FR/PR can be comprised of three distinct parts: i) the load carried by concrete cover area subjected to only FRP confinement, ii) the load carried by concrete core area under the combined confinement from steel transverse reinforcements and FRP jacket, and iii) the load carried by steel longitudinal bars. Accordingly, at a given axial strain (ε_c), the corresponding average axial load (N) can be expressed as:

$$N = f_c^{Core} A_c + f_c^{Cover}\left(A_g - A_c\right) + f_{sl} A_{slb} \tag{32}$$

in which

$$f_{sl} = E_{sl}\varepsilon_c \le f_{yl} \tag{33}$$

where f_c^{Core} and f_c^{Cover} are the axial stress acting on the concrete core and cover areas, respectively; A_g is the total area of the concrete section; A_c is the total area of the concrete core; A_{slb} is the total cross-section area of steel longitudinal bars; f_{sl} is the axial stress of steel longitudinal bars corresponding to ε_c; E_{sl} and f_{yl} are the elasticity modulus and yield stress of steel longitudinal bars, respectively. Accordingly, by calculating f_c^{Core} and f_c^{Cover} for a range of ε_c, not only can the axial stress-strain relations of the concrete core and cover areas be found, but also the axial load (N) versus axial strain relation of FR/PR can be calculated using Eq. (32).

In this study, the well- known concept of '*Active Confinement Approach*' was adopted to determine the axial responses of f_c^{Core} and f_c^{Cover} of FR/PR subjected to different confinement pressures. The axial response of FRP confined concrete (passive confinement) is derived based on an axial stress-strain base relation model originally developed for actively-confined concrete, by modifying its failure surface function to make it applicable to passively-confined ones [14, 19, 35, 53-56]. By following the axial stress-strain base relation model suggested by Popovics [32], at a given ε_c, f_c^{Core} carried by concrete core area under $f_{l,f}$ and $f_{l,s}$ can be obtained as

$$f_c^{Core} = f_{cc}^{Core} \frac{\left(\varepsilon_c / \varepsilon_{cc}^{Core}\right) n_1}{n_1 - 1 + \left(\varepsilon_c / \varepsilon_{cc}^{Core}\right)^{n_1}} \tag{34}$$

in which

$$\frac{\varepsilon_{cc}^{Core}}{\varepsilon_{c0}} = 1 + 5\left[\frac{f_{cc}^{Core}}{f_{c0}} - 1\right] \tag{35}$$

$$n_1 = \frac{E_c}{E_c - f_{cc}^{Core} / \varepsilon_{cc}^{Core}} \simeq \frac{1}{1 - 0.27 f_{c0}^{0.25}\left(1 - \alpha_1\right)} \tag{36}$$

$$\alpha_1 = 1.15 f_{c0}^{-0.1}\left(\frac{f_{l,f} + f_{l,s}}{f_{c0}}\right)^{0.4} \leq 0.85 \tag{37}$$

where f_{cc}^{Core} is the failure surface function as the peak axial stress of the axial stress-strain base relation of the confined (by steel transverse reinforcement and FRP) concrete core; ε_{cc}^{Core} is the axial strain corresponding to f_{cc}^{Core} to be determined using Eq. (35) recommended by Mander *et al.* [13]; n_1 introduces the concrete brittleness term that can be calculated using the recommendation of Carreira and Chu [52] by Eq. (36) (with a slight rearrangement); E_c defines the elasticity modulus of concrete.

Similarly, for the case of the concrete cover, the axial stress-strain base relation model can be expressed by

$$f_c^{Cover} = f_{cc}^{Cover} \frac{\left(\varepsilon_c / \varepsilon_{cc}^{Cover}\right) n_2}{n_2 - 1 + \left(\varepsilon_c / \varepsilon_{cc}^{Cover}\right)^{n_2}} \tag{38}$$

in which

$$\frac{\varepsilon_{cc}^{Cover}}{\varepsilon_{c0}} = 1 + 5\left[\frac{f_{cc}^{Cover}}{f_{c0}} - 1\right] \tag{39}$$

$$n_2 = \frac{1}{1 - 0.27 f_{c0}^{0.25}\left(1 - \alpha_2\right)} \tag{40}$$

$$\alpha_2 = 1.15 f_{c0}^{-0.1}\left(\frac{f_{l,f}}{f_{c0}}\right)^{0.4} \leq 0.85 \tag{41}$$

where f_{cc}^{Cover} is the failure surface function as the peak axial stress of the axial stress-strain base relation of the confined (by FRP) concrete cover; ε_{cc}^{Cover} is the axial strain corresponding to f_{cc}^{Cover} ; n_2 introduces the brittleness term of the concrete cover. According to Eqs. (34-41), to calculate the axial stress-strain relations of the concrete core and cover areas (f_c^{Core} versus ε_c curve, and f_c^{Cover} versus ε_c curve), f_{cc}^{Core} and f_{cc}^{Cover} as failure surface functions are required to be determined as input parameters.

It is now well-known that at the same level of confinement pressure, there is a remarkable difference in the level of enhancements provided by passively- and actively-confinement systems in which the confinement pressure is varying and constant, respectively, during axial loading. According to the studies conducted by Lai *et al.* [57, 58] and Ho et al. [59], the confinement path effect (Φ) can be computed quantitatively as the difference of the peak strength obtained from the failure surface functions of passively- and actively-confined concrete ($f_{cc}^{Passive}$ and f_{cc}^{Active}, respectively). Hence, Φ can be calculated by $\Phi = f_{cc}^{Passive} - f_{cc}^{Active}$ where $\Phi < 0$ reveals that confinement-induced enhancements in a passively-confined concrete is less than those in an actively-confined concrete system. Studies [14, 35, 56-59] evidenced that by using a failure surface function (f_{cc}^{Active}) derived/calibrated based on actively-confined concrete columns, the enhancements offered by a passive confinement system (as confinement path-dependent) are overestimated, due to the significant difference of their confinement pressure paths ($\Phi < 0$). This phenomenon has been evaluated comprehensively in Lai *et al.* [57, 58], Ho *et al.* [59] and Shayanfar *et al.* [14, 35].

In the present study, the confinement stiffness-based failure surface function recommended by Shayanfar *et al.* [14], calibrated based on a large test database of both FC and PC (passively-confined concrete columns), was adopted. Accordingly, f_{cc}^{Core} and f_{cc}^{Cover} can be calculated as:

$$\frac{f_{cc}^{Core}}{f_{c0}} = 1 + \frac{R_1}{R_2}\left(\frac{f_{l,f} + f_{l,s}}{f_{c0}}\right)^{R_2} \tag{42}$$

$$\frac{f_{cc}^{Cover}}{f_{c0}} = 1 + \frac{R_1}{R_2}\left(\frac{f_{l,f}}{f_{c0}}\right)^{R_2} \tag{43}$$

where R_1 and R_2 are the calibration terms. It should be noted that since the confinement pressure generated by steel transverse reinforcements ($f_{l,s}$) remains constant beyond steel yielding, the application of a failure surface function developed exclusively for passively-confined concrete might lead to underestimation in the calculation of the improvements induced by dual confinement mechanism of steel transverse reinforcements and FRP jacket ([56]). However, in this study, in a slight conservative manner, the effect of steel confinement on the determination of R_1 and R_2 was ignored, which can be considered practically correct for the case of RC columns with largely spaced steel transverse reinforcements due to its negligible effectiveness. Accordingly, by following the Shayanfar *et al.* [14]'recommendations, R_1 and R_2 can be calculated as (with a slight modification):

$$R_1 = \frac{24\rho_{K,f}{}^{0.67}}{\lambda_{fc}\lambda_{Rf}} \leq 4.25 \tag{44}$$

$$R_2 = 1.82\rho_{K,f}{}^{0.26} \geq 0.3 \tag{45}$$

in which

$$\rho_{K,f} = \frac{f_{l,f}\varepsilon_{c0}}{f_{c0}\varepsilon_{l,j}} = k_{v,f}k_{ff}{}^{PR}\frac{K_{Lc}w_f\varepsilon_{c0}}{\left(w_f + s_f\right)f_{c0}} \tag{46}$$

$$\lambda_{fc} = 0.75 + 0.008 f_{c0} \tag{47}$$

$$\lambda_{Rf} = 1 + 0.15R_f{}^{0.25} \tag{48}$$

where $\rho_{K,f}$ represents FRP confinement stiffness that considers the effect of non-homogenous distribution of concrete expansibility through $k_{ff}{}^{PR}$ in addition to vertical arching action ($k_{v,f}$) and FRP volumetric ratio in a partial confinement system (the term of $w_f/\left(w_f + s_f\right)$); λ_{fc} and λ_{Rf} are the partial calibration factors representing the impact of f_{c0} and R_f on R_1, respectively.

It should be noted that a lag between the axial strain development and confining strain/stress generation occurs with the increase of the concrete compressive strength (f_{c0}) due to the decrease of its lateral deformation [57-59]. Consequently, more confinement-induced enhancements would be achieved with the decrease of the concrete compressive strength class, which was reflected in the development of the proposed failure surface function through the consideration of the calibration term of λ_{fc} as a reduction factor for R_1. On the other hand, the dilation model developed in the present study for PR differs from that used by Shayanfar *et al.* [14] applicable to PC. Accordingly, since the dilation model has a significant influence on the confinement pressure and is coupled to the axial stress-strain relation, in this study, λ_{Rf} (Eq. (48)) was recalibrated based on regression analysis performed on the experimental axial stress-strain relations of 109 PC and PR specimens to ensure its reliability. The experimental values of λ_{Rf} were derived by trial-and-error procedure in such a way that full range axial stress-strain curves predicted by the developed analysis-oriented model could virtually coincide with those of the experimental relations. Fig. 10 demonstrates the variation of λ_{Rf}^{Exp} with $R_f = s_f / D$. As can be seen, there is an upward trend of λ_{Rf}^{Exp} by increasing R_f. Furthermore, Eq. (48) has a good agreement with experimental counterparts.

As a result, by calculating R_1 and R_2 by Eqs. (44) and (45), f_{cc}^{Core} and f_{cc}^{Cover} can be determined using Eqs. (42) and (43), respectively. Then, based on Eqs. (34) to (37) and Eqs. (38) to (41), the f_c^{Core} and f_c^{Cover} corresponding to ε_c are obtained, respectively. The incremental calculation process for determining the axial stress-strain response of FR/PR based on the developed analysis-oriented model is the following one:

1) Calculate k_{ff}^{PR} with Eq. (7)

2) Calculate $k_{v,f}$ with Eq. (16)

3) Calculate $k_{v,s}$ with Eq. (18)

4) Assume a value of concrete lateral strain ($\varepsilon_{l,j}$)

5) Calculate FRP confinement pressure ($f_{l,f}$) by Eq. (4)

6) Calculate steel confinement pressure ($f_{l,s}$) by Eq. (6)

7) Calculate axial strain (ε_c) by Eq. (24)

8) Calculate failure surface function of the concrete core (f_{cc}^{Core}) by Eq. (42)

9) Calculate failure surface function of the concrete cover (f_{cc}^{Cover}) by Eq. (43)

10) Calculate axial stress (f_c^{Core}) by Eqs. (34) to (37)

11) Calculate axial stress (f_c^{Cover}) by Eqs. (38) to (41)

12) Calculate the average axial load (N) by Eq. (32)

13) Continue the steps 4-12 up to ultimate axial strain

Accordingly, not only can N versus ε_c relation of FR/PR be found, but also f_c^{Core} versus ε_c and f_c^{Cover} versus ε_c relations of the concrete core and cover areas can be calculated.

It should be noted that a more reliable model could be always conducted by regression analysis through providing a comprehensive dataset having a broader range of the model variables. According to the database used to develop/calibrate Eqs. (42) and (43), concrete strength variable (f_{c0}) varies from 16 to 171 MPa with the mean and CoV values equal to 40 MPa and 0.53, respectively; confinement stiffness of the external jacket ($\rho_{K,f}$) has a range of 0.002 to 0.262 with the mean and CoV values equal to 0.037 and 0.85, respectively; column's diameter to total FRP's thickness ratio ($D/n_f t_f$) varies in the range of 40 to 1796 with mean and CoV values equal to 166 and 0.26, respectively; column aspect ratio (L/D) is in the range of 2 to 5 with mean and CoV values equal to 2.09 and 0.2, respectively. Accordingly, the proposed model is limited to the aforementioned range of the variables covered by the assembled database.

Studies [60-62] evidenced that slenderness effects have a detrimental influence on the load carrying and deformability capacity of FRP confined concrete/RC columns, leading to an underutilization of the FRP confinement potentialities and the necessity of considering the column buckling. However, in the present stage of the research program, the applicability of the developed model was only validated to the aforementioned interval of the relevant variables that govern the response of fully/partially FRP confined concrete/RC columns, and do not cover the cases where buckling is a design concern. Nevertheless, by developing the slenderness limit and its relative reduction factors in terms of load carrying and deformability capacity, the methodology proposed in the present work can be potentially extended to slender FRP confined RC columns, which will be the focus of a future study.

7- Model Validation

This section presents the verification of the proposed model to predict the axial and dilation responses of FR/PR under axial compressive loading. For this purpose, the results obtained from the developed analysis-oriented model were compared with those measured experimentally by [5-8, 11]. Furthermore, for the case of comparative assessment, the well-established model suggested by Teng *et al.* [19], developed exclusively for fully FRP confined circular columns, was selected and generalized for the case of partial confinement strategy based on the concept of confinement efficiency factor (Mander *et al.* 1988 as one of the most-cited approach). The generalized model of Teng *et al.* [19] can be found in Appendix A.

Fig. 11 compares the axial force(N)/stress ($f_c = N/A_g$)/versus axial strain (ε_c) curves of FR and PR obtained from the proposed model with those conducted experimentally by Barros and Ferreira [11], Eid *et al.* [8], and Wang *et al.* [5]. As shown in Fig. 11a, the developed model is able to predict accurately the global axial stress-strain curves of the FR specimens with the different values of R_s. In Fig. 11b-c, the developed model reveals efficient capability in simulating the experimental responses of FR with different values of f_{c0}, and with/without concrete cover, even though the initial axial behavior was underestimated slightly (in Fig. 11c, C2MP2N and C2N1P2N specimens were constructed without concrete cover). The comparisons in Fig. 11d-e demonstrate that the model is able to capture sufficiently the influence of FRP confining system on the axial stress-strain curves of FR and PR, regardless an underestimation associated with FL3S2C32. In Fig. 11f, a suitable performance of the developed model for the case of PR with the different values of R_f can be confirmed.

Fig. 12 and Fig. 13 compare the axial stress/force-strain curves of PR and FR obtained from the proposed model and the generalized Teng *et al.* [19]'s model with those conducted experimentally by Wang *et al.* [5], Kaeseberg *et al.* [6], Chastre and Silva [7], Eid *et al.* [8], and Barros and Ferreira [11]. In general, the developed model is able to predict closely the full range of the experimental counterparts. Furthermore, compared to the generalized Teng *et al.* [19]'s model, the developed model reveals a better predictive performance in terms of axial behavior of PR and FR with different types of confining arrangement.

For the further examination of the developed model in terms of axial and dilation responses, the axial stress versus volumetric strain (ε_v) curves of PC specimens reported by Barros and Ferreira [11] were simulated by the proposed model and the generalized Teng *et al.* [19]'s model, as shown in Fig. 14. Note that ε_v in this figure represents the concrete volumetric strain at the mid-plane of FRP strips during axial compressive loading. As can be seen, the developed model is capable of simulating closely the experimental volumetric variation. It is mainly attributable to the consideration of the effect of non-homogenous distribution of concrete lateral expansion along the height of PR in the developed model. By using Teng *et al.* [19]'s generalized model based on the concept of confinement efficiency factor suggested by Mander *et al.* [13], exclusively devoted to steel-confined RC columns, misleading predictions are obtained in terms of volumetric change evolutions.

The comparative assessment demonstrated in Figs. 11-14 not only evidences the reliability of the proposed analysis-oriented model for the prediction of axial and dilation behavior of FR and PR, but also confirms the validity of the conducted assumptions in the consideration of the effects of dual confinement mechanism of steel transverse reinforcements and FRP full/partial arrangement. Furthermore, the proposed model has a unified character for the case of FRP confined concrete (FC and PC) confirming its wide applicability.

Lastly, using the proposed model analysis on PR, Fig. 15 evaluates the dependence of FRP-steel confinement-induced enhancements on the distance between steel hoops (s_s), the distance between FRP strips (s_f) and the concrete compressive strength (f_{c0}). In this parametric study, an RC column with a diameter and height of 200 and 1000 mm was assumed. The data for the parameters of FRP confinement configuration were $n_f = 5$, $t_f = 0.167$ mm, $E_f = 249$ GPa and $w_f = 50$ mm

, while for the parameters of steel hoops were $d_{sth}=6$ mm, $f_{yh}=400$ MPa, $E_s=200$ GPa. Furthermore, for the case of the parameters of steel longitudinal reinforcements, the data were $d_{sth}=10$ mm, $f_{yl}=400$ MPa, $E_{sl}=200$ GPa. The concrete cover was considered 25 mm. Fig. 15a reveals the effect of s_s on the normalized concrete axial stress (f_c^{ave}/f_{c0}) versus ε_v relation of PR with $R_f=s_f/D=0.4$ and $f_{c0}=25$ MPa, where f_c^{ave} represents the area-weighted average axial stress carried by concrete core and cover areas. As can be seen, while s_s decreases from 150 mm to 50 mm, the volumetric change evolution tends to be reversed resulting in a higher axial strength and smaller volumetric expansion. It highlights the influence of steel hoop confinement in limiting the concrete tendency for an abrupt expansion. Similarly, as shown in Fig. 15b, for the case of PR with $s_s=100$ mm and $f_{c0}=25$ MPa, by decreasing R_f, the response changes from volumetric expansion to volumetric compaction, indicating a remarkable increase in FRP effectiveness in restraining concrete lateral dilation. In Fig. 15c-d, shows the effects of steel hoop and FRP spacing on f_c^{ave}/f_{c0} versus ε_v relation of PR with a higher concrete compressive strength ($f_{c0}=50$ MPa). As can be seen, FRP-steel confinement induced enhancements in the case of $f_{c0}=50$ MPa are not so pronounced compared to those in the case of $f_{c0}=25$ MPa (Fig. 15c-d), mainly attributable to smaller lateral deformations and a longer lag between the axial strain development and the confining strain/stress generation for higher strength concrete.

8- Summary and conclusions

In the present study, a generalized analysis-oriented model was developed for determining the axial compressive stress-strain relationship for circular cross-section RC columns of fully and partially confined with FRP systems and also including transverse steel reinforcements (FR and

PR, respectively). To derive the equivalent confinement pressures imposed by FRP jacket and steel transverse reinforcements, the effects of non-homogenous concrete transverse expansion along the column height and the vertical arching action were considered. An already existing dilation model was extended to the cases with partially imposed confinement pressure and dual FRP-steel confinement mechanism. With this information, a unified axial stress-strain model was developed for the establishment of the axial stress-strain relations of FR and PR. A comprehensive comparison to axial responses registered experimentally in available literature demonstrated that the proposed analysis-oriented model has a suitable agreement with the experimental counterparts. Based on the work presented in the current study, the conclusions can be drawn as follows:

- In contrast to the original concept of confinement efficiency factor, it is found that the consideration of the effect of non-homogenous concrete transverse expansion along the column height is critical to develop a rational and robust model for PC/PR. This consideration led to a significant enhancement in the model performance to simulate accurately axial and dilation responses of PC/PR concrete columns.
- An extended/improved version of Teng et al. (2015)'s dilation model for PC/PR is proposed, which demonstrated a suitable level of reliability for predicting lateral-to-axial strain relation of PC/PR, through addressing the substantial effects of additional axial deformations induced by damage evolution in unwrapped zones, peak Poisson's ratio, and non-homogenous concrete expansion distribution.
- The axial stress versus axial/lateral/volumetric strain relationship of PC/PR and FC/FR can be predicted accurately through the developed analysis-oriented model, consisting of a new confinement stiffness-based failure surface function that addresses the confinement path effect.

- The investigation undertaken in the current study has demonstrated that $R_f = s_f / D$ is the most influencing parameter on the confinement-induced improvements in PC/PR. By decreasing this parameter, the column response would drive from volumetric expansion to volumetric compaction, dependent on the confinement stiffness.
- The methodology adopted for the model development can be taken to recalibrate the key components of this model, resulting in a more reliable model, when more comprehensive databases are available. Furthermore, this methodology can be extended potentially to develop new confinement models for other concrete-type and confining materials, through the recalibration of the failure surface function of the proposed confinement model and its coupled dilation model.

Acknowledgments

This study is a part of the project ‘‘Sticker –Innovative technique for the structural strengthening based on using CFRP laminates with multifunctional attributes and applied with advanced cement adhesives’’, with the reference POCI-01-0247-FEDER-039755. The firs author also acknowledges the support provided by FCT PhD individual fellowship 2019 with the reference of “SFRH/BD/148002/2019”.

Data Availability Statement

All data, models, and code generated or used during the study appear in the submitted article.

References

[1] Lin, S., Zhao, Y. G., Li, J., & Lu, Z. H. (2021). Confining stress path-based compressive strength model of axially loaded FRP-confined columns. Journal of Composites for Construction, 25(1), 04020077.

[2] Wang, W., Martin, P. R., Sheikh, M. N., & Hadi, M. N. (2018). Eccentrically loaded FRP confined concrete with different wrapping schemes. Journal of Composites for Construction, 22(6), 04018056.

[3] Zeng, J. J., Guo, Y. C., Gao, W. Y., Chen, W. P., & Li, L. J. (2018). Stress-strain behavior of concrete in circular concrete columns partially wrapped with FRP strips. Composite Structures, 200, 810-828.

[4] Zeng, J., Guo, Y., Li, L., & Chen, W. (2018). Behavior and three-dimensional finite element modeling of circular concrete columns partially wrapped with FRP strips. Polymers, 10(3), 253.

[5] Wang, Z., Wang, D., Smith, S. T., & Lu, D. (2012). Experimental testing and analytical modeling of CFRP-confined large circular RC columns subjected to cyclic axial compression. Engineering Structures, 40, 64-74.

[6] Kaeseberg, S., Messerer, D., & Holschemacher, K. (2020). Experimental study on concrete under combined FRP–Steel confinement. Materials, 13(20), 4467.

[7] Chastre, C., & Silva, M. A. (2010). Monotonic axial behavior and modelling of RC circular columns confined with CFRP. Engineering Structures, 32(8), 2268-2277.

[8] Eid, R., Roy, N., & Paultre, P. (2009). Normal-and high-strength concrete circular elements wrapped with FRP composites. Journal of composites for construction, 13(2), 113-124.

[9] Yin, P., Huang, L., Yan, L., & Zhu, D. (2016). Compressive behavior of concrete confined by CFRP and transverse spiral reinforcement. Part A: experimental study. Materials and Structures, 49(3), 1001-1011.

[10] Zignago, D., & Barbato, M. (2021). Effects of Transverse Steel on the Axial-Compression Strength of FRP-Confined Reinforced Concrete Columns Based on a Numerical Parametric Study. Journal of Composites for Construction, 25(4), 04021024.

[11] Barros, J. A., & Ferreira, D. R. (2008). Assessing the efficiency of CFRP discrete confinement systems for concrete cylinders. Journal of composites for construction, 12(2), 134-148.

[12] Teng, J., Huang, Y. L., Lam, L., & Ye, L. P. (2007). Theoretical model for fiber-reinforced polymer-confined concrete. Journal of composites for construction, 11(2), 201-210.

[13] Mander, J. B., Priestley, M. J., & Park, R. (1988). Theoretical stress-strain model for confined concrete. Journal of structural engineering, 114(8), 1804-1826.

[14] Shayanfar, J., Barros, J. A., & Rezazadeh, M. (2021). Generalized Analysis-oriented model of FRP confined concrete circular columns. Composite Structures, 270, 114026.

[15] Shayanfar, J., Rezazadeh, M., & Barros, J. A. (2020). Analytical model to predict dilation behavior of FRP confined circular concrete columns subjected to axial compressive loading. Journal of Composites for Construction, 24(6), 04020071.

[16] Pellegrino, C., & Modena, C. (2010). Analytical model for FRP confinement of concrete columns with and without internal steel reinforcement. Journal of Composites for Construction, 14(6), 693-705.

[17] Hu, H., & Seracino, R. (2014). Analytical model for FRP-and-steel-confined circular concrete columns in compression. Journal of Composites for Construction, 18(3), A4013012.

[18] Jiang, T., & Teng, J. G. (2007). Analysis-oriented stress–strain models for FRP–confined concrete. Engineering Structures, 29(11), 2968-2986.

[19] Teng, J. G., Lin, G., & Yu, T. (2015). Analysis-oriented stress-strain model for concrete under combined FRP-steel confinement. Journal of Composites for Construction, 19(5), 04014084.

[20] Jansen, D. C., & Shah, S. P. (1997). Effect of length on compressive strain softening of concrete. Journal of engineering mechanics, 123(1), 25-35.

[21] Yang, K. H., Lee, Y., & Mun, J. H. (2019). A Stress-Strain Model for Unconfined Concrete in Compression considering the Size Effect. Advances in Materials Science and Engineering, 2019.

[22] Watanabe, K., Niwa, J., Yokota, H., & Iwanami, M. (2004). Experimental study on stress-strain curve of concrete considering localized failure in compression. Journal of Advanced Concrete Technology, 2(3), 395-407.

[23] ACI (American Concrete Institute) (2008). "Building code requirements for structural concrete (ACI 318-08) and commentary." ACI 318–08, Detroit.

[24] Bamforth P, Chisholm D, Gibbs J, Harrison T. Properties of Concrete for use in Eurocode 2. Blackwater, Camberley, Surrey, UK: The Concrete Center; 2008. 59 p.

[25] Sim, J. I., Yang, K. H., Kim, H. Y., & Choi, B. J. (2013). Size and shape effects on compressive strength of lightweight concrete. Construction and Building Materials, 38, 854-864.

[26] Bazant ZP, Planas J. Fracture and size effect in concrete and other quasibrittle materials. New York: CRC Press; 1998.

[27] Bazant ZP. Size effect in blunt fracture: concrete, rock, metal. J Eng Mech ASCE 1984;110(4):518–35.

[28] Kim JK, Eo SH. Size effect in concrete specimens with dissimilar initial cracks. Mag Concr Res 1990;42(153):233–8.

[29] Carpinteri, A., Ferro, G., & Monetto, I. (1999). Scale effects in uniaxially compressed concrete specimens. Magazine of Concrete Research, 51(3), 217-225.

[30] Dahl, K. K. B. (1992). "Uniaxial stress-strain curves for normal and high strength concrete." ABK Rep. No. R282, Dept. of Structural Engineering, Technical Univ. of Denmark, Kongens Lyngby, Denmark.

[31] Lim, J. C., & Ozbakkaloglu, T. (2014). Stress–strain model for normal-and light-weight concretes under uniaxial and triaxial compression. Construction and Building Materials, 71, 492-509.

[32] Popovics, S. (1973). A numerical approach to the complete stress-strain curve of concrete. Cement and concrete research, 3(5), 583-599.

[33] Fallahpour, A., Nguyen, G. D., Vincent, T., & Ozbakkaloglu, T. (2020). Investigation of the compressive behavior and failure modes of unconfined and FRP-confined concrete using digital image correlation. Composite Structures, 252, 112642.

[34] Shayanfar, J., Rezazadeh, M., & Barros, J. A. (2021). Theoretical Prediction of Axial Response of FRP Fully/partially Confined Circular Concrete Under Axial Loading. In International Conference on Fibre-Reinforced Polymer (FRP) Composites in Civil Engineering (pp. 1439-1449). Springer, Cham.

[35] Shayanfar, J., Barros, J. A., & Rezazadeh, M. (2022). Unified model for fully and partially FRP confined circular and square concrete columns subjected to axial compression. Engineering Structures, 251, 113355.

[36] Wei, Y., & Wu, Y. F. (2016). Experimental study of concrete columns with localized failure. Journal of Composites for Construction, 20(5), 04016032.

[37] Guo, Y. C., Gao, W. Y., Zeng, J. J., Duan, Z. J., Ni, X. Y., & Peng, K. D. (2019). Compressive behavior of FRP ring-confined concrete in circular columns: Effects of specimen size and a new design-oriented stress-strain model. Construction and Building Materials, 201, 350-368.

[38] Wu, Y. F., & Wei, Y. (2016). Stress–strain modeling of concrete columns with localized failure: An analytical study. Journal of Composites for Construction, 20(3), 04015071.

[39] Razvi, S., & Saatcioglu, M. (1999). Confinement model for high-strength concrete. Journal of Structural Engineering, 125(3), 281-289.

[40] Assa, B., Nishiyama, M., & Watanabe, F. (2001). New approach for modeling confined concrete. I: Circular columns. Journal of Structural Engineering, 127(7), 743-750.

[41] Shayanfar, J., Omidalizadeh, M., & Nematzadeh, M. (2020). Analysis-oriented model for seismic assessment of RC jacket retrofitted columns. Steel and Composite Structures, An International Journal, 37(3), 371-390.

[42] Shayanfar, J., & Akbarzadeh Bengar, H. (2017). Nonlinear analysis of RC frames considering shear behaviour of members under varying axial load. Bulletin of Earthquake Engineering, 15(5), 2055-2078.

[43] Kwan, A. K. H., Dong, C. X., & Ho, J. C. M. (2015). Axial and lateral stress–strain model for FRP confined concrete. Engineering Structures, 99, 285-295.

[44] Dong, C. X., Kwan, A. K. H., & Ho, J. C. M. (2015). A constitutive model for predicting the lateral strain of confined concrete. Engineering Structures, 91, 155-166.

[45] Lai, M., Hanzic, L., & Ho, J. C. (2019). Fillers to improve passing ability of concrete. Structural Concrete, 20(1), 185-197.

[46] Moran, D. A., & Pantelides, C. P. (2012). Elliptical and circular FRP-confined concrete sections: A Mohr–Coulomb analytical model. International Journal of Solids and Structures, 49(6), 881-898.

[47] Lim, J. C., & Ozbakkaloglu, T. (2015). Lateral strain-to-axial strain relationship of confined concrete. Journal of Structural Engineering, 141(5), 04014141.

[48] Shayanfar, J., Rezazadeh, M., Barros, J.A., Ramezansefat H. (2020). A new dilation model for FRP fully/partially confined concrete column under axial loading. The 3RD RILEM Spring Convention 2020 Ambitioning a Sustainable Future for Built Environment: Comprehensive Strategies for Unprecedented Challenges, Guimarães, Portugal.

[49] Yang, J., Wang, J., & Wang, Z. (2020). Axial compressive behavior of partially CFRP confined seawater sea-sand concrete in circular columns–Part I: Experimental study. Composite Structures, 246, 112373.

[50] Yang, J., Wang, Z., & Wang, J. (2022). Compressive Performance of Partially CFRP-Confined Square Seawater–Sea Sand Concrete Columns with Internal Epoxy-Coated Reinforcement. Journal of Composites for Construction, 26(2), 04021073.

[51] Zeng, J. J., Guo, Y. C., Gao, W. Y., Li, J. Z., & Xie, J. H. (2017). Behavior of partially and fully FRP-confined circularized square columns under axial compression. Construction and Building Materials, 152, 319-332.

[52] Carreira and Chu (1985). Stress-strain relationship for plain concrete in compression. In Journal Proceedings 1985;82(6):797–804.

[53] Shayanfar, J., & Akbarzadeh Bengar, H. (2018). A practical model for simulating nonlinear behaviour of FRP strengthened RC beam-column joints. Steel and Composite Structures, An International Journal, 27(1), 49-74.

[54] Nematzadeh, M., Mousavimehr, M., Shayanfar, J., & Omidalizadeh, M. (2021). Eccentric compressive behavior of steel fiber-reinforced RC columns strengthened with CFRP wraps: Experimental investigation and analytical modeling. Engineering Structures, 226, 111389.

[55] Yang, J. Q., & Feng, P. (2020). Analysis-oriented models for FRP-confined concrete: 3D interpretation and general methodology. Engineering Structures, 216, 110749.

[56] Lim, J. C., & Ozbakkaloglu, T. (2014). Unified stress-strain model for FRP and actively confined normal strength and high-strength concrete. Journal of Composites for Construction, 19(4), 04014072.

[57] Lai, M. H., Liang, Y. W., Wang, Q., Ren, F. M., Chen, M. T., & Ho, J. C. M. (2020). A stress-path dependent stress-strain model for FRP-confined concrete. Engineering Structures, 203, 109824.

[58] Lai, M. H., Song, W., Ou, X. L., Chen, M. T., Wang, Q., & Ho, J. C. M. (2020). A path dependent stress-strain model for concrete-filled-steel-tube column. Engineering Structures, 211, 110312.

[59] Ho, J. C. M., Ou, X. L., Chen, M. T., Wang, Q., & Lai, M. H. (2020). A path dependent constitutive model for CFFT column. Engineering Structures, 210, 110367.

[60] Mirmiran, A., Shahawy, M., & Beitleman, T. (2001). Slenderness limit for hybrid FRP-concrete columns. Journal of composites for construction, 5(1), 26-34.

[61] Fitzwilliam, J., & Bisby, L. A. (2010). Slenderness effects on circular CFRP confined reinforced concrete columns. Journal of Composites for Construction, 14(3), 280-288.

[62] Jiang, T., & Teng, J. G. (2013). Behavior and design of slender FRP-confined circular RC columns. Journal of Composites for Construction, 17(4), 443-453.

Appendix A

To determine axial stress versus axial strain curves of FRP fully confined RC columns (FR), Teng *et al.* [19] proposed an analysis-oriented model based on active confinement approach. In the present study, for the generalization of this model for the case of partial confinement arrangement (PR), the original concept of confinement efficiency factor recommended by Mander *et al.* (1988) was adopted.

Based on Teng *et al.* [19]'s model, at a certain level of concrete transverse expansion ($\varepsilon_{l,j}$) representing FRP hoop strain, the corresponding confinement pressures imposed by FRP strips ($f_{l,f}$) and steel transverse reinforcements ($f_{l,s}$) can be calculated as:

For the case of FRP full/partial arrangement:

$$f_{l,f} = 2k_{v,f} \frac{n_f t_f w_f}{b\left(s_f + w_f\right)} E_f \varepsilon_{l,j} \qquad \text{B-1}$$

in which

$$k_{v,f} = \left(1 - \frac{s_f}{2D}\right)^2 \qquad \text{B-2}$$

where $k_{v,f}$ is the reduction factor reflecting the effect of vertical arching action between FRP strips; n_f is the number of FRP layers; t_f is the thickness of a FRP layer; E_f is the FRP modulus of elasticity; w_f is the FRP width; s_f is the distance between FRP strips; D is the diameter of the circular cross-section.

For the case of steel transverse reinforcement:

$$f_{l,s} = 2k_{v,s}\frac{A_{sth}}{D_c s_s}E_s\varepsilon_{l,j} \qquad \text{for } \varepsilon_{l,j} < \varepsilon_{yh} \qquad \text{B-3a}$$

$$f_{l,s} = 2k_{v,s}\frac{A_{sth}}{D_c s_s}f_{yh} \qquad \text{for } \varepsilon_{l,j} \geq \varepsilon_{yh} \qquad \text{B-3b}$$

in which

$$k_{v,s} = \left(1-\frac{s_s}{2D_c}\right)^2 \qquad \text{for steel hoop reinforcement} \qquad \text{B-4a}$$

$$k_{v,s} = \left(1-\frac{s_s}{2D_c}\right) \qquad \text{for steel spiral reinforcement} \qquad \text{B-4b}$$

where $k_{v,s}$ is the reduction factor reflecting the effect of vertical arching action between reinforcements; D_c is the diameter of the concrete core; A_{sth} is the cross-sectional area of a steel spiral/hoop; s_s is the distance between reinforcements ; E_s , ε_{yh} and f_{yh} are the elasticity modulus, yield strain and stress of reinforcements, respectively. Subsequently, based on the dilation model, the average axial strain along the column height (ε_c) corresponding to $\varepsilon_{l,j}$ can be calculated as:

$$\varepsilon_c = 0.85\varepsilon_{c0}F_T\left\{\left[1+0.75\left(\frac{\varepsilon_{l,j}}{\varepsilon_{c0}}\right)\right]^{0.7} - \exp\left[-7\left(\frac{\varepsilon_{l,j}}{\varepsilon_{c0}}\right)\right]\right\} \qquad \text{B-5}$$

in which

$$F_T = 1+8\frac{f_{l,f}}{f_{c0}}+\alpha\frac{f_{l,s}}{f_{c0}} \qquad \text{B-6}$$

$$\alpha = 1.59 + 15.1\rho_{FS} \tag{B-7}$$

$$\rho_{FS} = \frac{K_{Lc} s_s D_c}{2k_{v,s} E_s A_{st}} \quad \text{for FR} \tag{B-8}$$

$$\rho_{FS} = \frac{k_{v,f} K_{Lc} s_s D_c}{2k_{v,s} E_s A_{st}} \left(\frac{w_f}{w_f + s_f} \right) \quad \text{for PR} \tag{B-9}$$

$$\varepsilon_{c0} = 0.000937 f_{c0}^{\ 0.25} \tag{B-10}$$

834 where ρ_{FS} is the ratio between the confinement stiffness of the FRP jacket and steel confining
835 systems; ε_{c0} is the axial strain corresponding to f_{c0}. Based on the active confinement approach,
836 the axial stress carried by concrete core area ($f_c^{\ Core}$) corresponding to ε_c can be calculated as

$$f_c^{\ Core} = f_{cc}^{\ Core} \frac{\left(\varepsilon_c / \varepsilon_{cc}^{\ Core}\right) n_1}{n_1 - 1 + \left(\varepsilon_c / \varepsilon_{cc}^{\ Core}\right)^{n_1}} \tag{B-11}$$

837 in which

$$\frac{f_{cc}^{\ Core}}{f_{c0}} = 1 + 3.5\left(\frac{f_{l,f}}{f_{c0}}\right) + 3.12\left(\frac{f_{l,s}}{f_{c0}\left[1 + 0.202\rho_{FS}^{\ 0.145}\right]}\right)^{0.736} \tag{B-12}$$

$$\frac{\varepsilon_{cc}^{\ Core}}{\varepsilon_{c0}} = 1 + 3.9\left[\frac{f_{cc}^{\ Core}}{f_{c0}} - 1\right]^{1.2} \tag{B-13}$$

$$n_1 = \frac{E_c}{E_c - f_{cc}^{\ Core} / \varepsilon_{cc}^{\ Core}} \tag{B-14}$$

$$E_c = 4730\sqrt{f_{c0}} \tag{B-15}$$

838 where $f_{cc}^{\ Core}$ is the failure surface function as the peak axial stress of the axial stress-strain base
839 relation of the concrete core; $\varepsilon_{cc}^{\ Core}$ is the axial strain corresponding to $f_{cc}^{\ Core}$; n_1 introduces the

concrete brittleness term; E_c defines the elasticity modulus of concrete. Similarly, the axial stress carried by concrete cover area (f_c^{Cover}) corresponding to ε_c can be calculated as

$$f_c^{Cover} = f_{cc}^{Cover} \frac{\left(\varepsilon_c / \varepsilon_{cc}^{Cover}\right) n_2}{n_2 - 1 + \left(\varepsilon_c / \varepsilon_{cc}^{Cover}\right)^{n_2}} \qquad \text{B-16}$$

in which

$$\frac{f_{cc}^{Cover}}{f_{c0}} = 1 + 3.5\left(\frac{f_{l,f}}{f_{c0}}\right) \qquad \text{B-17}$$

$$\frac{\varepsilon_{cc}^{Cover}}{\varepsilon_{c0}} = 1 + 17.5\left(\frac{f_{l,f}}{f_{c0}}\right)^{1.2} \qquad \text{B-18}$$

$$n_2 = \frac{E_c}{E_c - f_{cc}^{Cover} / \varepsilon_{cc}^{Cover}} \qquad \text{B-19}$$

where f_{cc}^{Cover} is the failure surface function as the peak axial stress of the axial stress-strain base relation of the concrete cover; ε_{cc}^{Cover} is the axial strain corresponding to f_{cc}^{Cover} ; n_2 introduces the brittleness term of the concrete cover.

The incremental calculation process of the generalized Teng *et al.* [19]'s model for determining the response of FR/PR in terms of f_c^{Core} versus ε_c and f_c^{Cover} versus ε_c relations of the concrete core and cover areas is as the following one:

1) Calculate $k_{v,s}$ with Eq. (B-4)
2) Calculate $k_{v,f}$ with Eq. (B-2)
3) Assume a value of concrete lateral strain ($\varepsilon_{l,j}$)

4) Calculate FRP confinement pressure ($f_{l,f}$) by Eq. (B-1)

5) Calculate steel confinement pressure ($f_{l,s}$) by Eq. (B-3)

6) Calculate axial strain (ε_c) by Eq. (B-5)

7) Calculate failure surface function of the concrete core (f_{cc}^{Core}) by Eq. (B-12)

8) Calculate failure surface function of the concrete cover (f_{cc}^{Cover}) by Eq. (B-17)

9) Calculate axial stress (f_c^{Core}) by Eqs. (B-11) to (B-15)

10) Calculate axial stress (f_c^{Cover}) by Eqs. (B-16) to (B-19)

11) Continue the steps 3-10 up to ultimate axial strain

By repeating the aforementioned calculation procedure for a range of $\varepsilon_{l,j}$, f_c^{Cover} versus ε_c and f_c^{Core} versus ε_c relations of the concrete core and cover areas can be determined. It is noted that that for large-sized RC specimens, Teng *et al.* [19] considered f_{c0} to be $0.85 f'_{c0}$ based on ACI 318's recommendation [23].

Figure 1

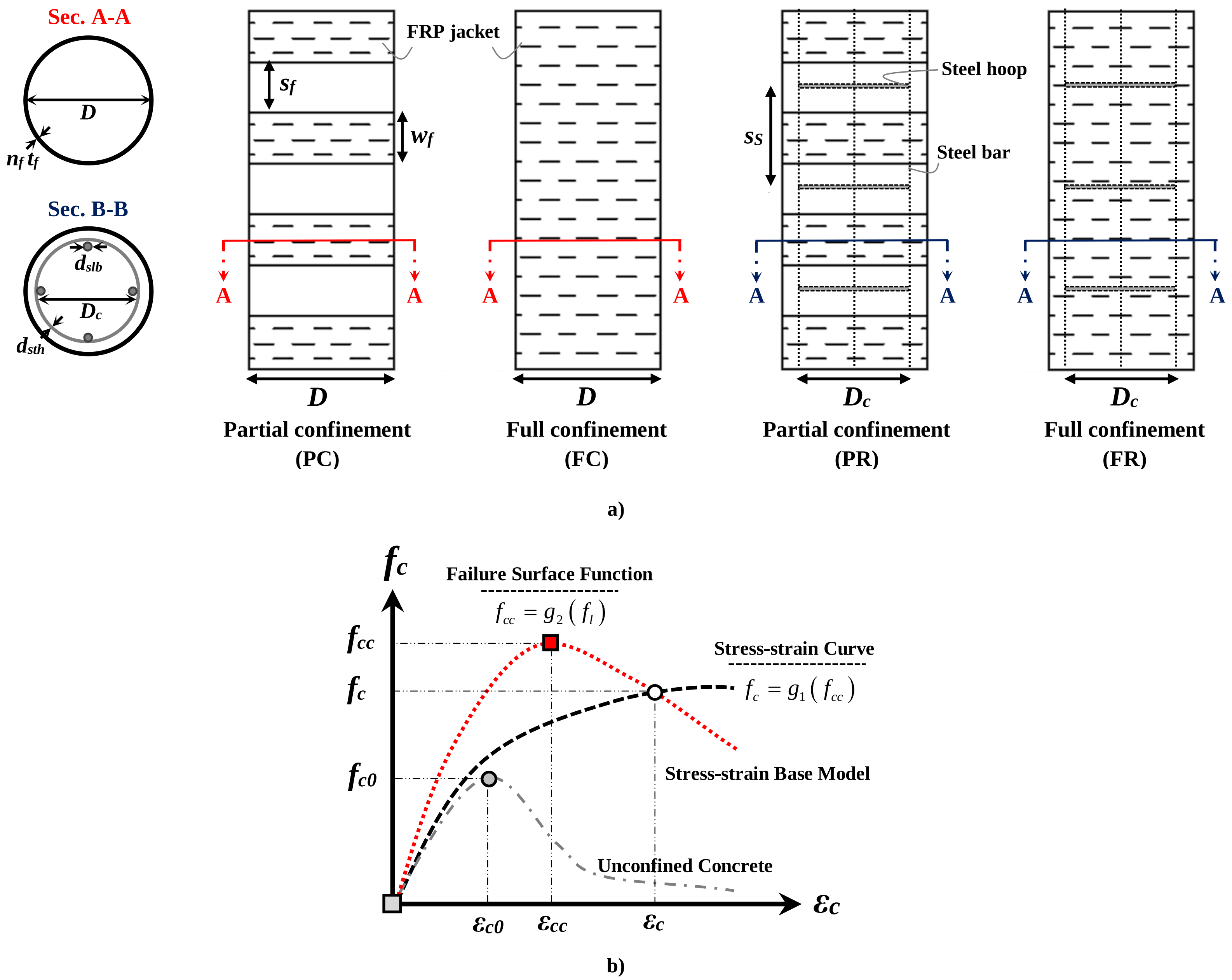

Fig. 1. a) Different confinement configurations; b) Development of axial stress-strain curve of FRP confined concrete

Note: FC: Fully FRP confined concrete column; **PC:** Partially FRP confined concrete column; **FR:** Fully FRP confined RC column; **PR:** Partially FRP confined RC column

Figure 2

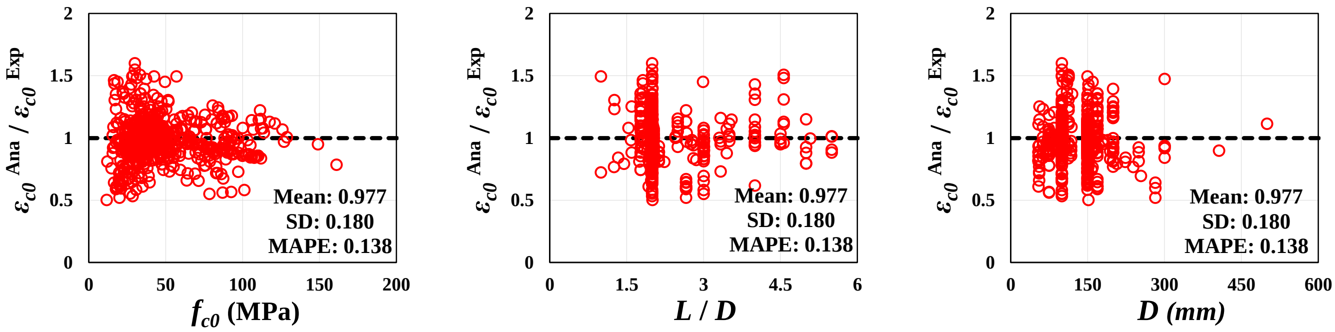

Fig. 2. Predictive performance of Eq. (2)

Figure 3

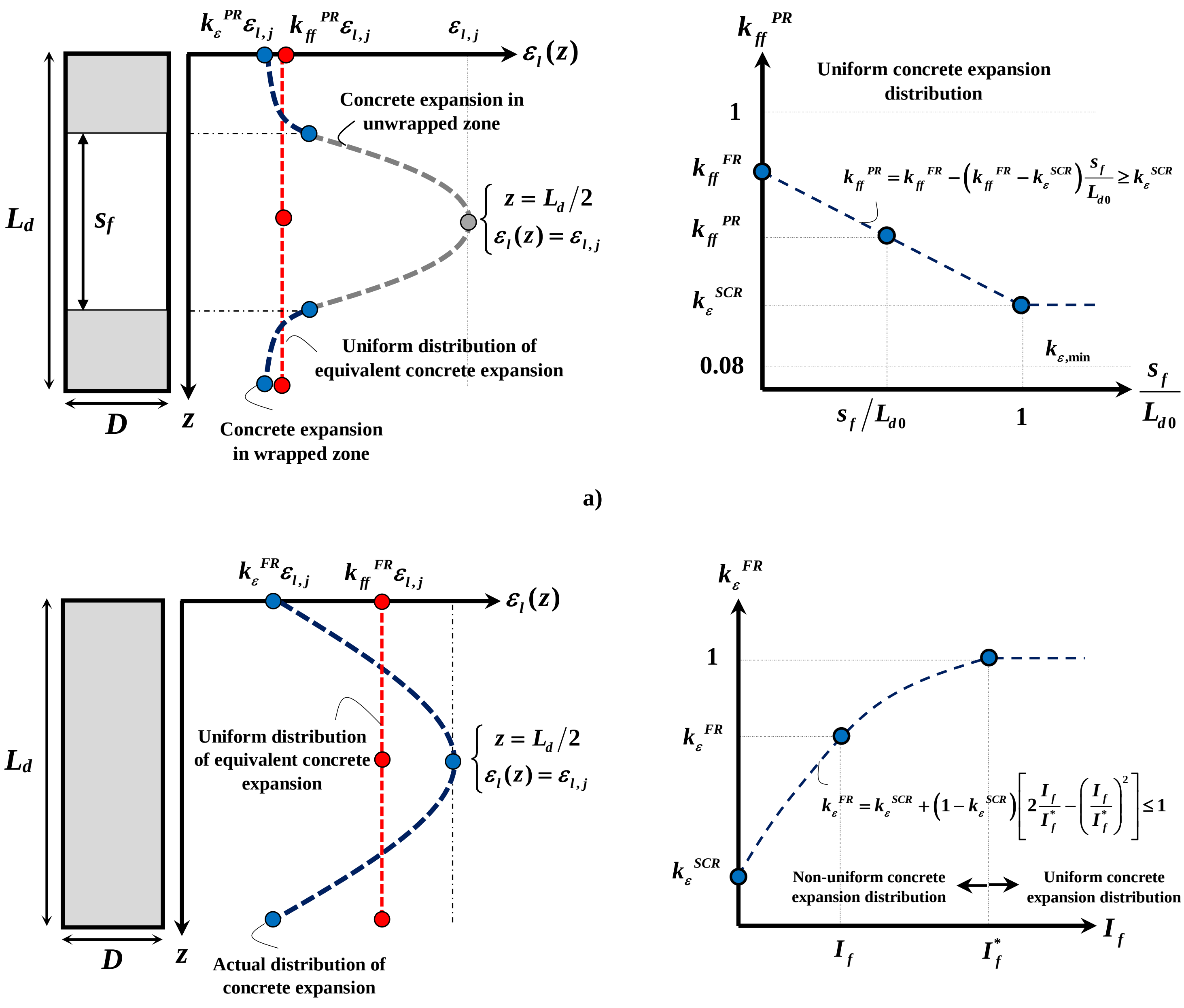

Fig. 3. Schematic distribution of concrete lateral expansion along the damage zone : a) Partial confinement configuration; b) Full confinement configuration

Note: $\varepsilon_l(z)$ defines the function of concrete lateral expansion along z-axis (damage length zone)

Figure 4

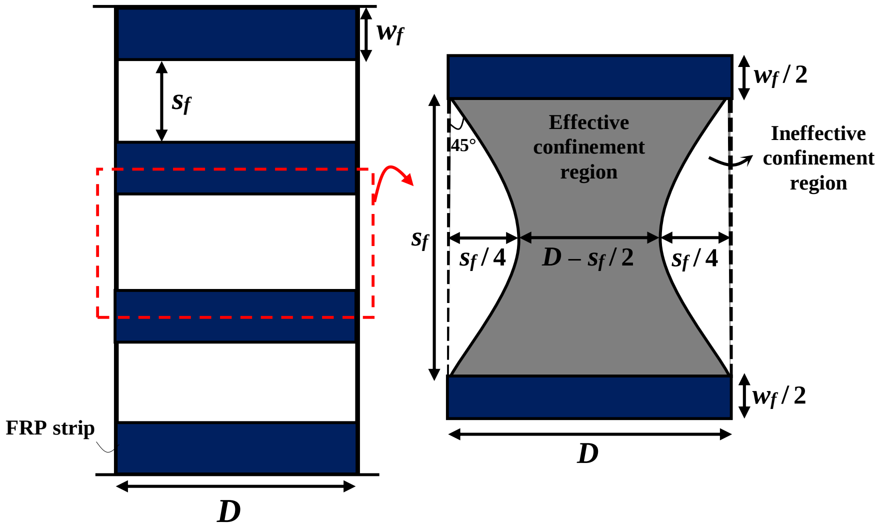

a)

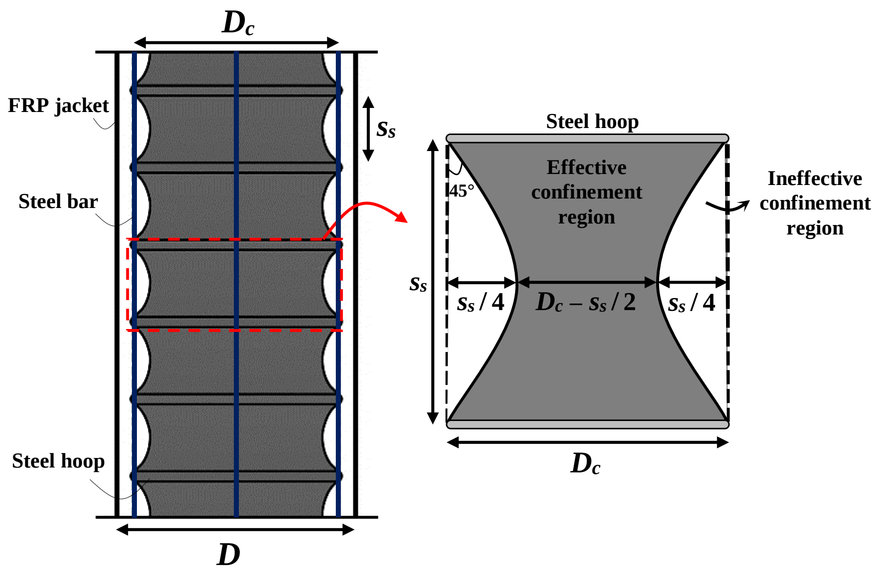

b)

Fig. 4. Vertical arching action between a) FRP strips and b) steel transverse reinforcements

Figure 5

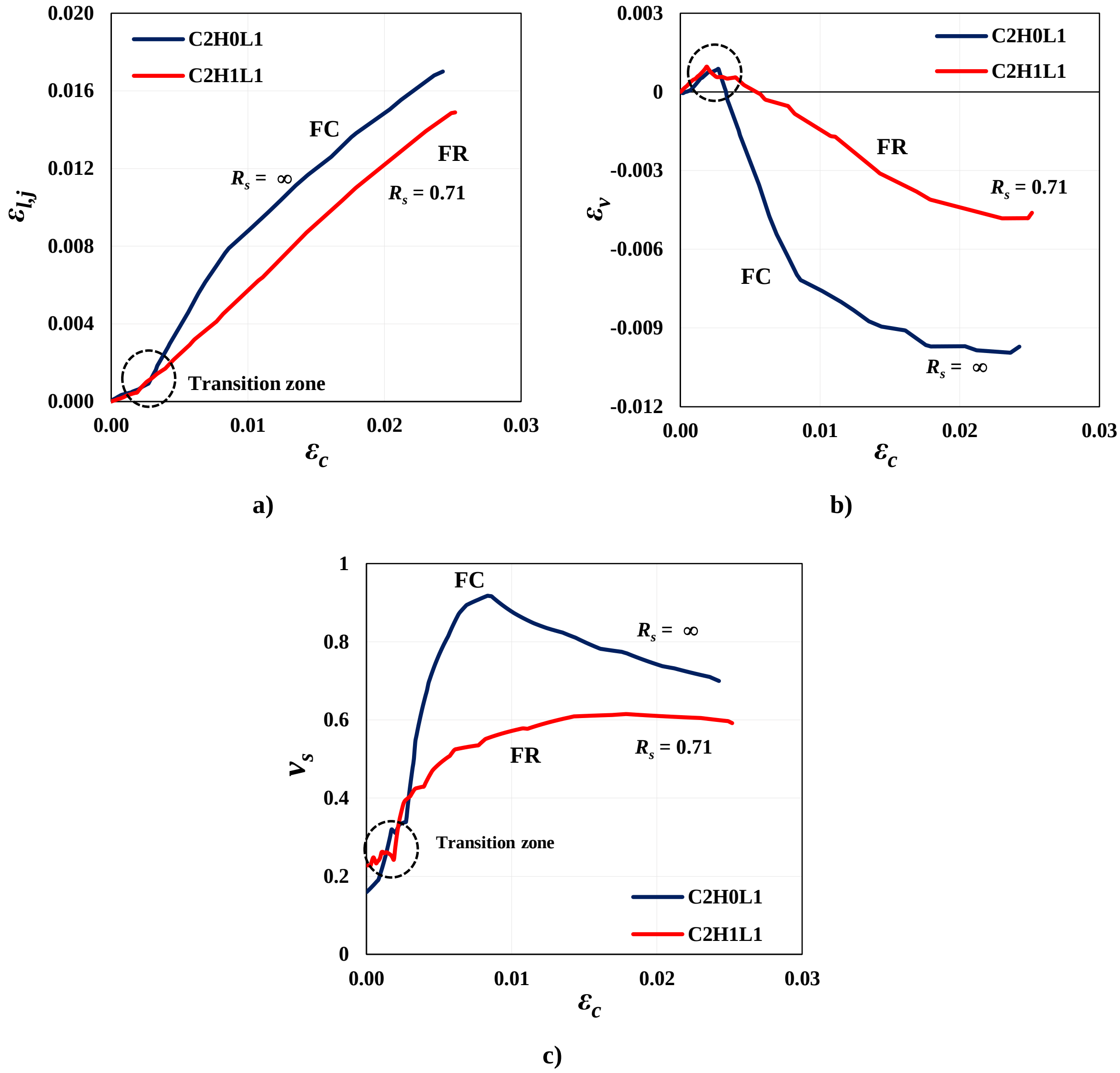

Fig. 5. Effect of steel confining hoops on the dilation characteristics of FR

Figure 6

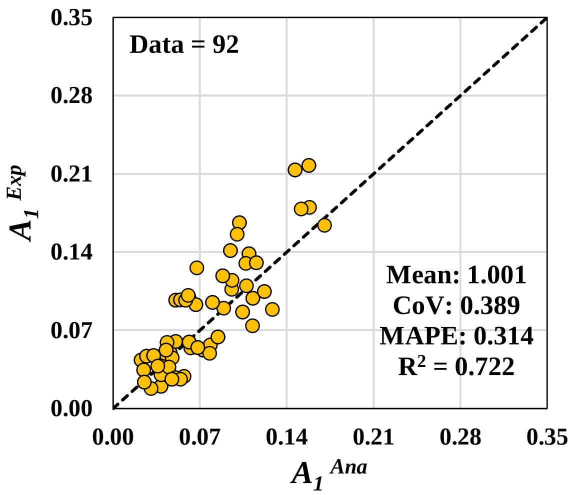

Fig. 6. Predictive performance of Eq. (31)

Figure 7

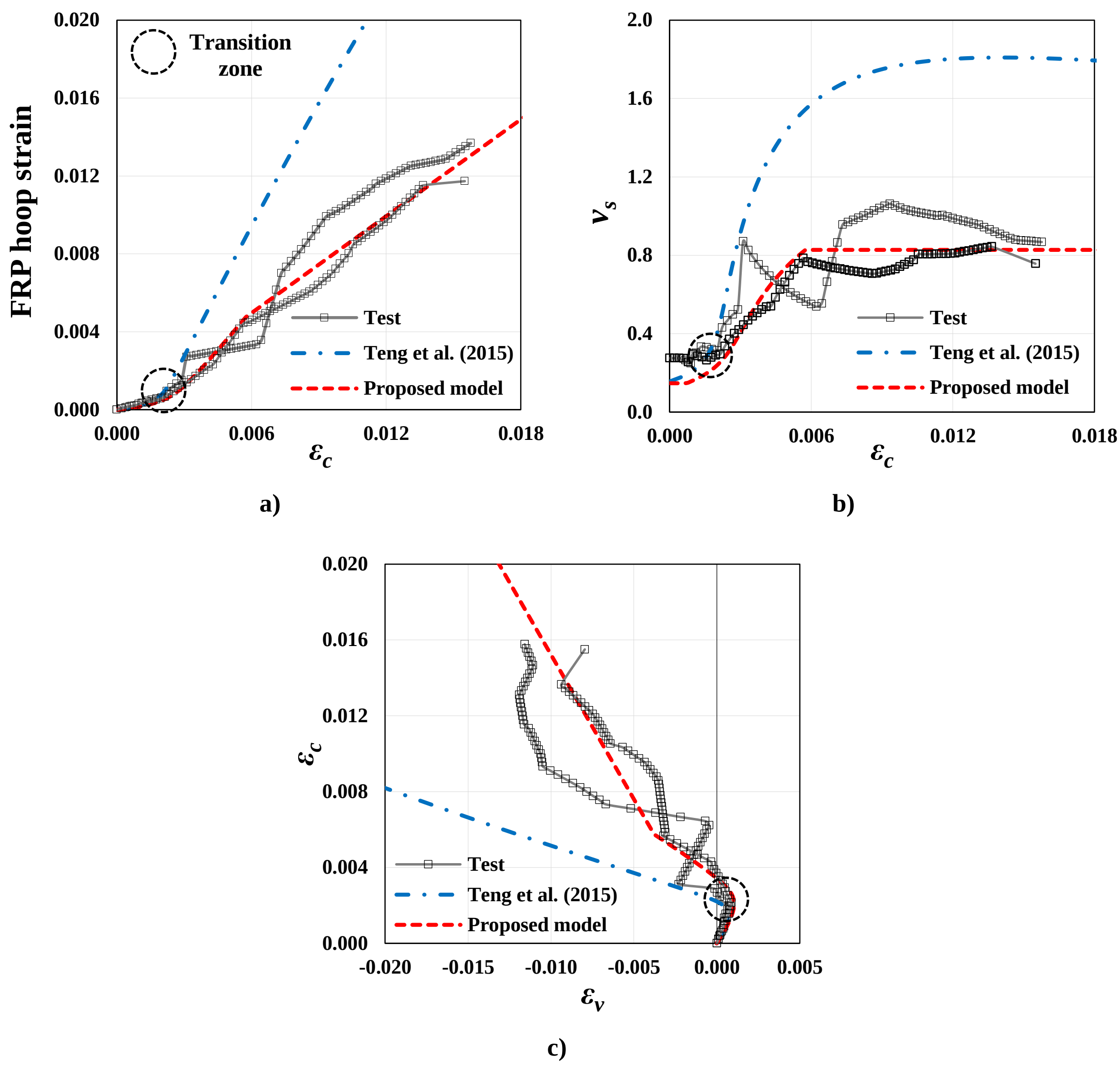

Fig. 7. Comparison of the developed approach with that proposed by Teng *et al.* [19]: a) FRP hoop strain versus axial strain (ε_c); b) secant Poisson's ratio (v_s) versus axial strain (ε_c); c) axial strain (ε_c) versus volumetric strain (ε_v)

Figure 8

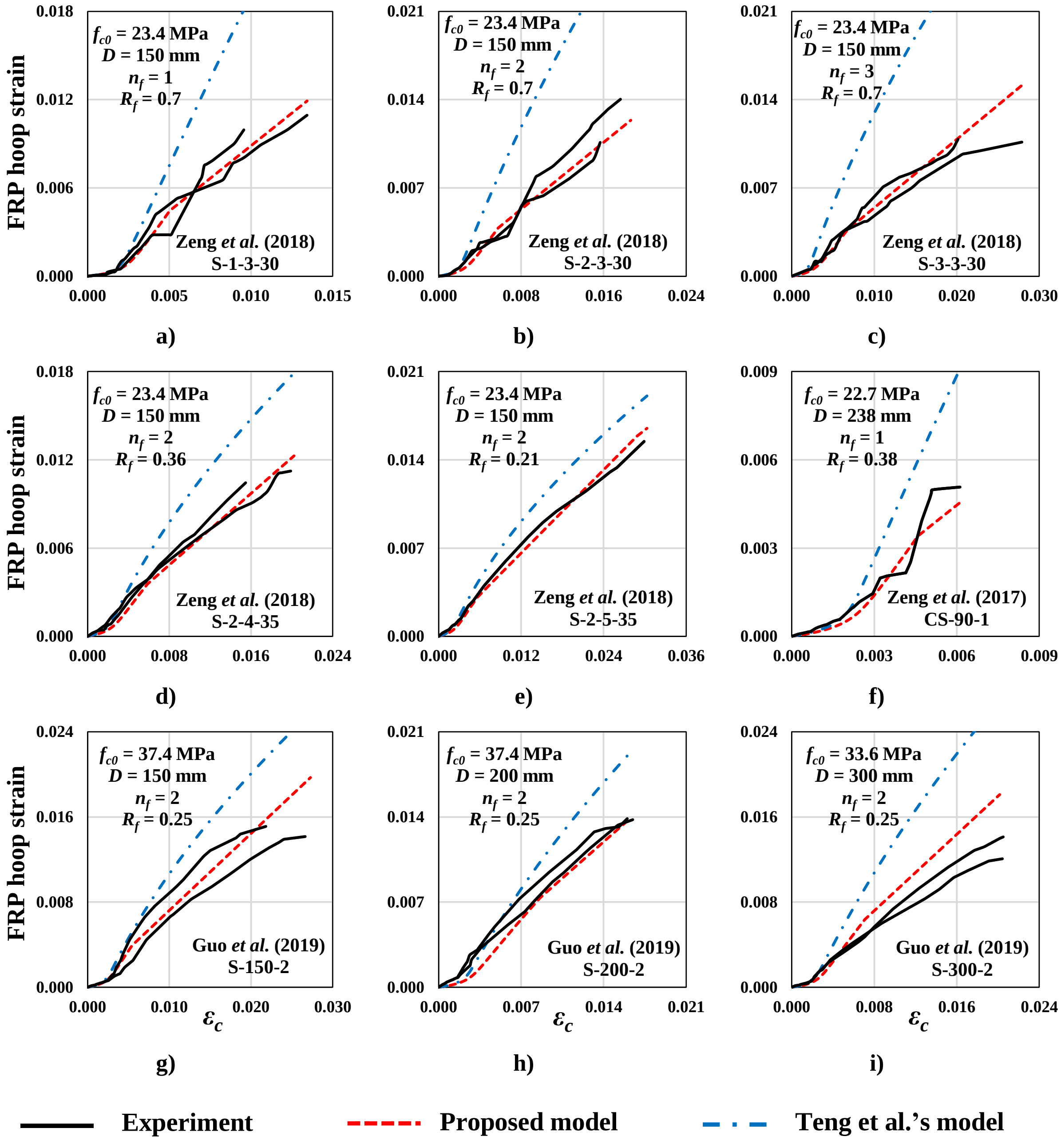

Fig. 8. Analytical simulations versus experimental results of PC tested by Zeng *et al.* [3, 51] and Guo *et al.* [37]

Figure 9

Click here to access/download;Figure (Do not upload picture, .svg format. Upload only PDF, eps or tiff format);Figure 9.docx

Figure 9

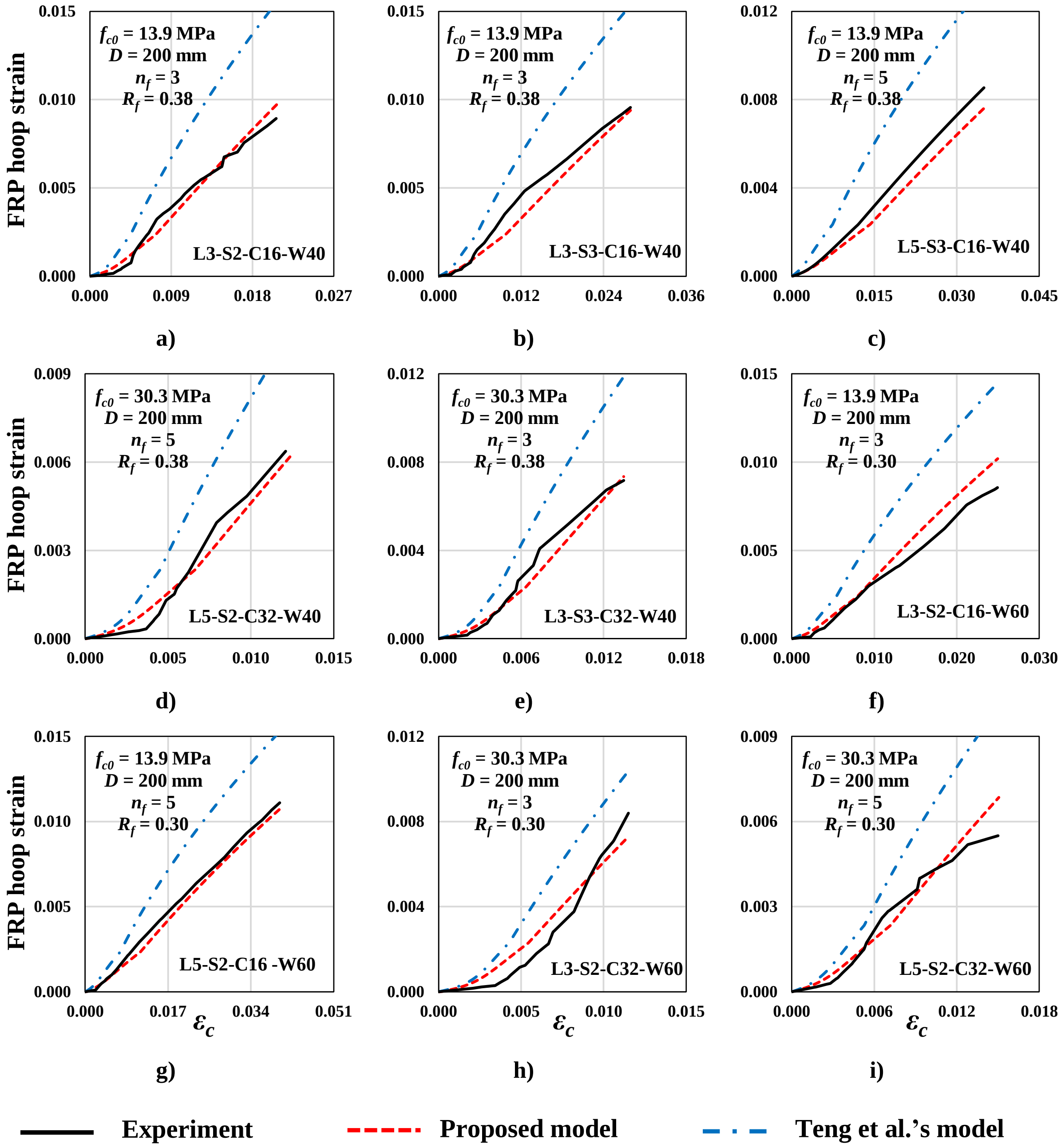

Fig. 9. Analytical simulations versus experimental results of PR tested by Barros and Ferreira [11]

Figure 10

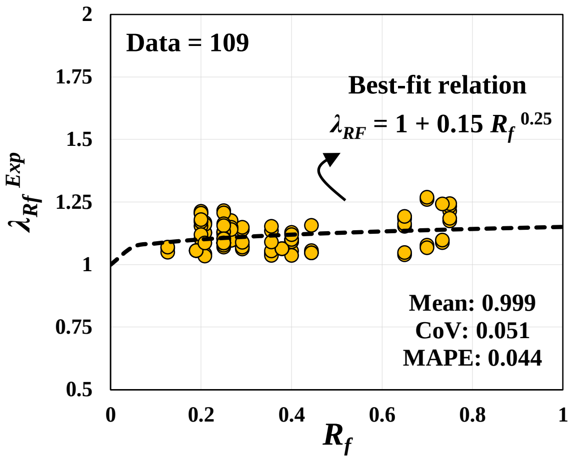

Fig. 10. Performance of Eq. (48)

Note: the experimental values were extracted from the experiments conducted by Barros and Ferreira [11], Zeng *et al.* [3, 4, 51], Guo *et al.* [37]

Figure 11

Click here to access/download;Figure (Do not upload picture, .svg format. Upload only PDF, eps or tiff format);Figure 11.docx

Figure 11

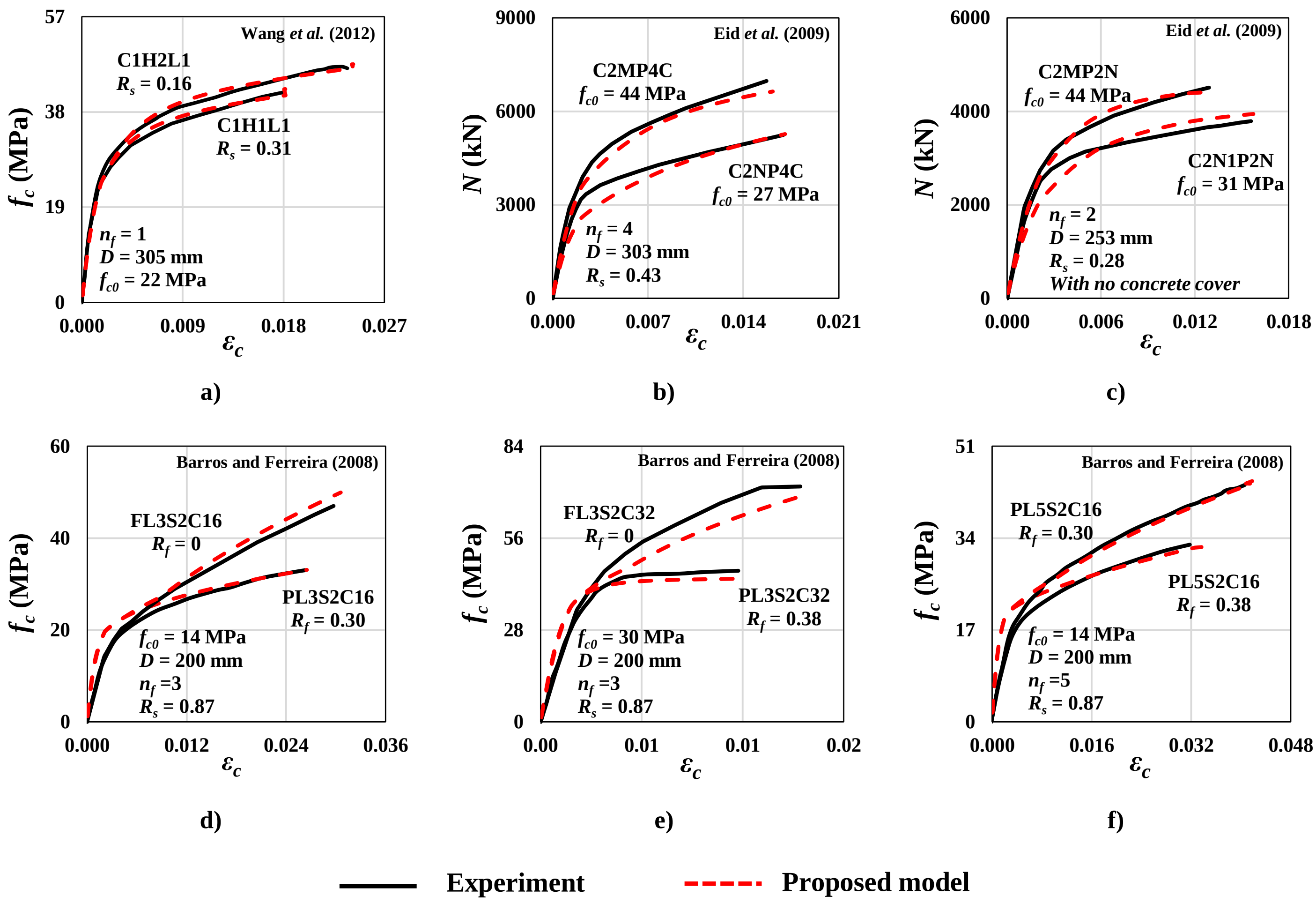

Fig. 11. Analytical simulations versus experimental results of FR/PR tested by [5, 8, 11]

Figure 12

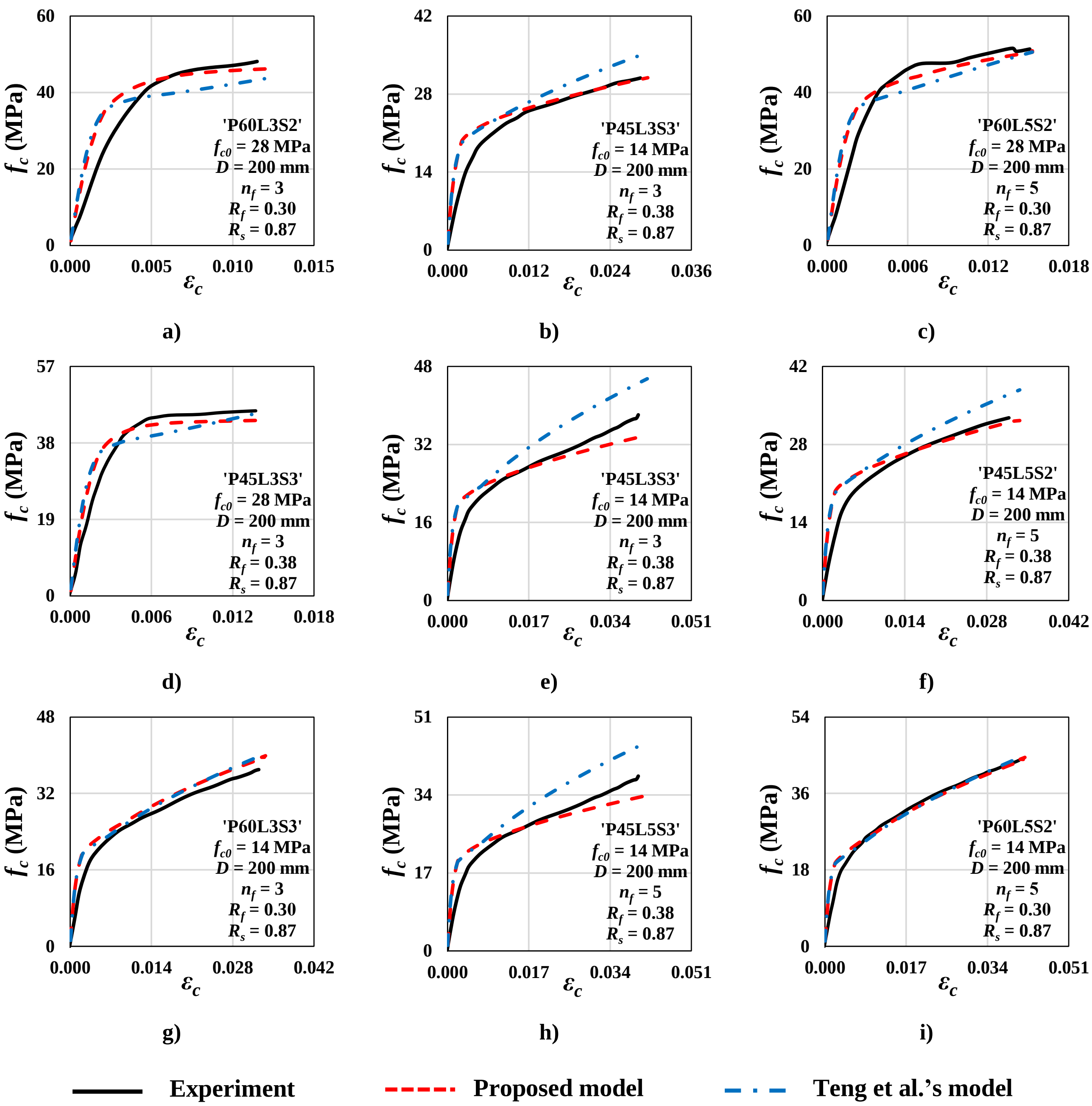

Fig. 12. Analytical simulations versus experimental results of PR tested by [11]

Figure 13

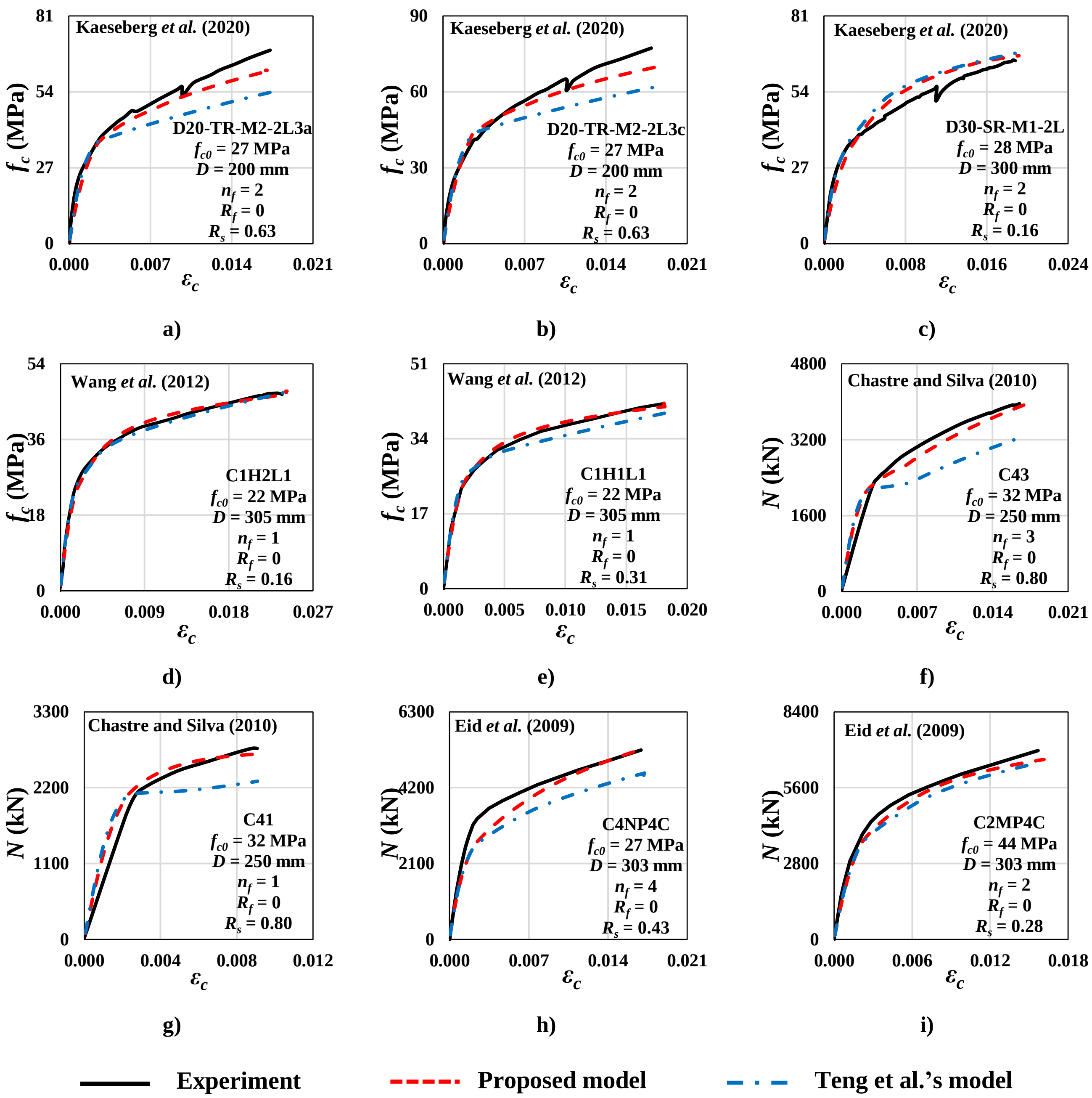

Fig. 13. Analytical simulations versus experimental results of FR tested by [5-8]

Figure 14

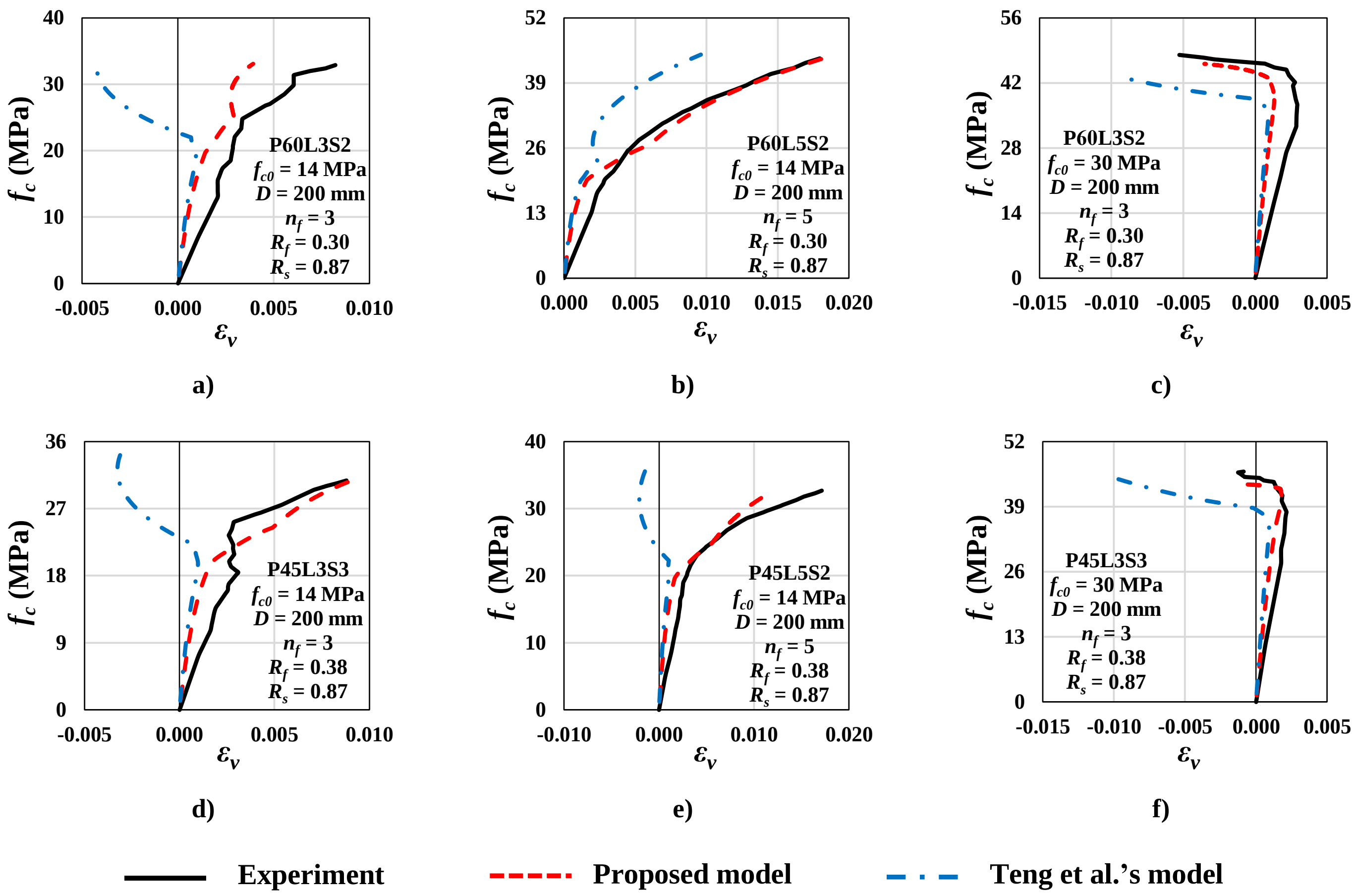

Fig. 14. Analytical simulations versus experimental results tested by Barros and Ferreira [11] in terms of axial stress versus volumetric strain relation

Figure 15

Click here to access/download;Figure (Do not upload picture, .svg format. Upload only PDF, eps or tiff format);Figure

Figure 15

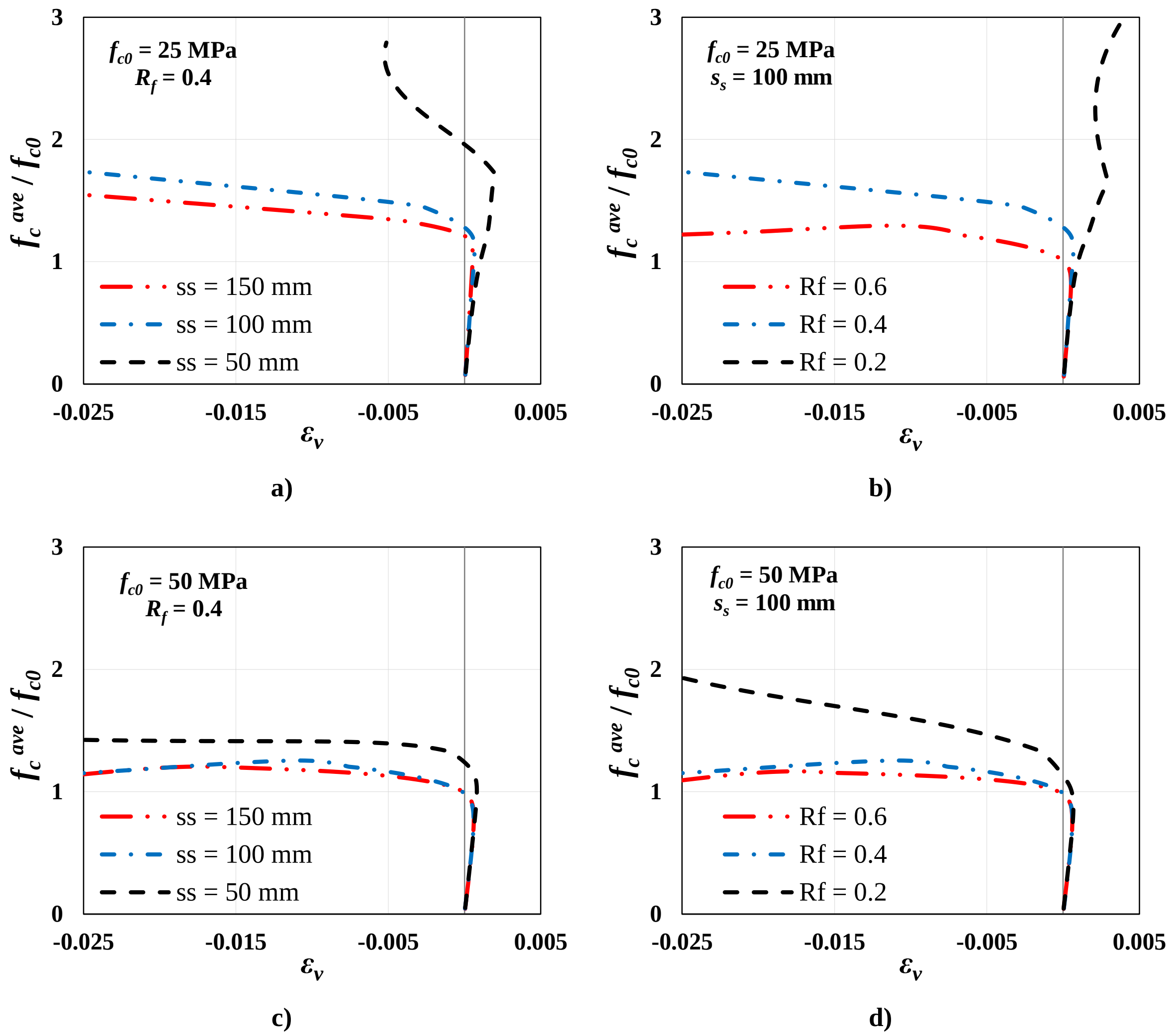

Fig. 15. Effects of steel hoop and FRP spacing, and concrete compressive strength on the normalized concrete axial stress versus volumetric strain relation

Table 1

Table 1. Summary of the compiled database.

Number of datasets		f_{c0} range (MPa)	ε_{c0} range	L/D range	D range (mm)
604	Min.	11.6	0.0012	1.0	54
	Max.	204.0	0.0051	5.5	500
	Mean	51.2	0.0025	2.2	133.4
	CoV	0.534	0.233	0.297	0.339

Table 2

Table 2. Comparative performance of Eq. (2) with existing expressions

Model	Expression	Test Data	Assessment indicators		
			Mean	SD	MAPE
Proposed model	$\varepsilon_{c0} = 0.0011\left(\frac{f_{c0}D}{L}\right)^{0.25}$	604	**0.977**	**0.180**	**0.138**
Lim and Ozbakkaloglu [25]	$\varepsilon_{c0} = 0.001 f_{c0}^{0.225}\left(\frac{152}{D}\right)^{0.1}\left(\frac{2D}{L}\right)^{0.13}$	604	0.988	0.186	0.143
Popovics [26]	$\varepsilon_{c0} = 0.000937 f_{c0}^{0.25}$	604	1.009	0.192	0.147